

August 2015

Fluoride and Phosphate Removal From Industrial and Domestic Wastewaters Using Cerium Chloride

John Michael Gonzales

University of Nevada, Las Vegas, gonza982@unlv.nevada.edu

Follow this and additional works at: <https://digitalscholarship.unlv.edu/thesesdissertations>



Part of the [Civil Engineering Commons](#), and the [Environmental Engineering Commons](#)

Repository Citation

Gonzales, John Michael, "Fluoride and Phosphate Removal From Industrial and Domestic Wastewaters Using Cerium Chloride" (2015). *UNLV Theses, Dissertations, Professional Papers, and Capstones*. 2476. <https://digitalscholarship.unlv.edu/thesesdissertations/2476>

This Thesis is protected by copyright and/or related rights. It has been brought to you by Digital Scholarship@UNLV with permission from the rights-holder(s). You are free to use this Thesis in any way that is permitted by the copyright and related rights legislation that applies to your use. For other uses you need to obtain permission from the rights-holder(s) directly, unless additional rights are indicated by a Creative Commons license in the record and/or on the work itself.

This Thesis has been accepted for inclusion in UNLV Theses, Dissertations, Professional Papers, and Capstones by an authorized administrator of Digital Scholarship@UNLV. For more information, please contact digitalscholarship@unlv.edu.

FLUORIDE AND PHOSPHATE REMOVAL FROM INDUSTRIAL AND DOMESTIC
WASTEWATERS USING CERIUM CHLORIDE

by

John Michael Gonzales

Bachelor of Engineering in Civil and Environmental Engineering
University of Nevada, Las Vegas
2013

A thesis submitted in partial fulfillment
of the requirements for the

Master of Science in Engineering - Civil and Environmental Engineering

Department of Civil and Environmental Engineering and Construction
Howard R. Hughes College of Engineering
The Graduate College

University of Nevada, Las Vegas
August 2015

August 10, 2015

This thesis prepared by

John Michael O. Gonzales

entitled

Fluoride and Phosphate Removal from Industrial and Domestic Wastewaters Using
Cerium Chloride

is approved in partial fulfillment of the requirements for the degree of

Master of Science in Engineering – Civil and Environmental Engineering
Department of Civil and Environmental Engineering and Construction

Jacimaria Batista, Ph.D.
Examination Committee Chair

Kathryn Hausbeck Korgan, Ph.D.
Graduate College Interim Dean

Daniel Gerrity, Ph.D.
Examination Committee Member

David James, Ph.D.
Examination Committee Member

Spencer Steinberg, Ph.D.
Graduate College Faculty Representative

ABSTRACT

by

John Michael Gonzales

Dr. Jacimaria Batista, Examination Committee Chair
Professor, Department of Civil and Environmental Engineering and Construction
University of Nevada, Las Vegas

The use of cerium chloride (CeCl_3) to remove fluoride and phosphate from waters is addressed in this study. High concentrations of fluoride exist in groundwater especially in developing countries. Consumption drinking water containing high levels of fluoride can lead to serious cases of dental and skeletal fluorosis. Current defluoridation technologies are limited, especially for high levels of fluoride, and are expensive. Industrial wastewaters contribute to the highest fluoride contamination in the world. With the increasing production of electronic materials, the global fluoride concentration and fluoride-contaminated waters have grown tremendously. Excessive discharge of phosphate into the environment promotes eutrophication of lakes and rivers. The major sources of phosphate pollution are agricultural and urban runoff and domestic wastewater discharges. Cerium chloride, a newly available coagulant is expected to remove both fluoride and phosphate from waters A commercially available cerium chloride e (i.e. Sorbx-100) which is a non-hazardous rare-earth salt solution developed for faster coagulation and flocculation of phosphate in wastewater has been recently made available(Molycorp Minerals Incorporated, n.d.). The objectives of this research are to determine the efficiency efficacy of cerium chloride in removing fluoride and phosphate from waters. Batch jar testing was performed to evaluate fluoride removal under different conditions. Column testing was used to test the phosphate removal efficiency of various

media impregnated with cerium chloride Batch tests were used to support central composite design (CCD) model to evaluate the impact of major parameters (e.g. fluoride concentration, pH, and cerium dose) on the removal of fluoride from industrial wastewater. In addition, batch tests were also used to investigate the interference of competing ions on the removal of fluoride using cerium chloride.

The CCD model achieved an R-squared = 0.8615 and adjusted R-squared = 0.7368. The model was deemed to be statistically significant. The results showed that the highest removal (> 90%) was achieved at pH of 4.75 at cerium dose of 25 mM, regardless fluoride concentration. The results revealed that sulfate and phosphate have a positive impact on fluoride removal. Bicarbonate was shown to have as a negative impact on fluoride removal. For an actual industrial wastewater containing fluoride and with high alkalinity, no fluoride removal was observed with addition of cerium chloride. The observed fluoride removals can be attributed to two mechanisms: direction precipitation of cerium fluoride, and adsorption of fluoride ions and fluoride complexes onto the surfaces of cerium hydroxides and/or cerium carbonate. Impregnation of various filter media with cerium chloride and using various techniques was proven unsuccessful for phosphate ($\text{PO}_4^{-3}\text{-P}$) removal. Analysis of the cerium on the column effluent samples showed cerium leaching out of the media. Therefore, all methods for preparing impregnated media were ineffective.

ACKNOWLEDGEMENTS

First and foremost, I would like to thank God Almighty for giving me this opportunity. Second, I would like to thank my parents, my sister and brother for their unconditional love and undying support throughout my undergraduate and graduate studies. Third, I would like to thank my committee members, Dr. Gerrity, Dr. James, and Dr. Steinberg for their valuable feedbacks throughout this endeavor. Fourth, I would like to thank my friends, Robert, Mike, Mark, Ashley, Greg, Sichu, Joao, and Henrique for spending their time with me and accommodating me in their lives. I would also to thank all the new friends I made through these years. Fifth, I would like to thank the research and development department at Molycorp, Inc., especially Mr. Joey Lupo, Dr. Mason Haneline, and Dr. Carol Landi for their support and entrusting me with the research and executive office at Molycorp, Inc.

Last but not the least, I would like to acknowledge and greatly thank Dr. Jaci Batista for her faith, trust, guidance, and encouragement through this project. Without her support, I wouldn't be here. And, thank you very much for trusting me and providing me the knowledge necessary during my undergraduate and graduate studies.

TABLE OF CONTENTS

ABSTRACT.....	iii
ACKNOWLEDGEMENTS.....	v
LIST OF TABLES.....	ix
LIST OF FIGURES.....	x
LIST OF EQUATIONS.....	xii
CHAPTER 1: INTRODUCTION AND OBJECTIVES.....	1
CHAPTER 2: LITERATURE REVIEW.....	6
2.1. Fluoride in Natural and Industrial Waters.....	6
2.1.1. Occurrence of Fluoride.....	6
2.1.2. Health Concerns of Fluoride.....	9
2.1.3. Fluoride Removal Technologies.....	11
2.1.3.1. Fluoride Removal Using Common Coagulants.....	11
2.1.3.2. Adsorption and Ion-Exchange.....	11
2.1.3.3. Electrochemical Process.....	16
2.1.3.4. Membrane Processes.....	17
2.2. Phosphate in Wastewater.....	18
2.2.1. Occurrence of Phosphate ($\text{PO}_4^{3-}\text{-P}$).....	18
2.2.2. Phosphate Removal Technologies.....	19
2.2.2.1. Precipitation Using Typical Coagulants.....	19
2.2.2.2. Enhanced Biological Phosphorus Removal (EBPR).....	19
2.3. Phosphate and Fluoride Removal using Typical Coagulants.....	20
2.4. Rare-Earth Elements as a New Coagulant.....	27
2.4.1. Background.....	27
2.5. Response Surface Methodology: Central Composite Design.....	34
CHAPTER 3: MATERIALS AND METHODS.....	38
3.1. Developing Central Composite Design (CCD).....	38
3.2. Experiments Based on the Central Composite Design (CCD).....	40
3.2.1. Batch Test for CCD Model.....	40
3.2.2. Batch Tests for Effect of pH, Cerium Dose, and Initial Fluoride Concentration.....	41
3.2.3. Batch Tests to Evaluate the Effect of Fluoride Concentration and Cerium Dose.....	43
3.2.4. Batch Tests to Evaluate the Effect of Bicarbonate and Cerium Dose.....	43
3.2.5. Batch Tests for Actual Industrial Wastewater.....	44
3.3. Media Impregnation and Column Testing for Phosphate Removal.....	44

3.3.1. Granular Activated Carbon and Anthracite Preparation	45
3.3.2. Column Testing with Impregnated Media for Phosphate (PO_4^{-3} as P) Removal	45
3.3.3. Modifications on Initial GAC Preparation and for Zeolite Preparation	48
3.4. Materials	50
3.4.1. Solutions	50
3.4.1.1. Synthetic Fluoride Wastewater	50
3.4.1.2. Synthetic Phosphate Water	50
3.4.1.3. Industrial Wastewater	51
3.4.1.4. Cerium Chloride Solution	51
3.4.2. Analytical Methods	52
3.4.2.1. pH Measurement	52
3.4.2.2. Orthophosphate, Nitrate, and Sulfate Analyses	52
3.4.2.3. Fluoride Analysis	53
3.4.2.4. Total Alkalinity as Bicarbonate	53
3.4.2.5. X-Ray Fluorescence (XRF) Detection	54
3.4.2.6. Trace Cerium Analysis	54
3.5. Quality Assurance and Quality Control	55
3.5.1. Quality Assurance	55
3.5.2. Quality Control Measures	55
CHAPTER 4: REMOVAL OF HIGH LEVELS OF FLUORIDE FROM WATERS USING CERIUM CHLORIDE	56
4.1. Batch Test Results for Central Composite Design	56
4.1.1. CCD Model Results	56
4.1.2. Contour Plot from CCD Model	65
4.2. Effect of pH and Cerium Dose on Fluoride Removal	70
4.3. Effect of Dose and Fluoride Concentration on Fluoride Removal	71
4.4. Impact of Competing Ions	73
4.5. Testing the Impact of Alkalinity on Fluoride Removal Using an Actual Fluoridated-Industrial Wastewater	86
CHAPTER 5: REMOVAL OF PHOSPHATE USING CERIUM CHLORIDE IMPREGNATED MEDIA	90
5.1. Adsorption of Impregnated Anthracite	92
5.2. Adsorption of Impregnated Natural Zeolite	93
5.3. Adsorption of Impregnated GAC	94
5.4. Results of XRF Analysis and Oxide Distribution	98
CHAPTER 6: CONCLUSIONS, IMPLICATIONS AND FUTURE WORK	100

6.1. Conclusion.....	100
6.2. Implications of the Research Results to the Treatment of Industrial Waters Contaminated with Fluoride	103
6.3. Future Work	104
REFERENCES	105
CURRICULUM VITAE.....	114

LIST OF TABLES

Table 1: Typical sources of fluoride in industrial wastewaters	8
Table 2: Health effects of varying fluoride concentrations in drinking water	10
Table 3: Common adsorbents for fluoride removal	13
Table 4: Adsorptive capacities for fluoride removal with the optimal pH levels	15
Table 5: Fluoride removal through precipitation using typical coagulants.....	27
Table 6: Common applications of highest weighted rare-earth elements	29
Table 7: Solubility products for various reactions of tri- and divalent metals.....	30
Table 8: Coded and un-coded levels of each factor for the Central Composite Design for fluoride removal – changing pH level, molar ratio, and fluoride concentration...	39
Table 9: Experimental matrix for the effect of pH, cerium dose, and fluoride concentration.....	42
Table 10: Experimental matrix to evaluate the effect of cerium dose and initial fluoride concentration.....	43
Table 11: Experimental matrix evaluate the effect of cerium dose and bicarbonate concentration.....	44
Table 12: Media Preparation for Column Testing Using Activated Carbon and Anthracite, and Natural Zeolite.....	46
Table 13: Industrial wastewater characteristics	51
Table 14: Experimental data points and response used in Central Composite Design with predicted fluoride removal	57
Table 15: Estimated regression coefficients of the quadratic model for the Central Composite Design model (1) for fluoride removal.....	59
Table 16: Percent differences between experimental responses and predicted responses	61
Table 17: Estimated regression coefficients of the quadratic model for the revised Central Composite Design model (2) for fluoride removal.....	62
Table 18: Comparison of R-squared and adjusted R-squared values	63
Table 19: Analysis of variance for the developed CCD model for fluoride removal efficiency.....	65
Table 20: Distribution of sulfate, fluoride and cerium for batch tests examining the impact of sulfate on fluoride removal by cerium chloride precipitation.....	79
Table 21: Distribution of phosphate, fluoride and cerium for batch tests examining the impact of phosphate on fluoride removal	80
Table 22: Media Preparation for Column Testing Using Activated Carbon and Anthracite, and Natural Zeolite.....	91

LIST OF FIGURES

Figure 1: Electro-coagulation process typically with aluminum or iron cathode (+) and anode (-) for industrial treatment (Meas et al., 2010)	16
Figure 2: Enhance biological phosphate removal process. Illustration adapted from (Greaves et al., 1999; Stratflul et al., 1999)	20
Figure 3: Removal mechanisms of particulate matter during coagulation process. Illustration adapted from (Sillanpaa & Matilaninen, 2014).....	21
Figure 4: Media preparation with different reactants. a) virgin GAC; b) GAC with KOH and Sorbx-100; c) GAC after furnace dry at 400 °C; d) virgin anthracite; e) anthracite with KOH and Sorbx-100; f) anthracite after furnace dry at 400 °C. ..	47
Figure 5: Media preparation with modified media preparation with 0.4 M SORBX-100 5% (w/w) with zeolite. a) virgin zeolite; b) zeolite with Sorbx-100 anthracite after furnace dry at 600 °C	48
Figure 6: Media preparation with modified media preparation with 0.4 M Sorbx-100 5% (w/w) with activated carbon. a) virgin activated carbon; b) activated carbon with Sorbx-100 anthracite after furnace dry at 600 °C	49
Figure 7: Modified column design and preparation set-up. a) virgin set-up (left) and modified zeolite (right) with HRT of 1.2 min; b) modified activated carbon (left) and modified zeolite (right) at HRT of 2.2 min.	49
Figure 8: Contour plot of predicted fluoride removal efficiency as a function of initial fluoride concentration at cerium dose of 12.50 mM and 1% salinity	67
Figure 9: Contour plot of predicted fluoride removal efficiency as a function of initial fluoride concentration at cerium dose of 25.0 mM and 1% salinity	68
Figure 10: Contour plot of predicted fluoride removal efficiency as a function of initial fluoride concentration at pH level of 4.75 and % salinity	69
Figure 11: Fluoride removal efficiency as a function of pH and differential cerium dose (6.25, 12.5, and 25 mM), and with 1% salinity	70
Figure 12: Fluoride removal efficiency as a function of Ce/F molar ratio and differential initial fluoride concentrations with 1% salinity, sulfate concentration of 20 mg/L, and final pH of 4.79 ± 0.24	72
Figure 13: Fluoride and sulfate removal as a function of increasing initial sulfate concentration at initial fluoride concentration of 961 mg/L, molar ratio Ce/F of 0.33, and 1% salinity	74
Figure 14: Fluoride and phosphate removal as a function of increasing initial phosphate concentration at initial fluoride concentration of 991 mg/L, molar ratio Ce/F of 0.33, and 1% salinity	77
Figure 15: Fluoride removal as a function of increasing nitrogen concentration at an initial fluoride concentration of 1,001 mg/L, molar ratio Ce/F of 0.33, and 1% salinity	81

Figure 16: Effect of bicarbonate on fluoride removal with an initial fluoride concentration of 974 mg/L and Ce/F ratio of 0.33 and with initial bicarbonate concentrations from 50 to 1250 mg/L as HCO_3^{-1}	83
Figure 17: Effect of bicarbonate on fluoride removal with an initial fluoride concentration of 952 mg/L and Ce/F ratio of 0.33 and with initial bicarbonate concentrations from 500 to 8,900 mg/L as HCO_3^{-1}	83
Figure 18: Fluoride removal as a function of Ce/F molar ratio and varying initial alkalinities, with constant initial fluoride concentration, and 1% salinity	84
Figure 19: Final pH solution as a function of Ce/F molar ratio and varying initial alkalinities, with constant initial fluoride concentration, and 1% salinity	85
Figure 20: Sludge production with increasing cerium dose on SCS solution, with initial fluoride concentration 41 mg/L	87
Figure 21: Sludge production and distribution, as a function of cerium dose (12.5, 12, 50, 100, and 200 mM).	88
Figure 22: Fluoride removal efficiency as a function of cerium dose, with an initial fluoride concentration of 41 mg/L	88
Figure 23: Relationship between C/Co and bed volumes passed (anthracite) with feed concentration (Co) of 3 ppm PO_4^{-3} -P (C=effluent concentration, Co=influent/feed concentration). The column was then run with an average hydraulic retention time of 0.60 to 1.0 minute	92
Figure 24: Relationship between C/Co and bed volumes passed (modified zeolite preparation) with feed concentration (Co) of 3 ppm PO_4^{-3} -P (C=effluent concentration, Co=influent/feed concentration).	94
Figure 25: Relationship between C/Co and bed volumes passed (GAC) with feed concentration (Co) of 3 ppm PO_4^{-3} -P (C=effluent concentration, Co=influent/feed concentration).The column was then run with an average hydraulic retention time of 0.60 to 1.2 (#5) minutes.	95
Figure 26: Tracer cerium analysis for modified GAC preparation (#5) as a function of phosphate (PO_4^{-3} -P) remaining	97
Figure 27: XRF analysis for all GAC preparation and identification of metal oxides on impregnated GAC	99

LIST OF EQUATIONS

Equation 1: Reaction in electro-coagulation using aluminum anodes and the formation of aluminum hydroxides (Meas et al., 2010).....	16
Equation 2: a) Phosphate precipitation using aluminum (e.g. aluminum sulfate) salts; (b) phosphate precipitation using iron (e.g. ferric chloride) salts.....	22
Equation 3: Metal hydroxide formations for co-precipitation and adsorption of phosphates - (a) aluminum salt and (b) iron salts. Equation adapted from (MWH Global, 2012).	22
Equation 4: Phosphate precipitation using metal salts with other constituent considerations – where r values are 1.6 for iron salts, and 0.80 for aluminum salts. Equation adapted from (Metcalf & Eddy, 2014)	23
Equation 5: Fluoride precipitation reactions. (a) Fluoride precipitation using aluminum salts, (b) magnesium salts, and (c) calcium salts.	24
Equation 6: Fluoride precipitation with aluminum salt - (a) co-precipitation and (b) adsorption. Equation adapted from (Hu et al., 2005).....	25
Equation 7: Formation of metal hydroxides and the acidification of solution based on the stoichiometric equation. (a) Reaction of aluminum sulfate when added to water; (b) reaction of ferric chloride when added to water.....	25
Equation 8: Corresponding reactions for adding (a) caustic soda and (b) lime to negate pH decrease and increase alkalinity	26
Equation 9: Stoichiometric equation of cerium to (a) fluoride and (b) phosphate. Lanthanum molar ratio equation is similar of that cerium formation.	31
Equation 10: Central Composite design equation using a second-order model (i.e. quadratic model)	35
Equation 11: Equation to calculate halfway points for the coded and uncoded levels.	40
Equation 12: Stock solution calculation for cerium chloride solution. (a) Conversion of weigh-to-weight ratio to weight-to-volume. (b) to (c) Conversion of concentration to molar ratio as cerium (III).....	52
Equation 13: Total alkalinity measurement and calculation as calcium carbonate	53
Equation 14: Stoichiometric equation of calcium carbonate with addition of water, and carbon dioxide to calcium bicarbonate.	53
Equation 15: Conversion of alkalinity as calcium carbonate (mg/L) to alkalinity as bicarbonate (mg/L).....	54
Equation 16: Predicted surface response equation for the CCD model for fluoride removal efficiency using the uncoded units.....	59
Equation 17: Predicted surface response equation for the CCD model (2) for fluoride removal.....	63
Equation 18: Complex formation of lanthanides (expressed as Ln) with sulfate and then with a fluoride ion (Haas et al., 1995)	75

Equation 19: Equation for lanthanide complexes with phosphate and with fluoride in natural waters (Haas et al., 1995) 78

CHAPTER 1: INTRODUCTION AND OBJECTIVES

This research focuses on the use of a new coagulant, cerium chloride (i.e. Sorbx-100) to remove fluoride and phosphate from waters. Cerium chloride has recently become commercially available in the United States, due to the mining of rare-earth ores in Mountain Pass, at the California/Nevada Border. Rare-earth chlorides, particularly cerium chloride, are one of the useful by-products of rare-earth mining. Rare-earth elements (REE) – commonly known as lanthanides – consist of lanthanum to lutetium (atomic number from 57 to 71) including yttrium (atomic number of 39). Cerium is the most abundant rare-earth element on earth's crust and greater in abundance compared to copper or lead (Castor & Hedrick, n.d.; Bleiwas & Gambogi, 2013).

Fluoride can be found naturally in waters or it can be added – artificial fluoridation for teeth health concerns. A community can be exposed to fluoride primarily from drinking water, food, dental products and various forms of pesticides. The greatest source of non-dietary requirement of fluoride is through dental products, primarily from toothpaste (National Research Council, 2006). Fluoride is a naturally occurring ion on the earth's crust with typical groundwater concentrations ranging from 0 mg/L to 41 mg/L (Ayoob & Gupta, 2006; Vithanage & Bhattacharya, 2015) and can go as high up to 205 mg/L groundwater, particularly in Ethiopia (National Research Council, 2006; Vithanage & Bhattacharya, 2015). In recent studies, it has been found that high concentrations of fluoride exists in groundwater, especially in developing countries such as India, China, and some parts of Southeast Asia (Mohapatra et al., 2009) where the potential implementation of treatment technologies is limited by cost. Endemic fluorosis

has been devastating southern and northern India. Tanzania, Kenya, Uganda, Ethiopia, and parts of Africa are also greatly affected because of limited resources and treatment technologies (McGill, 1995). The U.S. EPA has established a drinking water MCL (maximum contaminant level) of 4 mg/L of fluoride in waters; in the State of California the MCL is 2 mg/L. With the continuing stringent contaminant goals for drinking water for fluoride, it is necessary to find effective treatment technologies, particularly for countries limited by treatment and costs.

Industrial wastewaters contribute to the highest fluoride contamination in the world. With the increasing production of electronic materials, the global fluoride concentration and fluoride-contaminated waters have grown tremendously. The major contributors of fluoride contaminated wastewaters are semiconductor manufacturers, and industrial plants specializing in photovoltaic materials, plastics and textiles (Mohapatra et al., 2009). Hydrofluoric acid solutions are typically used as etchant for metal processing manufacturers. With the decreasing demands for hydro-fluorocarbon as etching agents, the demand for HF will continuously increase as well as the need for electronic materials (Kirschner, 2005). With the international increase of electronic materials use, the World Health Organization established an international maximum concentration goal of 1.5 mg/L, primarily designed for health benefits. Therefore, in the case of industrial wastewater with high fluoride concentrations (e.g. 500-1,000 mg/L), it is necessary to find technologies that are able to remove a very high percentage of the fluoride present.

The removal of fluoride can be accomplished by several technologies; the most acceptable and widely used technologies for fluoride removal include adsorption onto activated alumina (Feenstra et al., 2007; Tomar & Kumar, 2013; Renuka & Pushpanjali,

2013), ion-exchange resins(Renuka & Pushpanjali, 2013; Tomar & Kumar, 2013), electrochemical processes and membrane techniques including reverse osmosis, and electro-dialysis (Na & Park, 2010), and precipitation using aluminum salts or lime (Renuka & Pushpanjali, 2013; Tomar & Kumar, 2013).

Phosphate is a well-known contaminant of waters that promote eutrophication of rivers and lakes. Major sources of phosphate include agriculture runoff and domestic wastewater treatment plant discharges (Litke, 1999). The vast majority of wastewater treatment plants in the U.S. are required by law to remove phosphate from their wastewater before it can be discharged to rivers and lakes. The amount of phosphate to be removed depends on the water quality standards established for the body of water where the treated wastewater effluent is discharged. Typically, most plants have to remove phosphate to 1 mg/L (Litke, 1999; Jenkins et al., 1971; Parsons & Smith, 2008). Several plants, however, have to remove phosphate ($\text{PO}_4^{-3}\text{-P}$) to below 1 mg/L. In Southern Nevada, local wastewater treatment plants are required to remove phosphate ($\text{PO}_4^{-3}\text{-P}$) below 0.25 mg/L before discharging to Lake Mead.

Phosphate can be removed biologically and through chemical addition (Metcalf & Eddy, 2014; Jenkins et al., 1971). Enhanced biological phosphorus removal (EBPR) is currently practiced in many wastewater treatment plants (Parsons & Smith, 2008). It is less expensive and generates less sludge than chemical phosphate removal. However, EBPR is not very effective in colder climates where sufficient volatile fatty acids (VFAs) can be generated to sustain the process. On the other hand, chemical phosphate removal can be used widely (Greaves et al., 1999; Parsons & Smith, 2008). A drawback of chemical phosphate removal is the chemical cost and the large amount of sludge

produced and its associated disposal cost (Parsons & Smith, 2008). Notwithstanding, coagulation/precipitation, using various coagulants, is the most used technology for phosphate from wastewater. Typical coagulants used for phosphate removal are aluminum sulfate, ferric sulfate, ferric chloride, and lime. A phosphate removal efficiency of between 80 to 90 % can be achieved with chemical precipitation (Metcalf & Eddy, 2014; Thistleton et al., 2002; Parsons & Smith, 2008). Even in plants where EBPR is practiced, there is still need to use some amount of coagulant. In these plants, coagulants are added before filtration to add the removal of solids, which in EBPR are loaded with polyphosphate. Coagulants are also added to treat return streams (i.e. from centrifuges) where secondary phosphate release may occur (Morse et al., 1998). Furthermore, coagulants are also added before digestion to prevent the formation of struvite ($MgNH_4PO_4 \cdot 6H_2O$), a scale that can form in EBPR systems that use sludge digestion (Parsons & Smith, 2008).

Both fluoride and phosphate can be removed by coagulation/precipitation. For fluoride removal, typical coagulants used are aluminum sulfate and lime. Lime is the most common chemical used for fluoride removal from industrial wastewaters with 90 % removal efficiency. However, lime increases the total alkalinity of the wastewater. Fluoride removal using aluminum sulfate is independent of pH. However, optimal pH with lime for fluoride precipitation occurs at 6.50. Excluding coagulation method, all other technologies – adsorption, electrochemical process, and membrane process – requires pH adjustment. However, the presence of sulfate, bicarbonate, and phosphate decreases the effectiveness of these technologies for fluoride removal (Drouiche et al., 2008). This research aims to investigate the effectiveness of cerium chloride precipitation

as a treatment technology to remove fluoride and phosphate from waters. While the research on fluoride focus on using coagulation/precipitation, the research on phosphate removal focus on impregnating media with cerium chloride for use in wastewater filters. The removal of phosphate from wastewater by coagulation using cerium chloride is the subject of the thesis of another member of our research group.

The specific objectives of this research are:

1. To investigate the removal of fluoride from industrial wastewater using cerium chloride as the coagulant
2. To evaluate the removal of phosphate from wastewaters using various media impregnated with cerium chloride.

CHAPTER 2: LITERATURE REVIEW

2.1. Fluoride in Natural and Industrial Waters

2.1.1. Occurrence of Fluoride

Fluoride can be found in natural waters or as an additive compound – artificial fluoridation for health concerns. However, some communities are exposed to fluoride primarily from drinking water, food, dental products and forms of pesticides. The greatest source of non-dietary requirement of fluoride is through dental products, primarily from toothpaste. Other contamination sources of fluoride include some pharmaceuticals, and atmospheric contributions from pesticides manufacturers (National Research Council, 2006).

Fluoride (F^-) is the ionic form of the fluorine element with a molecular weight of 19 grams per mole. Fluoride is a naturally occurring ion on the earth's crust, and typical groundwater concentrations range from 0 mg/L to 41 mg/L (Ayoob & Gupta, 2006; Vithanage & Bhattacharya, 2015) and can go as high up to 205 mg/L groundwater, particularly in Ethiopia (National Research Council, 2006; Vithanage & Bhattacharya, 2015).

Fluoride is typically found in soil, water and in trace amounts in plant. Fluoride species occur mainly as sellaite (MgF_2), fluorspar (CaF_2), cryollite (Na_3AlF_6) and fluoroapatite [$3Ca_3(PO_4)_2 \cdot Ca(F,Cl)_2$] (Mohapatra et al., 2009). Fluorspar can be found in sedimentary rocks and cryollite can be found from igneous rocks. Fluoride concentration is controlled by pH, total dissolved solids (TDS), hydroxyl and carbonate alkalinity, and

rock materials among other things. In the circum-neutral pH range from 6.50 to 8.50, fluorosilicates naturally dissociate into fluoride ion, hydrofluoric acid (HF), and silicic acid ($\text{Si}(\text{OH})_4$). Fluoride ions and fluoride compounds form a reversible reaction to and from hydrofluoric acid (HF), and also form complexes with aluminum (National Research Council, 2006). Hydrofluoric acid (HF) is a weak acid with a pKa value of 3.40 and that would make it strong.

In recent years, the industrial production of electronic materials has contributed to the increase in global fluoride concentration and contamination of waters. The major contributors of fluoride contaminated wastewaters are semiconductor manufacturers, and industrial plants manufacturing hydrofluoric acid, photovoltaic materials, plastics, and textiles (Shen et al., 2003). These major contributors produce and discharge fluoride contaminated wastewaters that far exceed the maximum contaminant level (MCL) of 4 mg/L. Table 1 enumerates the typical fluoride contaminated wastewaters and typical fluoride concentrations found in these waters:

Table 1: Typical sources of fluoride in industrial wastewaters

Type of wastewater	Fluoride (mg/L)	pH range	Reference
Semiconductor fabrication	217	2.18	(Drouiche et al., 2008)
	83	6.38	(Zhang et al., 2010)
	350 – 1000	-	(Gurtubay et al., 2010)
	743	3.5	(Huang & Liu, 1999)
	500 - 2000	-	(Drouiche et al., 2008)
Steel fabrication industry	5 - 35	7	(Khatibikamal et al., 2010)
	40 – 65	8.8-9.3	(Gurtubay et al., 2010)
Aluminum process industry	80 – 90	-	(Zhang et al., 2010)
Photovoltaic energy manufacturers	217	2.18	(Drouiche et al., 2008)
	1000	-	(Drouiche et al., 2008)
	500 – 2000	-	(Gurtubay et al., 2010)
Beryllium extraction plants	>1000	-	(Gurtubay et al., 2010)

Fluoride-contaminated wastewaters come from using hydrofluoric acid (HF) as an etchant or cleaning agent for semiconductors, photovoltaic plates, and for metal-plating or metal manufacturing industries as listed above. HF acid is also added as a chemical catalyst in the alkalytion process in the oil-processing. Alkalytion increases the octane levels in gasoline. Furthermore, the increased demand for HF acid is due to the need to replace hydrofluorocarbons (HCFCs) as etching solutions for the metal industry. The continued growth in all aspects of electronic production will show a furthering spike in the demand of HF acid solutions (Kirschner, 2005), and thereby increasing fluoride contaminated wastewater.

2.1.2. Health Concerns of Fluoride

The Safe Drinking Water Act enacted by the U.S. Environmental Protection Agency (EPA) established maximum contaminant level (MCL) for various contaminants for public drinking-water systems. The U.S. EPA established the maximum contaminant level goals (MCLGs) and (MCLs) that protect people from potential of adverse health effects from consuming fluoride-containing waters (National Research Council, 2006). MCLGs are not regulated; however, MCLs are enforced based on the allowable and established analytical methods. The MCLG established for fluoride is 4 milligrams per liter (mg/L) and a secondary MCL (SMCL) of 2 mg/L. However, for fluoride, the MCLG and MCL is the same. Under the U.S. Public Health Service for water fluoridation, an optimal range between 0.70 to 1.40 mg/L for cavities prevention and control enamel fluorosis. Approximately 162 million people in the United States consume artificially fluoridated drinking water (National Research Council, 2006).

However, excessive ingestion of fluoride through water is a serious health hazard that could cause dental and skeletal fluorosis. More than 260 million people internationally consume more than 1 mg/L of fluoride (Jagtap et al., 2012). Fluorosis is classified into industrial and endemic. Industrial fluorosis is defined by prolonged exposure to high fluoride atmospheric concentrations through aluminum and steel industries. Endemic fluorosis occurs through the consumption of fluoride-contaminated drinking water. In recent studies, it has been found that high concentrations of fluoride exists in groundwater, especially in India, China, and some parts of Southeast Asia (Mohapatra et al., 2009). Endemic fluorosis has been devastating southern and

northern India, as well. Tanzania, Kenya, Uganda, Ethiopia, and parts of Africa are also greatly affected (McGill, 1995).

Upon ingestion, fluoride infiltrates the bones and increases the total bone mass. Continual ingestion of fluoride produces ossification of the bones and ligaments (McGill, 1995), bone deterioration and a severe case of osteoporosis (Mandinic et al., 2010). More than 99% of human bones contain fluoride (National Research Council, 2006). Table 2 lists the fluoride concentrations corresponding to the health benefits and effects in drinking water.

Table 2: Health effects of varying fluoride concentrations in drinking water

Fluoride Concentration (mg/L)	Health Effects
No fluoride	Limited growth
0 to 0.5 mg/L	Dental caries/cavities
0.5 to 1.5 mg/L	Tooth decay prevention
1.5 to 4.0	Dental fluorosis
4 to 10 mg/L	Dental and skeletal fluorosis
More than 10 mg/L	Crippling fluorosis

Adapted from (Edmunds & Smedley, 2013)

In the study conducted by the National Research Council on behalf of the U.S. EPA, the research committee unanimously identified the risk of fluoride in public drinking water. The study recommended a lower MCGL (MCGL=MCL) of less than 4 mg/L to prevent developing severe enamel and skeletal fluorosis in children (National Research Council, 2006).

2.1.3. Fluoride Removal Technologies

Defluoridation, a water treatment process, reduces the fluoride level to the permissible concentration for drinking water (Mohapatra et al., 2009). The most acceptable and widely used defluoridation techniques include precipitation and coagulation, adsorption, and membrane techniques including reverse osmosis, and electro-dialysis (Na & Park, 2010).

2.1.3.1. Fluoride Removal Using Common Coagulants

Coagulation and precipitation methods are the addition of chemicals and the subsequent precipitation of insoluble materials. Aluminum sulfate, lime, poly-aluminum chloride, and poly-aluminum -hydroxyl sulfate are the most frequent coagulation aids to precipitate insoluble fluoride (Renuka & Pushpanjali, 2013). Chemical removal of fluoride will be further discussed in the subsequent sections.

2.1.3.2. Adsorption and Ion-Exchange

Adsorption techniques for fluoride removal are used for polishing step. Adsorbents include activated alumina, modified activated carbon, hydroxyapatite, plant carbon, zeolites, bone, bone char, clay pots and fluoride-specific ion-exchange resin (Na & Park, 2010). Synthetic resins are readily available for fluoride removal using ion-exchange processes. Adsorption technology provides greater accessibility of adsorbents, lower costs compared to chemical precipitation, simplicity of operation, and a wider range of adsorbents as mentioned earlier (Habuda-Stanic et al., 2014; Mohapatra et al.,

2009). The adsorption mechanisms of fluoride in water include three phases – fluoride mass transfer from bulk liquid to the surface of the adsorbent, adsorption of fluorides on the adsorbent surfaces, and transfer of fluorides onto the porous adsorbents (Mohapatra et al., 2009; Fan et al., 2003)

Adsorption is effective in reducing fluoride concentrations, but in general, the adsorptive mechanism for fluoride has low selectivity, making the process less effective. In recent studies, impregnations of adsorbents with rare-earth solutions have shown a significant increase in fluoride selectivity and fluoride adsorption (Loganathan et al., 2013).

Studies have shown that to increase the adsorptive capacity of alumina, they can be impregnated with rare-earth solutions, typically with lanthanum or yttrium (Tomar & Kumar, 2013). However, fluoride removal efficiency through adsorption depends on the initial fluoride concentration, pH level, temperature, empty-bed contact time, and amount of adsorbent used (Bhatnagar et al., 2011; Fan et al., 2003; Tomar & Kumar, 2013).

Commonly used adsorbents for fluoride removal under fixed-bed, required dose, interferences, and optimal operating pH are listed in Table 3:

Table 3: Common adsorbents for fluoride removal

Adsorbent	Removal	Adsorption Capacity	Interference	Optimal pH
Activated carbon	≥ 90%	Variable	Many	< 3
Plant carbon	≥ 90%	300 mg F/kg	-	-
Defluoron 2	-	360 g F/m ³	Alkalinity	
Zeolite	≥ 90%	100 mg F/kg	-	-
Clay pots	60-70%	80 mg F/kg	-	Non-specific
Activated alumina	80-95%	100mg-F/mg-alumina	Alkalinity	5.5
Bone	-	900 g F/m ³	Arsenic	>7
Bone char	-	1,000 g F/m ³	Arsenic	>7

Adapted from (Feenstra et al., 2007; Tomar & Kumar, 2013; Renuka & Pushpanjali, 2013; Edmunds & Smedley, 2013)

Loganathan et al. (2013) identified that pH levels, co-existing anions, temperature and adsorption kinetics influences the adsorption mechanism the most. The study identified that pH is the most influential factor in fluoride removal by adsorption. Fluoride adsorption had the maximum removal at a pH range of 4 to 8. However, this removal decreases at very low pH and at very high pH. At a pH below 4, fluoride reacts with the hydrogen ion and produces a weak hydrofluoric (HF) acid. At pH 7 to 8, the removal slightly decreases because of carbonate and hydroxyl alkalinity, bicarbonate, and silicate ions. Therefore, the efficacy of fluoride adsorption is highest at circum-neutral pH around 6.5 to 8.5 (Loganathan et al., 2013; Fan et al., 2003; Bhatnagar et al., 2011). In addition to pH, co-existing and competing anions affect the adsorption mechanism. Interfering anions include phosphate (PO₄⁻³), chloride (Cl⁻), sulfate (SO₄⁻²), bromide (Br⁻) and nitrate (NO₃⁻). The adsorption process decreases at lower temperatures (5°C to 10°C). At temperatures greater than 25°C, the adsorption process increases. However, at higher

temperatures at around 50°C, there are no changes in fluoride adsorption. The adsorption rate increases with increased adsorbent dose and at low initial fluoride concentration.

Commonly, ion exchange resins are classified either as cation or anion based resins (Kumar & Jain, 2013). Strong-base ion exchange resins and chloride and hydroxide forms are typically used for fluoride removal. Some of the available resins are Polyanion, Tul-sion A-27, Deacedite FF, Amberlite IRA 400, Lewatit MIH-59 and Amberlite XE-75 resins (Renuka & Pushpanjali, 2013). The fluoride capacity of available resins depends on the initial fluoride concentrations and competing anions in the water (Patil & Ingole, 2012). For example, Polyanion resins have a capacity of 862 mg fluoride/kg of resins and 1040 mg fluoride/mg of resins for waters with fluoride-concentration of 2.80 and 8.10 mg/L. Rao and Bhaskaran (1998) studied various aluminum salts, alumina, magnesium, lime, activated carbon, and sulphonated resins. The study observed that sulphonated resins were able to remove fluoride concentrations of 5 mg/L (Rao & Bhaskaran, 1998). Bhakuni (1970) studied the effectiveness of Lewatt S-100 resins with waters in fluoride concentrations of 4 mg/L and alkalinity concentration of 400 mg/L as CaCO₃. The study shows loss of fluoride capacity with increasing alkalinity concentration (Patil et al., 1970). Renuka and Pushpanjali (2013) also determined that sulfate (>100 mg/L) and bicarbonate (> 200 mg/L) in water reduced the resin capacity by more than 33 % (Renuka & Pushpanjali, 2013). Ion-exchange resin regeneration requires regeneration and large amount of regenerant. Fluoride removal with specialized ion-exchange resins produces brine solutions with extremely high fluoride concentrations (Feenstra et al., 2007). Defluoridation techniques through ion-exchange resins are complex and extremely expensive (Renuka & Pushpanjali, 2013).

Activated alumina is the most common and efficient fluoride adsorbent for fluoride-contaminated waters. Maximum fluoride uptake and removal was observed at pH 5.5- 6.5 with adsorptive capacity of 1,200 mg-F/m³ (Feenstra et al., 2007; Tomar & Kumar, 2013). However at acidic conditions, adsorption of fluoride was decreased. Langmuir and Freundlich isotherm models described fluoride removal through non-specific adsorption. Table 4 shows the adsorptive capacities of fluoride with activated alumina (Tomar & Kumar, 2013).

Table 4: Adsorptive capacities for fluoride removal with the optimal pH levels

Adsorbent	Adsorptive Capacity (mg-F/g-alumina)	pH	References
Acidic alumina	8.4	3.6 – 11.6	(Goswami & Purkait, 2012)
Activated alumina (α -Al ₂ O ₃)	88	5 – 6	(Bahena et al., 2002)
Activated alumina (Grade OA-25)	2	7	(Ghorai & Pant, 2004)

Data adapted from (Tomar & Kumar, 2013)

However, alkalinity and pH can highly impact fluoride removal by activated alumina. Regeneration solution from activated alumina contains significantly high fluoride concentrations (Feenstra et al., 2007). The literature indicates that for other coagulants. The presence of sulfate, bicarbonate, nitrate, and phosphate negatively impact fluoride removal. Therefore, it is necessary to investigate what other ions compete with fluoride removal when cerium chloride is used.

2.1.3.3. Electrochemical Process

The basic principle of electro-coagulation is the in situ generation of trivalent metal ions by electro-dissolution of sacrificial anodes, commonly aluminum or iron metal plates. At the optimal pH, hydroxide ions combine with the aluminum ions and allow for the formation and polymerization of aluminum hydroxides. Figure 1 shows the electro-coagulation process.

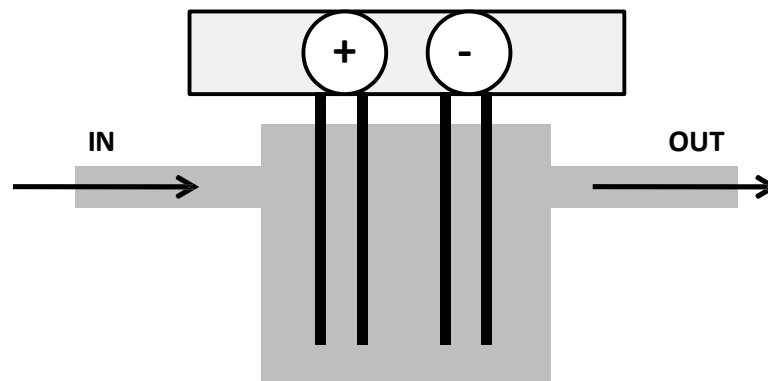
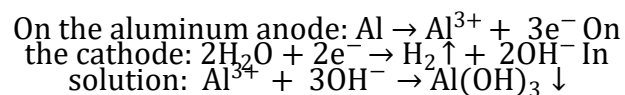


Figure 1: Electro-coagulation process typically with aluminum or iron cathode (+) and anode (-) for industrial treatment (Meas et al., 2010).

In electro-coagulation, the precipitates are removed through sedimentation or flotation process (Meas et al., 2010). The equation using aluminum anode plates is expressed as:



Equation 1: Reaction in electro-coagulation using aluminum anodes and the formation of aluminum hydroxides (Meas et al., 2010).

Electro-coagulation (EC) has been shown to be very effective in removing fluoride using aluminum electrode plates (Drouiche et al., 2012). Drouiche et al. (2012) investigated fluoride removal through electrochemical treatment with electro-coagulation for photovoltaic wastewaters. The study identified that some cations and anions interfered with fluoride removal in the photovoltaic wastewater. The presence of sulfate (SO_4^{-2}), bicarbonate (HCO_3^-), dihydrogen phosphate (H_2PO_4^-), reduced fluoride removal (Drouiche et al., 2012). In addition, Hu et al. (2005) identified that co-existing anions – sulfate, alkalinity, and phosphate – impacts fluoride removal using electro-coagulation. The study revealed that the interferences of these anions were mitigated by increasing the amount of calcium added to the solution (Hu et al., 2005). These results were also observed using electrochemical treatment to remove fluoride from photovoltaic manufacturing wastewaters as a polishing treatment.(Drouiche et al., 2008).

2.1.3.4. Membrane Processes

Membrane processes include reverse osmosis, nano-filtration, ultrafiltration, and microfiltration. In both membrane filtration and reverse osmosis processes, contaminated water is passed through a semi-permeable membrane and contaminants are left behind depending on the particle size and pressure on the membrane. Both membrane processes require lots of chemicals and produce brine solutions. However, both processes have no ion selectivity. In particular, reverse osmosis produces high fluoride residual for disposal (Loganathan et al., 2013). Clogging and scaling are also expected in a reverse osmosis system. However, reverse osmosis can achieved fluoride removal between 45 to 90%at Ph levels of 5.5 to 7.0(Loganathan et al., 2013; Vithanage & Bhattacharya, 2015).

Schneiter and Middlebrooks (1983) reported fluoride removal using reverse osmosis up to 59-67% at a pH of 6.40 (Schneiter & Middlebrooks, 1983).

Electrodialysis, particularly Donnan dialysis technique, is also an acceptable method for defluoridation of brackish water by passing of ions through membranes with an electric current (Loganathan et al., 2013; Vithanage & Bhattacharya, 2015).

Membrane processes for fluoride removal have high capital and maintenance costs, and are extremely prone to fouling. They require high expertise in operation and skillful operators (Vithanage & Bhattacharya, 2015).

2.2. Phosphate in Wastewater

2.2.1. Occurrence of Phosphate ($\text{PO}_4^{-3}\text{-P}$)

Phosphate can be present as either orthophosphate, polyphosphates, meta-phosphates, and as organophosphates. The presence of excess phosphate in any body of water can cause eutrophication (De Gregorio et al., 2011). Typical domestic wastewater would contain phosphate ($\text{PO}_4^{-3}\text{-P}$) concentrations from 3 mg/L to 11 mg/L (Metcalf & Eddy, 2014). Another source of phosphate in waters is agricultural and urban runoff (Parsons & Smith, 2008; Minton & Carlson, 1972)

2.2.2. Phosphate Removal Technologies

2.2.2.1. Precipitation Using Typical Coagulants

Phosphate can be removed from waters biologically or chemically. Normally, chemical precipitation of phosphate is achieved with the addition of multivalent metal coagulants. Typical multivalent metal ions used for phosphate precipitation include calcium, aluminum and iron salts (Metcalf & Eddy, 2014). Chemical removal of phosphate will be discussed in the subsequent sections (Litke, 1999; Jenkins et al., 1971; Parsons & Smith, 2008).

2.2.2.2. Enhanced Biological Phosphorus Removal (EBPR)

Phosphate removal is required for all wastewater treatment facility to reduce the risk of eutrophication and algal growth in receiving waters. Phosphate can be removed chemically (coagulant/precipitation) or biologically (enhanced biological phosphate removal) (Metcalf & Eddy, 2014). An effective EBPR treatment process can lead to 80 to 90 % phosphate ($\text{PO}_4^{-3}\text{-P}$) removal (Greaves et al., 1999) and can produce an effluent phosphate ($\text{PO}_4^{-3}\text{-P}$) less than 1 mg/L (Metcalf & Eddy, 2014). In EBPR process, polyphosphate accumulating organisms (PAOs) release phosphate under anaerobic conditions, and under aerobic conditions release phosphate (Greaves et al., 1999; Metcalf & Eddy, 2014).

Under anaerobic conditions (absence of oxygen and nitrate), PAOs take up volatile fatty acids (VFAs), such as butyrate, acetate, propionate and break down polyphosphate to release orthophosphate (soluble phosphate) for energy generation

(Greaves et al., 1999). The process then introduces significant soluble phosphate in the mixed liquor and converts large amounts of soluble VFAs to polyhydroalkanoates (PHAs) (Greaves et al., 1999; Metcalf & Eddy, 2014; Stratflul et al., 1999). Under aerobic conditions (presence of oxygen), PAOs consume and store soluble phosphate beyond the required phosphate for biomass production; when PAOs consume excess phosphate, the process is called -luxuryll uptake(Greaves et al., 1999; Stratflul et al., 1999). Thus, in a typical activated sludge process to treat wastewater, when EBPR is practiced, the sludge contains a high concentration of polyphosphate. By wasting the sludge during clarification, phosphate is then removed from the wastewater (Morse et al., 1998).

Figure 2 shows the EBPR process in a wastewater treatment facility.

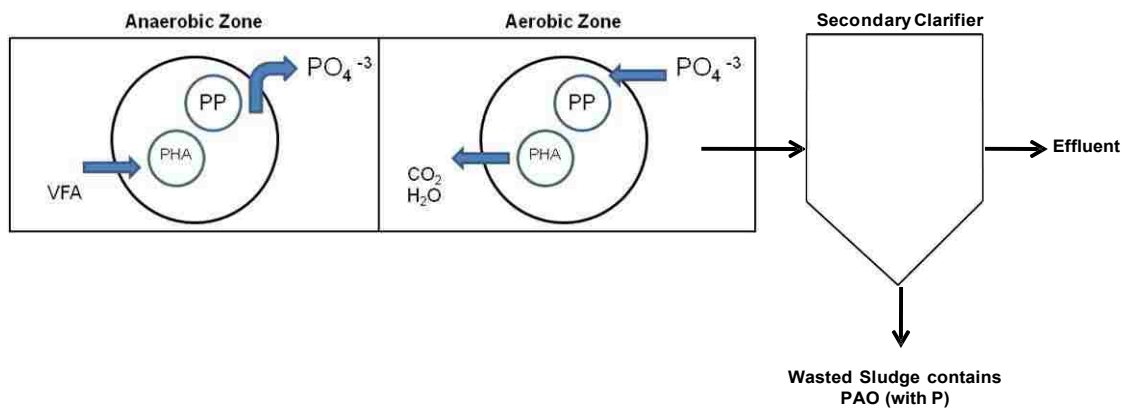


Figure 2: Enhance biological phosphate removal process. Illustration adapted from (Greaves et al., 1999; Stratflul et al., 1999).

2.3. Phosphate and Fluoride Removal using Typical Coagulants

Coagulation/precipitation is the process of adding chemical to water to destabilize particles and/or to form precipitates of target soluble contaminants. The mechanism of soluble contaminant removal by precipitation typically involves precipitate formation and adsorption of the soluble contaminants to the surface of the precipitate (MWH Global,

2012). In natural waters, coagulation/precipitation involves the reaction between coagulant chemicals, natural organic matter (NOM), and the surface of particles or precipitates to produce micro-particles. When these micro-particles collide, they form larger particles, called -flocs (Sillanpaa & Matilaninen, 2014) that precipitate out of water and can be removed by sedimentation and/or filtration (Johnson & Amirtharajah, 1983; Metcalf & Eddy, 2014). Coagulation has been used in water treatment primarily to reduce turbidity also to promote the precipitation of soluble contaminants (Sillanpaa & Matilaninen, 2014). The four primary mechanisms in particle removal and colloidal particles are enmeshment or entrapment, charge neutralization or destabilization, adsorption for inter-particle bridging (Johnson & Amirtharajah, 1983), and complexation or precipitation (Sillanpaa & Matilaninen, 2014). Figure 3 below provides the different coagulation mechanisms.

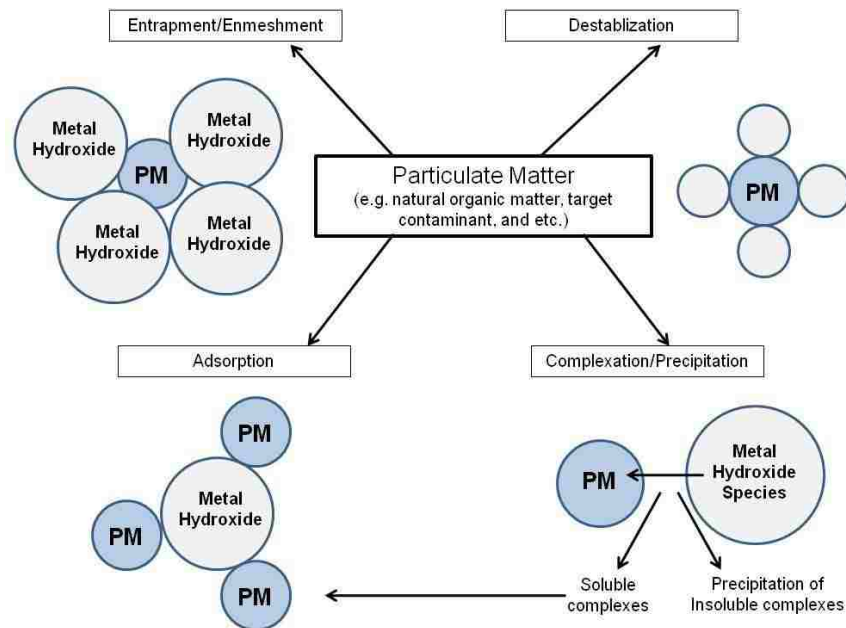
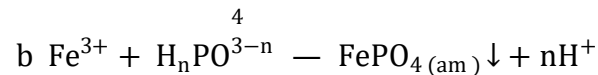
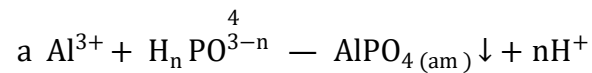


Figure 3: Removal mechanisms of particulate matter during coagulation process. Illustration adapted from (Sillanpaa & Matilaninen, 2014).

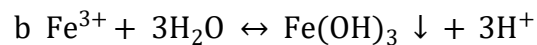
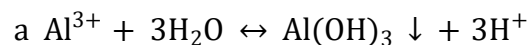
Aluminum sulfate (i.e. alum), ferric chloride, and lime are the most common coagulants used for coagulation/precipitation of phosphates (i.e. phosphate) in domestic wastewaters (MWH Global, 2012; Metcalf & Eddy, 2014).

These chemicals rapidly hydrolyze in waters and immediately remove phosphates. The reaction for alum and ferric chloride are shown in the following (Metcalf & Eddy, 2014):



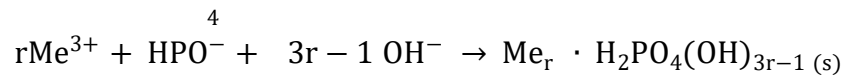
Equation 2: a) Phosphate precipitation using aluminum (e.g. aluminum sulfate) salts; (b) phosphate precipitation using iron (e.g. ferric chloride) salts.

When metal salts are added in excess, these metal ions can produce metal oxides or hydroxides (e.g. aluminum hydroxide and ferric hydroxide) to which soluble contaminants can be adsorbed. This reaction can occur both for phosphate and fluoride removal in any water. Phosphates can be removed through co-precipitation and adsorption onto metal hydroxides. The mechanisms can be expressed with the following equations:



Equation 3: Metal hydroxide formations for co-precipitation and adsorption of phosphates - (a) aluminum salt and (b) iron salts. Equation adapted from (MWH Global, 2012).

Aside from the aforementioned considerations, water quality parameters such as alkalinity, presence of other ions (e.g. sulfate, nitrate, fluoride, and etc.), and other trace elements found in wastewaters also impact phosphate precipitation. The equation below describes the potential reactions that can occur in waters (Metcalf & Eddy, 2014):



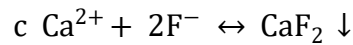
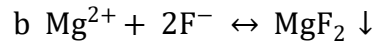
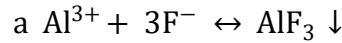
Equation 4: Phosphate precipitation using metal salts with other constituent considerations – where r values are 1.6 for iron salts, and 0.80 for aluminum salts. Equation adapted from (Metcalf & Eddy, 2014).

However, the precipitation of phosphates in waters is not generally simple. Competing ions and other reactions must be considered in order to remove phosphates or target contaminants from waters.

Besides using aluminum and iron salts, calcium can also be added to remove phosphates in water; calcium-based solutions such as quick lime or slurry lime are typically used for phosphate precipitation. Phosphate removal using lime requires large amounts of chemicals and produces more sludge compared to aluminum and iron salts (U.S. Environmental Protection Agency, 2000).

Coagulation/precipitation is also the most widely-used and well-established process in fluoride treatment. Typical coagulants used for fluoride coagulation/precipitation include alum (aluminum sulfate), gypsum and fluorite lime (Edmunds & Smedley, 2013), calcium oxide, calcium chloride (Edmunds & Smedley, 2013), magnesium oxide (Vithanage & Bhattacharya, 2015), and, sequential addition of alum and lime (i.e. Nalgonda technique) (Renuka & Pushpanjali, 2013; Vithanage

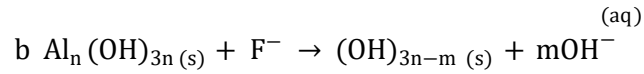
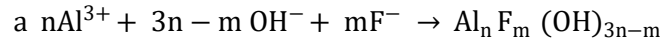
&Bhattacharya, 2015). The reaction for fluoride precipitation using aluminum-, calcium-, and magnesium-based salts are seen below:



Equation 5: Fluoride precipitation reactions. (a) Fluoride precipitation using aluminum salts, (b) magnesium salts, and (c) calcium salts.

Coagulation/precipitation can provide more than 90% fluoride removal, depending on the coagulant. Removal efficiencies are non-specific for fluoride removal; however, pH does make an impact on the solubility constants of the precipitates (Vithanage & Bhattacharya, 2015).

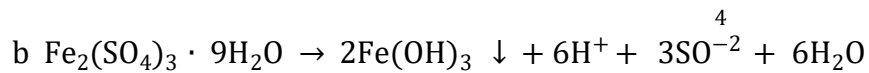
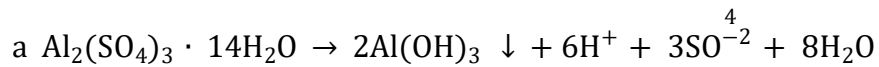
At high fluoride concentrations, lime precipitation is commonly used and is the least expensive way to remove fluoride and precipitate as calcium fluoride (CaF₂). However, this process can only reduce the fluoride concentration to 17 to 20 mg/L (Renuka & Pushpanjali, 2013; Edmunds & Smedley, 2013). The significant addition of lime results in higher alkalinity and hardness (Drouiche et al., 2008). Aluminum salts are also viable coagulants for fluoride removal. Co-precipitation or adsorption precipitation can occur when excess amount of aluminum salt is added to remove fluoride-containing solutions. Fluoride removal through aluminum co-precipitation and adsorption is expressed by the following equation.



Equation 6: Fluoride precipitation with aluminum salt - (a) co-precipitation and (b) adsorption. Equation adapted from (Hu et al., 2005)

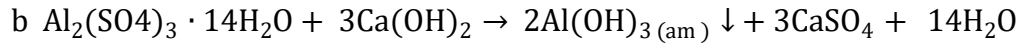
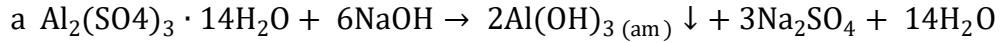
2.3.1. Effect of Dose, pH and Alkalinity for Phosphate and Fluoride Removal

Equation 7 describes the stoichiometric addition of alum or iron salt and the precipitation of metal hydroxides. When aluminum and iron salts are added to water, it immediately hydrolyzes and produces strong acids – sulfuric and hydrochloric acid; the reaction will lower the pH and will consume majority of the alkalinity. These reactions are expressed by the following equation:



Equation 7: Formation of metal hydroxides and the acidification of solution based on the stoichiometric equation. (a) Reaction of aluminum sulfate when added to water; (b) reaction of ferric chloride when added to water.

To reduce the effects of pH depression when strong acids are added, caustic soda (i.e. sodium hydroxide) or lime (i.e. calcium hydroxide) can be added to the water following the addition of coagulants (MWH Global, 2012; Metcalf & Eddy, 2014). The overall reaction of aluminum salt with the addition of alkalinity through caustic soda or lime can be expressed as:



Equation 8: Corresponding reactions for adding (a) caustic soda and (b) lime to negate pH decrease and increase alkalinity.

Phosphate precipitation with aluminum and iron salts is highly effective between the pH ranges of 6-8.5 (Mohammed & Shanshool, 2009). For calcium salts, the optimum pH was determined as greater than 10 (Mohammed & Shanshool, 2009). Other studies have identified that alum precipitation is effective between pH of 5.5 to 6.5 (Mohammed & Shanshool, 2009) and 6.50 to 7.50 (Ebeling et al., 2003); consequently, the optimum pH for iron salts is from 4.5 to 5.0 (Mohammed & Shanshool, 2009) and have identified pH from 4 to 11 (Ebeling et al., 2003).

Given the stoichiometric equation of metal ions to phosphates, phosphates can be removed given a 1:1 molar ratio (Metcalf & Eddy, 2014). However, it has been described that a 1.5 to 2 molar ratio is required for phosphate removal. A higher molar dose is required because of various competing ions – sulfate, nitrate, and carbonate - in wastewaters (Szabo et al., 2008). The amount of lime used for phosphate precipitation in wastewater is typically 1.4 to 1.50 times more than the alkalinity in water (Metcalf & Eddy, 2014). However, pH adjustment is necessary after lime addition.

Alum and lime have proven to be effective in fluoride removal in a wider pH range. The required doses for fluoride removal are listed in Table 5.

Table 5: Fluoride removal through precipitation using typical coagulants

Coagulant	Removal	Required Dose
Aluminum Sulfate (i.e. Alum)	$\geq 90 \%$	150 mg/mg F
Lime	$\geq 90 \%$	30 mg/mg F
Alum + Lime (i.e. Nalgonda)	70 - 90 %	(150 mg alum + 7 mg lime)/mg F
Gypsum + Fluorite	Not Listed	(5 mg gypsum + < 2mg fluorite)/mg F
Calcium Chloride	$\geq 90 \%$	3 mg CaCl ₂ /mg F

Adapted from (Feenstra et al., 2007; Tomar & Kumar, 2013; Renuka & Pushpanjali, 2013)

Alum and lime provides more than 90-% fluoride removal. However, the Nalgonda technique – addition of alum and lime – produces 70% to 90% fluoride removal efficiencies at the optimal pH of 6.5. Calcium chloride only works at an optimum pH of 6.5-8.0 for fluoride removal (Feenstra et al., 2007). Therefore, pH plays a significant role on fluoride removal using typical coagulants.

2.4. Rare-Earth Elements as a New Coagulant

2.4.1. Background

The use of rare-earth solutions – for precipitation of fluorides, phosphates, and oxides – has shown great potential in removing phosphate and fluoride in groundwater. Rare-earth based products such as lanthanum oxide (LaO₃), cerium chloride (CeCl₃), cerium oxide (CeO₃), lanthanum nitrate (La(NO₃)₃), and yttrium oxide (YtO₃) have been developed for water treatment. Rare-earth elements (REE) – commonly called lanthanides – consist of lanthanum to lutetium (atomic number from 57 to 71) including

yttrium (atomic number of 39). China produces more REEs than any other country. In 2001, China had an annual REE production of 80,600 metric tons of rare-earth oxide (REO), followed by United States (5,000 metric tons of REO equivalent), and Kyrgyzstan (3,800 metric tons of REO equivalent) (Castor & Hedrick, n.d.).

REEs are commonly used in automotive applications for pollution control, oil-refinery fluid cracking, pharmaceuticals, semiconductors and capacitors, aluminum alloys, and glass-polishing compounds (Castor & Hedrick, n.d.). In addition, increased growth is expected for REEs in lasers, fiber optics, and for automotive pollution catalysts (Castor & Hedrick, n.d.). These elements are also prevalent in high-tech consumer products such as cell phones, flat-screen televisions, computer monitors, external hard drives, and electric cars. REEs have also found use in various military products such as smart bombs, guided missiles, and other military munitions (Bleiwas & Gambogi, 2013). Table 6 lists the common applications of rare-earth elements with highest weight percent by oxide.

Table 6: Common applications of highest weighted rare-earth elements

Application	Rare-Earth Element				
	Yttrium	Lanthanum	Cerium	Prasedymium	Neodymium
Alloys	X	X	X	X	X
Batteries		X	X	X	X
Catalysts	X	X	X	X	X
Ceramics	X	X	X	X	X
Electronics	X	X	X	X	X
Fertilizers		X	X		X
Glass	X	X	X	X	X
Lamps	X	X	X	X	
Lasers	X	X	X	X	X
Magnets			X	X	X
Medical uses		X	X		X
Neutron adsorption	X		X		
Phosphors	X	X	X		

Table adapted from (Bleiwas & Gambogi, 2013)

Most of cerium based precipitates are insoluble, particularly cerium phosphate and cerium fluoride. Solubility products allow determining the formation of complexes, and the removal of ions from waters (Metcalf & Eddy, 2014). Solubility products for various possible reactions with tri- and divalent metal coagulants are listed in Table 7.

Table 7: Solubility products for various reactions of tri- and divalent metals

Compound	Formula	Solubility Product
Cerium (III) sulfate ^A	Ce ₂ (SO ₄) ₃ · 2H ₂ O	9.84
Aluminum (III) fluoride ^A	AlF ₃	0.670
Cerium (III) hydroxide ^A	Ce(OH) ₃	9.00 x10 ⁻⁰⁵
Calcium hydroxide ^B	Ca(OH) ₂	5.02 x10 ⁻⁰⁶
Calcium fluoride ^B	CaF ₃	3.45 x10 ⁻¹¹
Cerium (III) phosphate ^A	CePO ₄	7.43 x10 ⁻¹¹
Cerium (III) fluoride ^B	CeF ₃	8.00 x10 ⁻¹⁶
Iron (II) hydroxide ^B	Fe(OH) ₂	8.00 x10 ⁻¹⁶
Lanthanum (III) fluoride ^B	LaF ₃	7.00 x10 ⁻¹⁷
Aluminum (III) phosphate ^B	AlPO ₄	9.84 x10 ⁻²¹
Lanthanum (III) hydroxide ^B	La(OH) ₃	2.00 x10 ⁻²¹
Iron (III) phosphate ^B	FePO ₄	1.30 x10 ⁻²²
Lanthanum (III) phosphate	LaPO ₄	7.08 x10 ⁻²⁷
Calcium phosphate ^B	Ca ₃ (PO ₄) ₂	2.00 x10 ⁻²⁹
Aluminum (III) hydroxide ^B	Al(OH) ₃	3.00 x10 ⁻³⁴
Iron (III) hydroxide ^B	Fe(OH) ₃	4.00 x10 ⁻³⁸

↑
MORE SOLUBLE↓
LESS SOLUBLE

A – Temperature at 293 K

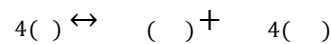
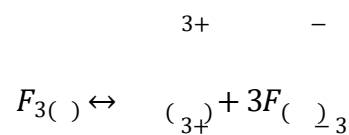
B – Temperature at 298 K

Table adapted from (Firsching & Brune, 1991; Haynes, 2015)

The solubility products of lanthanum-fluoride and lanthanum-phosphate are 7×10^{-17} (Haynes, 2015) and 7.08×10^{-27} (Firsching & Brune, 1991), respectively. Likewise, the solubility products of cerium fluoride and cerium phosphate are 8×10^{-16} (Haynes, 2015) and 7.43×10^{-11} (Haynes, 2015), respectively.

Solubility and pH play an important role in the formation of soluble and insoluble complexes, sludge production, and removal mechanism. At high pH levels, the net surface charge of the metal-hydroxides will be negatively charged. At low pH levels, the surface charge is positively charged. Therefore, at high pH levels, adsorption of anions is not likely favored (MWH Global, 2012).

Comparing lanthanum-based precipitates, the coagulation and precipitation of fluoride and phosphates produce significantly less insoluble materials. In addition, the stoichiometric equation produces a molar ratio of 1:1 for cerium or lanthanum to phosphate and 1:3 for cerium or lanthanum to fluoride, as seen in the equation below:



Equation 9: Stoichiometric equation of cerium to (a) fluoride and (b) phosphate. Lanthanum molar ratio equation is similar of that cerium formation.

The precipitation process with the rare-earth salt, lanthanum salts, has been shown to be a better process of phosphates precipitation compared to aluminum (i.e as Al^{3+}) and iron (i.e. as Fe^{3+}) salts addition with a wider pH range of 4.5 to 8.5(Recht et al., 1970).

Aside from coagulant use, rare-earth salts are known to inhibit bacterial growth in small dosages; however, there is limited information about toxicity with different micro-organisms. Burkes and McCleskey (1947) examined the bacterio-static activity of cerium, lanthanum, and thallium salts. They determined inhibition through plate count after 1, 2, 3 and 5 day incubation. The study provided inhibition data for more than 40 species of

microorganisms. Selected species were from this developed pool of testing species by Burkes and McCleskey (1947). Results from the study showed relatively good bacteriostatic activity for the 39 species tested. Cerium chloride with concentrations from 0.0006 M to 0.0012 M showed growth inhibition to 39 out of 40 species tested; using lanthanum chloride with concentrations of 0.0002 M to 0.0008 M; and with concentrations of thallium nitrate from 0.0005 M to 0.0010 M (Burkes & McCleskey, 1947). In recent years, development of cerium oxide powders and nanoparticles has shown applicability for antibacterial usage (Pelletier et al., 2010). Pelletier et al. (2010) studied variations of cerium oxide nanoparticle concentrations with changing incubation period (0, 1, 5, and 24 hour incubation). Bacteriological toxicity were quantified by disk diffusion test, determination of minimum inhibitory concentrations (MICs), CFU measurements and plate counts, live/dead viability assays, superoxide production, and through micro-array hybridization and analysis (Pelletier et al., 2010). The study showed growth inhibition for *E. coli* and *B. subtilis* as a function of nanoparticle concentration and size. The result can be related to the interaction of nanoparticles in aqueous solutions and the different metabolic mechanisms of each bacterium. The fact that rare earth salts have been proven to have some disinfection properties shows the need to study this property for application in drinking and wastewater treatment.

Rare-earth metals lanthanum and cerium-doped natural adsorbents have shown potential particularly in fluoride removal. Na et al. (2010) identified that lanthanum hydroxide adsorbent had an adsorption capacity of 242.2 mg of fluoride/g of adsorbent at $\text{pH} < 7.5$. However, the adsorption capacity decreased at a pH greater than 10 to 24.8 mg/g. In a previous study, Raichur et al. (2001) identified increased fluoride

adsorbed(>90%) with increased adsorbent dose (>3 mg/L) at a final pH of 6.5. A (>90%) adsorption and maximum adsorption was achieved at a pH of 6 to 6.5; the optimal fluoride adsorption was determined to be between pH 5 to 7. However at lower pH levels, the adsorption ranged from 40% to 60%, because of the formation of weak hydrofluoric acid. Furthermore, the fluoride adsorption greatly decreased at alkaline pH level. This can be attributed to the competition of hydroxyl ions with the fluoride ions onto the adsorbents. Nitrate and sulfate interferences were studied. The adsorption capacity, with 100 mg/L sulfate, decreased from 85% to 84%; consequently, the presence of nitrate (100 mg/L) reduced the capacity from 85% to 80% (Raichur & Basu, 2001)

In a recent study by Strileski (2013) at UNLV, lanthanum chloride was shown to better remove phosphate from wastewater than alum and ferric chloride. A 99% phosphate removal was achieved with 1:1 molar ratio (La:PO₄⁻³). Furthermore, the study determined a phosphate removal efficiency of 85-% even at pH of 2. Compared to alum and ferric chloride, lanthanum showed greater removal at lower pH level (Strileski, 2013). This makes rare earth coagulants very suitable for phosphate removal from waste streams with low pH levels.

In addition to fluoride removal, rare-earth doped adsorbents have been recently investigated due to their effective phosphate adsorptive capacity. Rare-earth doped adsorbents that have been used include cerium (III) exchanged natural zeolite (Haron et al., 2008; Lee & Rees, 1987), cerium oxides incorporated onto natural zeolite (Hashimoto et al., 1997), lanthanum doped activated carbon fiber(Zhang et al., 2012), lanthanum-impregnated silica gels (Wasay et al., 1996), lanthanum-doped zeolites (Li et al., 2005; Li

et al., 2009; Ning et al., 2008), lanthanum-doped chelex resin (Wu et al., 2007), and lanthanum-doped silicates (Qu et al., 2007; Zhang et al., 2010).

2.5. Response Surface Methodology: Central Composite Design

Response surface methodology (RSM) is a mathematical and statistical analysis of relationship between a response (Y), and various associated independent variables or factors that control the response (Khuri & Mukhopadhyay, 2010). Independent variables (X_1 , X_2 , and X_3) are experimental variables or factors that can be changed, independent from each other. In this study, independent variables comprise pH, initial fluoride concentration, and coagulant (e.g. cerium chloride) dose. Experimental response or dependent variable is the measured result from the experimental analysis (Bas & Boyaci, 2007; Bezerra et al., 2008), which in this study is fluoride removal.

RSM is developed to empirically model experimental response, and to overcome limitations of one-factor optimization. RSM allows for multivariate statistical analysis, and simultaneously optimize these independent variables to attain the highest probable response (e.g. fluoride removal) (Bezerra et al., 2008). RSM offers several advantages compared to other statistical methods. RSM predicts responses based on a very small amount of experimental data. In addition, RSM provides the interaction between independent variables on the response. RSM is widely used for optimization of chemical and biochemical process (Bas & Boyaci, 2007). One drawback of RSM, however, is the fitting the data to quadratic equation (Lundstedt et al., 1998; Bas & Boyaci, 2007).

RSM can be classified into first- or second order design models. First-order model can be used when there is no curvature on the predicted response surface. However, in cases where linear model cannot describe the experimental results or responses, quadratic responses surfaces are used, which include: full-factorial, central composite, Box-Behnken, and Doehlert designs. In practice, designs such as Box-Behnken, central composite, and Doehlert designs are typically used to accommodate fewer sample runs (Bezerra et al., 2008; The Pennsylvania State University, 2015). The second-degree model can be described as:

$$= b_0 + b_1x_1 + b_2x_2 + b_3x_3 + b_{12}x_1x_2 + b_{13}x_1x_3 + b_{23}x_2x_3 + b_{11}x_1^2 + b_{22}x_2^2 + b_{33}x_3^2$$

Equation 10: Central Composite design equation using a second-order model (i.e. quadratic model)

Where the model coefficients $b_0 \dots b_3$ are the linear regression coefficients of the quadratic predicted response; $b_{11} \dots b_{33}$ are the cross-product coefficients for each parameter.

In this study, a central composite design (CCD) model was used to predict fluoride removal. CCD models have been previously used to identify optimal conditions for chromium (VI) removal from ion-exchange brine solutions (Pakzadeh & Batista, 2011; Zaroual et al., 2009) and for optimization of Fenton process for COD removal (Asghar et al., 2014). Response surface model – Box-Behnken model – was to use optimize seed extract dose for fluoride removal in drinking water (Jafari et al., 2014).

A CCD consists of the following: (1) full-factorial points, (2) a star (axial) points which are experimental points at distance from its center, and (3) center points (Bas

&Boyaci, 2007; Lundstedt et al., 1998). A full-factorial experiment design consists of 2^k experiments, $2k$ for star (axial) points, and n_c center points, where k is total number of factors (e.g. pH, initial fluoride concentration, and coagulant dose) being investigated. In general, star (axial) points are at some $+\alpha$ (alpha) and $-\alpha$ (alpha) distance from each axis that allow for the estimate of quadratic coefficients of the model. For a 3 factor-level CCD model, there will be 8 factorial points, 8 star points, and 5 center points; thereby, total of 20 experimental runs.

The CCD factors are entered as coded level as (-) minus for low levels, and (+) plus for high levels. The low and high levels should correspond to the range of values for each factor being investigated. A zero-level is also included to represent the middle range of the investigated variables (Lundstedt et al., 1998). There are three types of central composite design which are: (1) circumscribed (CCC), inscribed (CCI), and face-centered (CCF). Circumscribed (CCC) and inscribed (CCI) models are typically used when evaluating operating conditions with five levels for each independent variable. The former is used when the area of operability – region where the independent variables can vary – lies with the area of concern. And, the latter is used when the region of operability and concern coincide each other. On the other hand, face-centered (FCC) models are used when the axial (i.e. alpha or star) points must correspond to the defined low and high levels of the independent factor; the axial points of the FCC match the surface of the cubic (National Institute of Standards and Technology, 2003). In face-centered design, the axial points fall at the center of each face of the factorial design, so α (alpha) = ± 1 (National Institute of Standards and Technology, 2003; The Pennsylvania State University, 2015). All FCC designs are composed of three levels for each independent

variable (Yang, 2008). A face-centered central composite design was used to optimize fluoride removal on industrial wastewater, since three-level and three factors (e.g. pH, fluoride concentration, and cerium dose) are being evaluated.

CHAPTER 3: MATERIALS AND METHODS

To determine the effectiveness of cerium chloride to remove fluoride and phosphate from waters, both batch and column bench tests were performed. Column adsorption tests were performed to investigate the removal of phosphate using various media (i.e. GAC, zeolite, and anthracite) impregnated with cerium chloride. Batch tests were used to support central composite design (CCD) model to evaluate the impact of major parameters on the removal of fluoride from industrial wastewater. In addition, batch tests were also used to investigate the interference of competing ions on the removal of fluoride using cerium chloride.

3.1. Developing Central Composite Design (CCD)

In this study, a three-factorial and three-level CCD with duplicate experiments for non-centered and six-center points was performed to investigate the most important variables involved in the removal of fluoride from waters using cerium chloride. The model resulted in 20 distinct batch tests and 40 batch tests, after including replication.

The major parameters - pH, initial fluoride concentration, and molar dose – were designated as X_1 , X_2 , and X_3 for the un-coded variables, respectively. The statistical program, SAS JMP, was used to develop and predict responses, and to calculate parameter coefficients, lack of variance, and lack of fit analyses. Table 8 lists the coded and un-coded values for the central composite design. The coded values were assigned (-

1), 0 and, (+1). Values for the high and low levels are based on data reported in the literature for typical fluoride contaminated industrial wastewaters.

Table 8: Coded and un-coded levels of each factor for the central composite design for fluoride removal – changing pH level, molar ratio, and fluoride concentration

Independent Variables (Uncoded)	Unit	Symbol	Coded Level		
			-1	0	1
pH	Value	X ₁	2.0 ±0.2	4.75 ±0.5	6.50 ±0.7
Initial Fluoride Concentration	mg/L	X ₂	10 ±1	100 ±10	1,000 ±100
Cerium Dose (mM)	Value	X ₃	6.25	12.5	25.0

After determining the independent variables that impact fluoride removal and their typical values, each factor is then entered into the response surface design of choice. In this study, a central composite design (CCD) was selected and SAS JMP statistical program was used to create the CCD model. A face-centered CCD model was selected because study involves 3-level independent variables, which meant that the axial (star) points are $+\alpha$ and $-\alpha$ on the axial surface. In some cases where five levels are being evaluated, a circumscribed (CCC) or inscribed (CCI) would be the appropriate CCD design model.

After establishing the axial distance, the program generates a table with the experiment runs, and independent variables based on the high, middle, and low level variable provided. The experimental run and run order for this study can be seen on Table 14 (Chapter 4), columns 1 to 4. Batch experiments were run based on the run order of the program's output (Table 14, column one). After running all batch experiments with

duplicate, experimental responses were then logged into the program. The model generates an equation, and predicts responses (i.e. fluoride removal) based on the equation.

Since the quadratic equation utilizes coded levels for prediction, it was necessary to determine equivalent distance and value for each un-coded levels to estimate fluoride removal and plot the data as contour plots. The equation used to calculate the halfway point for the coded and uncoded levels is:

$$H l w y \quad i = \frac{z}{2}$$

Equation 11: Equation to calculate halfway points for the coded and uncoded levels.

Where, halfway point is the distance between two points for the coded (i.e. +1, 0,-1) and un-coded levels (e.g. fluoride = 10, 100, and 1,000 mg/L). Each point then represents the actual values for pH, fluoride concentration, and cerium dose.

3.2. Experiments Based on the Central Composite Design (CCD)

3.2.1. Batch Test for CCD Model

Aliquots of stock solutions were transferred to 50-mL plastic bottles and then diluted with distilled water to obtain the desired concentrations. The pH of the solutions was adjusted using 0.01 N HCl, 0.01 N KOH, bicarbonate and 0.10 N NaOH to achieve pH levels ranging from 2.0 to 6.75. Because Sorbx-100 is very acidic (pH = 3.20 to 3.50), it was necessary to develop titration curves using concentrated solutions for pH adjustment purposes.

After all stock solution preparations, the sealed bottles were shaken vigorously for 1 minute and placed onto a shaker at 200 rpm for 15 minutes. Preliminary kinetic testing showed that mixing time showed no impact on precipitation using cerium chloride. Samples were transferred into 50-mL plastic vials and placed in a Sorvall Legend RT centrifuge (Thermo Fisher Scientific Inc., USA) at 2500 rpm for 5 minutes. Decant volumes were transferred to 100-mL plastic bottles for storage and filtered through a 0.20 μm Whatman glass fiber filter. Filtered samples were analyzed for the compounds of interest.

3.2.2. Batch Tests for Effect of pH, Cerium Dose, and Initial Fluoride Concentration

The model results and batch experiments guided the next series of batch experiments. Furthermore, the results of statistical calculation using the model design identified the major effects of each factors. To identify the major effect of pH, a series of batch tests were performed with initial fluoride concentrations of 1,000 mg/L (52.63 mM) with increasing cerium dose (6.25, 12.5 and 25 mM), and varying pH levels from 2 to 8. Since the cerium chloride solution is very acidic and depresses the pH, higher cumulative volumes of cerium added to the solution led to a significant decrease in pH. Titration curves were necessary to identify the optimal amount of sodium hydroxide to add to the solution to maintain a pH greater than 6.0. Higher removal efficiencies were achieved at fluoride concentrations of 100 mg/L. However, this is not a great representation of the fluoride concentrations in industrial waters. As previously cited, fluoride concentrations

in industrial wastewater can range from 100 mg/L (5.26 mM) to 1,000 mg/L (52.63 mM) (Table 1) (Hu et al., 2005; Hamdi & Srasra, 2007; Gurtubay et al., 2010).

The impacts of sulfate, nitrate, and bicarbonate on fluoride were investigated. Sulfate can be found in fluoride-contaminated wastewater. Typical sulfate concentrations in fluoride-contaminated wastewater can range up to 3,700 mg/L (60.0mM). However, preliminary testing determined that sulfate concentration less than 100 mg/L (1.04 mM) showed no impact on fluoride concentration. A sulfate concentration of 20 mg/L (0.21 mM) was added to all batch solutions (Hu et al., 2005). Chloride concentration in industrial wastewater typically ranges from 13 mg/L (0.37 mM)(Hu et al., 2005) to 25,300 mg/L (714.7 mM)(Gurtubay et al., 2010)and sodium concentrations from 900 mg/L (39.1 mM)(Hamdi & Srasra, 2007) to 10,000 mg/L (434.8 mM)(Gurtubay et al., 2010). Therefore, 1% salinity (10,000 mg/L as NaCl) was maintained throughout the entire experiments to somewhat simulate industrial wastewaters.

All batch experiments were run in duplicate to reduce experimental errors. Table 9 summarizes the batch tests performed to evaluate the effect of pH, cerium dose, and fluoride concentration.

Table 9: Experimental matrix for the effect of pH, cerium dose, and fluoride concentration

#	Cerium Dose (mM)	Fluoride (mg/L)	Fluoride (mM)	pH				
1	6.25 ¹	1,000	52.63	2	3.5	4.75	7.50	8.75
2	12.5 ²	1,000	52.63	2	3.5	4.75	7.50	8.75
3	25.0 ³	1,000	52.63	2	4.75	5.50	¹ -	² -

1 – pH > 5 is attained without adding exaggerated amount
2 – pH > 5 is attained without adding exaggerated amount

3.2.3. Batch Tests to Evaluate the Effect of Fluoride Concentration and Cerium Dose

To investigate the effect of fluoride concentration and cerium doses, six additional batch tests were performed. Solutions with fluoride concentrations of 100 mg/L (5.26 mM) and 1,000 mg/L (52.63 mM) were prepared with increasing cerium dose (6.25, 12.5 and 25 mM), with a constant pH of 4.75, 20 mg/L (0.21 mM) sulfate, and 1% salinity (10,000 mg/L as NaCl). All tests were performed twice to account variation between tests. Table 10 summarizes the batch tests performed to evaluate the effect of fluoride concentration and cerium dose.

Table 10: Experimental matrix to evaluate the effect of cerium dose and initial fluoride concentration

#	Fluoride (mg/L)	Fluoride (mM)	pH	Cerium Dose (mM)		
1	100	5.26	4.75	6.25	12.5	25.0
2	1,000	52.6	4.75	6.25	12.5	25.0

3.2.4. Batch Tests to Evaluate the Effect of Bicarbonate and Cerium Dose

To investigate the effect of bicarbonate concentration and cerium dose, six additional batch tests were performed. A fluoride concentration of 1,000 mg/L (52.6 mM) was maintained with 500 mg/L (8.20 mM) and 1,000 mg/L (16.4 mM) bicarbonate concentration, 20 mg/L sulfate (0.21 mM), and 1% salinity (10,000 mg/L as NaCl). Cerium dose (12.50, 25.0 and 50.0 mM) was increased for at the two bicarbonate concentrations. Table 11 summarizes the batch test done to evaluate the effect of increasing cerium dose, and bicarbonate concentrations.

Table 11: Experimental matrix evaluate the effect of cerium dose and bicarbonate concentration

#	Fluoride (mg/L)	Fluoride (mM)	HCO ₃ ⁻ (mg/L)	HCO ₃ ⁻ (mM)	Cerium Dose (mM)		
1	1,000	52.6	500	8.20	12.5	25.0	50.0
2	1,000	52.6	1,000	16.4	12.5	25.0	50.0

3.2.5. Batch Tests for Actual Industrial Wastewater

Coagulation tests were performed at room temperature using a Phipps and Bird six-plate stirrer. One hundred mL of the industrial wastewater from Radian Chemicals (Kingwood, Texas) were transferred to 1-liter glass beaker, and the amount of cerium chloride was then added, while mixing at 100 rpm for complete mixing. After the rapid mixing at 100 rpm, the stir setting was reduced to slow mix, at 30-33 rpm for 20 minutes to allow flocs formation. Right after slowly mixing, samples were allowed to settle for 30 minutes and were transferred into 50-mL plastic vials and placed in centrifuge Sorvall Legend RT centrifuge (Thermo Fisher Scientific Inc., USA) at 2500 rpm for 5 minutes. Decant volumes were transferred to 100-mL plastic bottles for storage and filtered through a 0.20 um Whatman glass fiber filter. Filtered samples were analyzed for the compounds of interest.

3.3. Media Impregnation and Column Testing for Phosphate Removal

Activated carbon (F-400, Calgon Carbon), natural zeolite (Bear River Idaho) and anthracite were used as a media for Sorbx-100 impregnation in the screening adsorption

tests. These tests were performed to investigate the removal of phosphate from waters using media impregnated with cerium chloride.

3.3.1. Granular Activated Carbon and Anthracite Preparation

Five hundred milliliters of media were rinsed thoroughly ten times with distilled water. The rinsed media was placed in clean trays lined with aluminum foils and were covered. All media were air dried for 24 hours. Desired amount of Sorbx-100 (Table 12) were mixed, using a wooden spoon, with 100 ml of activated carbon and anthracite, separately. Some media were also treated with 0.10 N KOH to increase the pH and therefore convert cerium chloride to cerium oxide. A portion of the media was also heated to 400°C and at 600°C for 30 minutes. The impregnated materials were air-dried for 24 hours (Table 12). For some effluent samples, the concentration of cerium in the effluent was determined by inductively coupled plasma (ICP), to establish if cerium was leaching out of the column materials.

3.3.2. Column Testing with Impregnated Media for Phosphate (PO_4^{-3} as P)

Removal

To test the capability of the impregnated media to adsorb contaminants, column tests were performed. The desired amount of media was placed in a plastic burette (1-inch OD) containing a small amount of glass beads at the bottom to support the Sorbx-impregnated media. Synthetic phosphate solution was then fed to the columns using a peristaltic pump (Cole Parmer, Chicago, Illinois). The effluent solution was then

collected for analysis. It was assumed that Sorbx-100 was fully attached to the media, since Sorbx-100 solution fully covered or adsorbed onto the media. Three parts per million or 3 mg/L of phosphate (PO_4^{-3} as P) was used as feed for the column testing.

Table 12 shows the techniques used to prepare the media used in the three columns. Column surface loading rate, SLR, of 5 gal/sq.ft.min was used to simulate loading used in full-scale filtration systems for water and wastewater treatment; typical surface loading rates ranges from 4-8 gal/sq.ft.min(Metcalf & Eddy, 2014)

Table 12: Media Preparation for Column Testing Using Activated Carbon and Anthracite, and Natural Zeolite

Parameter	Preparation				
	#1	#2	#3	#4	#5
Media Content	None	Sorbx-100	Sorbx-100	Sorbx-100	Sorbx-100
Preparation	None	Sorbx-100	0.10 N KOH	0.10 N KOH	0.10 N KOH
0.10 N KOH	None	None	15	15	15
Volume (mL)	None	None	15	15	15
Sorbx-100	None	15	15	15	-
Volume (mL)	None	15	15	15	-
Sorbx-100	None	2.09	2.09	2.09	0.40
Concentration (M)	None	2.09	2.09	2.09	0.40
Media	GAC Anthracite	GAC Anthracite	GAC Anthracite	GAC Anthracite	GAC Zeolite
Drying Method	None	Air-dried (24-hr)	Air-dried (24-hr)	Air-dried (24-hr)	Oven-dried (24-hr)
Furnace-Drying Temperature (°C)	None	None	None	400°C (30 min)	600°C (30 min)

Figures 4a-4c shows no considerable external physical changes with activated carbon with the addition of Sorbx-100 and after furnace calcinations at 400°C.

Subsequent to adding KOH and Sorbx-100 to anthracite, the anthracite showed significant aggregation of the media (Figure 4e-4f). After heating the anthracite media at 400 °C for 30 minutes, a significant amount was lost and a brownish precipitate was formed on the anthracite media. A hydraulic retention time (HRT) of 0.60 to 0.80 min was maintained throughout the column testing.



Figure 4: Media preparation with different reactants. a) virgin GAC; b) GAC with KOH and Sorbx-100; c) GAC after furnace dry at 400 °C; d) virgin anthracite; e) anthracite with KOH and Sorbx-100; f) anthracite after furnace dry at 400 °C.

3.3.3. Modifications on Initial GAC Preparation and for Zeolite Preparation

About 200 g of zeolite and activated carbon were washed ten times with distilled water. After rinsing, the media was soaked in 0.4 M of Sorbx-100 with (5% w (Sorbx-100)/w (GAC or zeolite, 5%). The excess reagent was then removed by filtering the mix through a coffee filter. Next the media was dried over night at 105⁰C and then placed in a furnace at 600⁰C for 30 minutes. Similar procedure has been used by Zhang et al. (2011). This media preparation is shown in Table 1 as preparation #5. Modified preparation for GAC and natural are shown on Figures 5 and 6. Figure 7 shows the column set-up for the modified column design with 1.20 min HRT and 2.20 min HRT for zeolite and activated carbon media.



Figure 5: Media preparation with modified media preparation with 0.4 M Sorbx-100 5% (w/w) with zeolite. a) virgin zeolite; b) zeolite with Sorbx-100 anthracite after furnace dry at 600°C.



(a) GAC only



(b) modified GAC 5% (w/w)

Figure 6: Media preparation with modified media preparation with 0.4 M Sorbx-100 5% (w/w) with activated carbon. a) virgin activated carbon; b) activated carbon with Sorbx-100 anthracite after furnace dry at 600°C.



(a) Column set-up with virgin zeolite (left) and zeolite with SORBX and after calcinations (right).



(b) Column set-up with GAC (left) and zeolite with SORBX and after calcinations (right).

Figure 7: Modified column design and preparation set-up. a) virgin set-up (left) and modified zeolite (right) with HRT of 1.2 min; b) modified activated carbon (left) and modified zeolite (right) at HRT of 2.2 min.

3.4. Materials

3.4.1. Solutions

3.4.1.1. Synthetic Fluoride Wastewater

ACS reagent grade sodium fluoride (NaF) salt (VWR Scientific), anhydrous sodium phosphate (Na_2HPO_4) powder (J.T. Baker), sodium nitrate (NaNO_3) salt (EMD), potassium sulfate (K_2SO_4) salt (EMD), and sodium bicarbonate (NaHCO_3) powder were used to prepare 10,000 mg/L stock solutions of fluoride, phosphate, nitrate, and bicarbonate in 1 liter of fluoride-free (distilled) water, respectively. ACS grade sodium chloride (NaCl) salt was used to prepare 330,000 mg/L saline solution in 1 liter of distilled water.

The use of distilled water was needed because the Las Vegas tap water contains fluoride, added intentionally, and fluoride is not removed during deionization by the Environmental Engineering Laboratory.

3.4.1.2. Synthetic Phosphate Water

ACS reagent grade of anhydrous sodium phosphate (Na_2HPO_4) powder (J.T. Baker) was used to prepare 1,000 mg/L stock solutions of phosphate in 1 liter distilled water.

3.4.1.3. Industrial Wastewater

Experiments were done with sulfidic caustic solutions taken from Radian Chemicals, Inc. (Kingwood, Texas). The initial pH of the industrial wastewater was 13. The industrial wastewater from oil-refining industry was analyzed prior to the addition of cerium chloride. Industrial wastewater characteristics used for the fluoride experiments with cerium chloride is seen on Table 13.

Table 13: Industrial wastewater characteristics

Constituent	Concentration	Unit
pH	13 – 14	-
Sulfate	16,000 – 17,000	mg/L
Total Alkalinity	99,500 – 100,000	mg/L as CaCO ₃
Fluoride	40 – 50	mg/L
Soluble COD	20,000	mg/L

3.4.1.4. Cerium Chloride Solution

Molycorp, Inc. provided (Mountain Pass, CA) cerium chloride (i.e. SORBX-100) solutions for this research. The solution has a pH of 3.0 to 4.0 with specific gravity of 1.4 to 1.6 g/mL. Sorbx-100 is composed of 65-69 % by weight of water and 31-35 % by weight of rare-earth chloride. For the entire batch testing, a concentration of 2.09 M as cerium (III) at a pH of 3.20 was used. The computation of the concentration of the solution followed the equations:

$$a \quad \text{Concentration} \frac{\text{g}}{\text{L}} = \text{Specific Gravity} \times \% \text{ Weight \%} \times 1000$$

$$b \quad \text{Concentration as Ce III M} \\ = \text{Concentration} \frac{\text{g}}{\text{L}} \times \frac{1 \text{ mole of CeCl}_3}{246.48 \frac{\text{g}}{\text{mole}}} \times \frac{1 \text{ mole of Ce (III)}}{1 \text{ mole of CeCl}_3}$$

$$c \quad \text{Concentration as Ce III M} = 2.00 \text{ to } 2.09 \text{ M as Ce (III)}$$

Equation 12: Stock solution calculation for cerium chloride solution. (a) Conversion of weigh-to-weight ratio to weight-to-volume. (b) to (c) Conversion of concentration to molar ratio as cerium(III).

3.4.2. Analytical Methods

3.4.2.1. pH Measurement

Final pH of all solutions was measured using AR 10 Fisher Scientific pH meter. The pH meter was calibrated using a two-point calibration using pH 4 and pH 7 buffers, and pH 7 and pH 10 buffers.

3.4.2.2. Orthophosphate, Nitrate, and Sulfate Analyses

For phosphate measurements, USEPA method 8048 (Ascorbic Method), using PhosVer 3 power pillows, was used. The detection range for this method is between 0.02 to 2.50 mg/L PO_4^{-3} . Nitrate was measured using Method 10020 (Chromotopic Acid Method) for high range nitrate concentrations (0.20 to 30.0 mg/L $\text{NO}_3\text{-N}$). Sulfate was measured using USEPA method 8051 (Turbidimetric Method) using Hach SulfaVer4 powder pillows for sulfate concentrations (0 to 70 mg/L SO_4^{-2}). All analyses were done spectrophotometrically using Hach DR 5000 spectrophotometer. Accuracy of all methods was checked by using standard solutions of the compounds of interest.

Concentrations measured in standards were less than 5% differential of the expected concentration.

3.4.2.3. Fluoride Analysis

Fluoride concentrations were determined spectrophotometrically using Hach DR 5000 spectrophotometer using USEPA Method 8029 (SPADNS Method). This method utilizes SPADNS reagent solution and the method detection range is 0.02 to 2.00 mg/L. This method provided an $R^2 = 0.998$ for fluoride detection following standard calibration.

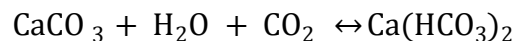
3.4.2.4. Total Alkalinity as Bicarbonate

Alkalinity was determined by titration method using Standard Methods for the Examination of Water and Wastewater and Hach Method 8221 for Total Alkalinity. The following equation was used to calculate total alkalinity:

$$\text{Alkalinity as HCO}_3^- = \frac{\text{volume of titrant ml} \times \text{normality of titrant} \times 50,000}{\text{volume of sample (mL)}}$$

Equation 13: Total alkalinity measurement and calculation as calcium carbonate

In addition, by considering this equation for alkalinity as bicarbonate:



Equation 14: Stoichiometric equation of calcium carbonate with addition of water, and carbon dioxide to calcium bicarbonate.

Therefore, one mole of $\text{Ca}(\text{HCO}_3)_2$ equals to one mole of CaCO_3 and the conversion is as follows:

$$\text{Alkalinity as HCO}_3 \text{ (mg/L)} = 1.22 \times \text{Alkalinity as CaCO}_3 \text{ (mg/L)}$$

Equation 15: Conversion of alkalinity as calcium carbonate (mg/L) to alkalinity as bicarbonate (mg/L).

3.4.2.5. X-Ray Fluorescence (XRF) Detection

X-ray fluorescence is an x-ray analytical method that is commonly used for chemical analyses of sediments, rocks, and minerals. The various media preparations were sent to Molycorp, Inc. for XFR analysis to identify rare-earth metal formations. However, the exact method performed for XRF analysis is unknown.

3.4.2.6. Trace Cerium Analysis

Inductively coupled plasma (ICP) is an analytical method that measures trace elements, particularly metals, in aqueous solutions (Batsala et al., 2012). Effluent samples were sent to Molycorp, Inc. for ICP analysis to identify, if cerium leaches out of the column. Samples analyzed were from column #5 for GAC preparation with 0.40 M Sorbx-100 and 1.20 min HRT. Since samples were sent to Molycorp, exact method used for measuring tracer cerium concentrations is unknown.

3.5. Quality Assurance and Quality Control

3.5.1. Quality Assurance

The following procedures were implemented to assure quality and maintain the integrity of the samples.

- a. All samples were refrigerated and placed in 4°C when not in use.
- b. All samples are labeled accordingly based on the batch test with date and sampling number.
- c. To assure integrity of stock solutions, stock solution measurements were done prior to the batch test. All stock solutions are disposed of in the correct waste bin.
- d. All glassware were soaked in Micro-90 cleaning solution, rinsed, and then rinsed three times with distilled water prior to use.

3.5.2. Quality Control Measures

For all batch tests, duplicate runs were done for all samples to reduce the uncertainty in analysis. Analytical measurements were performed for all runs to ensure the quality of the data.

CHAPTER 4: REMOVAL OF HIGH LEVELS OF FLUORIDE FROM WATERS USING CERIUM CHLORIDE

RESULTS AND DISCUSSION

4.1. Batch Test Results for Central Composite Design

4.1.1. CCD Model Results

Preliminary batch tests were performed to support a CCD investigation of the major variables that affect fluoride removal from water by cerium chloride. Table 14 shows the experimental data points used for the CCD surface design models including the experimental responses (i.e. obtained from batch tests) and the predicted response (i.e. obtained from the CCD model).

Table 14: Experimental data points and response used in Central Composite Design with predicted fluoride removal

Run ^a	pH	Fluoride (mg/L)	Dose (mM)	Molar Ratio (Ce/F)	Experimental Response ^b	Predicted Response
1	-1 (2.06)	-1 (11)	1 (25.0)	45.0	44.3	36.3
2	-1 (2.08)	1 (970)	1 (25.0)	0.5	23.7	35.2
3	0 (4.83)	0 (105)	0 (12.5)	2.3	79.6	82.7
4	1 (6.58)	1 (1,000)	-1 (6.25)	0.1	42.7	52.9
5	0 (5.01)	0 (105)	-1 (6.25)	1.1	74.5	78.9
6	1 (6.32)	-1 (10)	1 (25.0)	47.5	62.3	73.2
7	-1 (2.11)	0 (103)	0 (12.5)	2.3	46.8	48.7
8	0 (4.84)	0 (105)	0 (12.5)	2.3	72.9	82.7
9	-1 (2.35)	1 (948)	-1 (6.25)	0.1	29.2	20.5
10	0 (4.83)	0 (105)	0 (12.5)	2.3	83.0	82.7
11	0 (4.78)	0 (105)	1 (25.0)	4.5	96.9	83.7
12	0 (4.84)	0 (105)	0 (12.5)	2.3	84.7	82.7
13	0 (4.84)	0 (105)	0 (12.5)	2.3	75.6	82.7
14	0 (4.91)	1 (943)	0 (12.5)	0.3	79.3	67.4
15	1 (6.38)	1 (965)	1 (25.0)	0.5	89.8	88.7
16	1 (6.40)	-1 (10)	-1 (6.25)	12.4	87.4	78.4
17	0 (4.86)	-1 (11)	0 (12.5)	22.3	77.4	80.5
18	-1 (2.06)	-1 (10)	-1 (6.25)	11.9	59.0	62.3
19	1 (6.51)	0 (91)	0 (12.5)	2.6	94.0	83.3
20	0 (4.84)	0 (105)	0 (12.5)	2.3	83.0	82.7

a – Two replicates were performed for runs 1 to 20

b – Average of two replicates are presented for runs 1 to 20

Listed in Table 14 are the un-coded and coded values including measured concentrations. Since cerium chloride is acidic (pH=3.2), pH depression was anticipated

and pH was adjusted using 0.10 N potassium hydroxide (0.10 N KOH). All pH measurements, seen on column 1, are well within 5% standard deviation of the anticipated levels. The experimental initial fluoride concentrations are listed in column 2; all measured fluoride concentrations are within 5% standard deviation as well.

Experimental and predicted responses are shown in columns 6 and 7.

In this study, the highest fluoride removal (96.9%) is obtained at a pH of 4.78 to 5.0, for an initial fluoride concentration of 105 mg/L (5.53 mM), and at cerium dose of 12.5 mM (Ce/F ratio of 4.5). Once all the experimental data were logged, Minitab and SAS JMP were used to predict the fluoride removal. In general, the results show that the predicted responses are lower than the experimental values, particularly for results for a pH of 4.75 and cerium doses of 12.50 and 25.0 mM. Furthermore, the lowest removal is achieved at the lower pH of 2 and cerium dose of 12.5 and 25.0 mM, independent of the initial fluoride concentration. In comparison, the model predicted similar fluoride removal at lower pH (<4.75). However, in some cases, a lower response (i.e. fluoride removal) is predicted compared to the actual removal from the batch experiments. The model cannot predict other reactions, other than direct fluoride removal with cerium.

Table 15 lists all the computed coefficients for the response equation used to predict fluoride removal in water with characteristics similar to that commonly found in industrial operations.

Table 15: Estimated regression coefficients of the quadratic model for the Central Composite Design model (1) for fluoride removal

Term	Source	Coefficient	Value	P-value ¹
Intercept	Constant	b ₀	82.716364	<0.0001
pH	X ₁	b ₁	17.32	0.001
Concentration	X ₂	b ₂	-6.57	0.089
Cerium Dose	X ₃	b ₃	2.42	0.503
pH*Concentration	X ₁ X ₂	b ₁₂	4.15	0.312
pH*Cerium Dose	X ₁ X ₃	b ₁₃	5.275	0.206
Concentration*Cerium Dose	X ₂ X ₃	b ₂₃	10.175	0.026
pH*pH	X ₁ X ₁	b ₁₁	-16.69091	0.031
Concentration*Concentration	X ₂ X ₂	b ₂₂	-8.740909	0.218
Cerium Dose*Cerium Dose	X ₃ X ₃	b ₃₃	-1.390909	0.838

1 - P, critical = > 0.05, non-significant factors

The finalized response equation with the coefficients based on the estimated regression coefficients (Table 15) from the CCD model to predict fluoride removal is:

$$\begin{aligned}
 \text{Removal (\%)} = & 82.72 + 17.32 \times \text{pH} - 6.57 \times \text{Fluoride} + 2.42 \times \text{Dose} \\
 & - 16.69 \times \text{pH}^2 - 8.74 \times \text{Fluoride}^2 - 1.39 \times \text{Dose}^2 \\
 & + 4.15 \times \text{pH} \times \text{Fluoride} + 5.28 \text{ pH} \times \text{Dose} + [10.18 \\
 & \times \text{Fluoride} \times \text{Dose}]
 \end{aligned}$$

Equation 16: Predicted surface response equation for the CCD model for fluoride removal efficiency using the uncoded units.

The estimated regression coefficients show the major impact of each parameter and interaction of each parameter with each other in predicting fluoride removal. The coefficients for each term determine the overall effect on fluoride removal. However, to

fully identify the significance of each factor, it is necessary to evaluate the correlation of the model with desired statistically significant P-values. P-values of not more than 0.05 was chosen based on previous CCD models for contaminant removal (Olmez, 2009; Jafari et al., 2014)

The analysis of variance (ANOVA) between linear, quadratic, and two-way interactions of each variable is listed on Table 15. As stated earlier, major variables affecting fluoride removal are pH, coagulant dose, and the initial fluoride concentration. Based on the p-values, the only significant variable, at the chosen level of significance, is pH ($0.001 < P\text{-value} < 0.05$). Cerium dosage and initial fluoride concentration show much higher P-values. Therefore, according to the model, fluoride concentration and cerium dose have a lower impact on fluoride removal when cerium chloride is used as the coagulant. To determine the sensitivity of the variables on the predicted fluoride removal response, the CCD was rerun and re-evaluated excluding linear, quadratic and two-interacting factors with $P\text{-value} > 0.05$ to obtain a revised CCD model. Table 16 shows the percent difference calculation between experimental responses, (i.e. obtained from batch tests), predicted responses (i.e. obtained from the CCD model), and predicted responses from revised CCD model.

Table 16: Percent differences between experimental responses and predicted responses

Run	Experimental	CCD Model (1)		CCD Model (2)		(1) and (2)
		Predicted	Difference ¹	Predicted	Difference ¹	Difference ²
1	44.3	36.3	20.0%	39.4	11.7%	8.3%
2	23.7	35.2	39.0%	46.6	65.2%	28.0%
3	79.6	82.7	3.8%	80.7	1.4%	2.5%
4	42.7	52.9	21.4%	56.1	27.1%	5.8%
5	74.5	78.9	5.7%	78.3	4.9%	0.8%
6	62.3	73.2	16.0%	74.1	17.2%	1.2%
7	46.8	48.7	4.0%	40.6	14.2%	18.2%
8	72.9	82.7	12.6%	80.7	10.1%	2.5%
9	29.2	20.5	34.9%	21.4	30.6%	4.3%
10	83.0	82.7	0.3%	80.7	2.8%	2.5%
11	96.9	83.7	14.6%	83.1	15.3%	0.8%
12	84.7	82.7	2.4%	80.7	4.8%	2.5%
13	75.6	82.7	9.0%	80.7	6.5%	2.5%
14	79.3	67.4	16.2%	74.1	6.8%	9.5%
15	89.8	88.7	1.3%	81.3	10.0%	8.7%
16	87.4	78.1	11.2%	89.6	2.5%	13.7%
17	77.4	80.5	4.0%	87.3	12.0%	8.0%
18	59.0	62.3	5.5%	54.9	7.1%	12.6%
19	94.0	83.3	12.0%	75.2	22.2%	10.2%
20	83.0	82.7	0.3%	80.7	2.8%	2.5%

1 – % difference between experimental response and the predicted response

2 – % difference between CCD models

Experimental and predicted responses (i.e. obtained from initial and revised model are shown in Table 16. CCD model (1) is the first developed model including both

significant and non-significant factors. CCD model (2) is the revised CCD model where non-significant factors were removed. Columns 4 and 6 show the percent differences between the experimental response and the CCD models. Column 7 shows the percent difference between the two developed CCD models. For both CCD models (1) and (2), the modified model had the highest percent difference. Predicted fluoride removal responses from CCD model (1) and CCD model (2) (35.2% and 46.6%, respectively) were higher compared to the actual removal (23.7%) obtained from the batch experiments. Comparing both developed CCD models, the modified model has the highest (28%) difference. Since both CCD models show relatively the same differences from the experimental data, removing the non-significant factors have a minimal impact and both equations can then be used to estimate fluoride removal using cerium chloride from industrial wastewaters. Table 17 lists all the computed coefficients for the revised response equation for CCD model (2).

Table 17: Estimated regression coefficients of the quadratic model for the revised Central Composite Design model (2) for fluoride removal

Term	Source	Coefficient	Value	P-value ¹
Intercept	Constant	b_0	80.69	<0.0001
pH	X_1	b_1	17.32	0.0003
Concentration	X_2	b_2	-6.57	0.0926
Cerium Dose	X_3	b_3	2.42	0.5169
Concentration*Cerium Dose	X_2X_3	b_{23}	10.175	0.0254
pH*pH	X_1X_1	b_{11}	-22.77	0.0006
1 - P, critical = > 0.05, insignificant factors				

The revised response equation to predict fluoride removal is shown below:

$$\text{Removal \%} = 82.72 + 17.32 \times \text{pH} - 6.57 \times \text{Fluoride} - 22.77 \times \text{pH}^2 \\ + 2.42 \times \text{Dose} + [10.18 \times \text{Fluoride} \times \text{Dose}]$$

Equation 17: Predicted surface response equation for the CCD model (2) for fluoride removal

In both, the original and the revised model cerium dosage and initial fluoride concentration show much higher P-values (>0.05) than for pH. Therefore, according to CCD models, fluoride concentration and cerium dose factors have a lesser impact on fluoride removal when using cerium chloride. The developed CCD model for this study estimated lower R-squared and adjusted R-squared values of 0.8615 and 0.7368 (Table 18), respectively. Excluding all non-significant factors from the previous model, the revised model has R-squared and adjusted R-squared values of 0.7884 and 0.7128 (Table 18), respectively.

Table 18: Comparison of R-squared and adjusted R-squared values

Source	R-squared	Adjusted R-squared
CCD Model (1)	0.8615	0.7368
CCD Model (2)	0.7884	0.7128

Even though both models are statistically significant, 25% of the total variation cannot be explained by the quadratic model. Initial CCD model had higher R-squared and adjusted R-squared values. Therefore, the initial CCD model is better at predicting variations of the data compared to the revised CCD model.

There exist several reasons for the variation between the CCD model prediction and the actual fluoride removal obtained. The cerium dosage added took into consideration only the stoichiometry for the formation of cerium fluoride (CeF_3); complex formation and the formation of cerium hydroxide and cerium carbonate were not accounted for. Therefore, the predicted fluoride removal response is lower than the experimental response. This shows the limitation of the CCD model. It is known that cerium chloride addition promotes the formation of cerium hydroxide and or cerium carbonate. There have been reports of the adsorption of fluoride to oxides and hydroxides of REEs (Na & Park, 2010; Raichur & Basu, 2001). Wood (1990) has identified formation of complexes with lanthanides with sulfates, phosphates, fluorides, hydroxides, and bicarbonates (Wood, 1990). Jafari et al. (2014) used a RSM – Box-Behnken Model – for process optimization for fluoride removal from drinking water using seed extract. The model predicted R-squared and adjusted R-squared values of 0.99 and 0.98, respectively. A CCD was previously developed in hexavalent chromium removal in IX brine solutions using calcium polysulfide (Pakzadeh & Batista, 2011). The CCD model estimated an R-squared and adjusted R-squared of 0.9655 and 0.9344, respectively. Olmez (2009) also used RSM for optimization of hexavalent chromium reduction by electro-coagulation. The response surface model predicted an R-squared of 0.875 (Olmez, 2009). The model developed for this study produced lower R-values compared to most of the previous studies using the RSM – CCD model.

The analysis of variance (ANOVA) and lack of fit responses for the predicted and experimental data are listed on Table 19.

Table 19: Analysis of variance for the developed CCD model for fluoride removal efficiency

Source	F-Value	F-Critical	P-Value ²
CCD Model (1)	6.91	3.020	0.003
CCD Model (2)	10.4353	2.958	0.0002
2 – P, critical = > 0.05			

Based on the calculated responses of the CCD models, F-values are significantly greater than the F-critical. Therefore, both equations can confidently predict real variances. All P-values are less than the P-critical (<0.05) therefore, both models are statistically significant.

4.1.2. Contour Plot from CCD Model

Using the quadratic equation generated for with the CCD model and related coefficients, contour plots can be developed to show fluoride removal forecast under various conditions.. Contour plots were created based on the CCD model (1) to predict fluoride removal at varying pH, cerium dose, and initial fluoride concentrations. The contour plots were based on the conditions where the highest experimental fluoride removal was achieved. Disregarding initial fluoride concentrations, the data indicated that doses of 12.50 and 25.0 mM and at pH of 4.75 to 5.00, had the highest (>80%) removal. However, in generating the plots, increasing fluoride concentration were considered.

Figure 8-9 show the predicted contour plots as a function of initial fluoride concentration, pH, and at fixed cerium doses of 12.5 mM (Figure 8) and 25.0 mM (Figure 9). Consequently, a contour plot, solely by fixing the pH, was created. Figure 10 shows the prediction contour plots as a function of initial fluoride concentration, increasing cerium dose, and at fixed pH of 4.75.

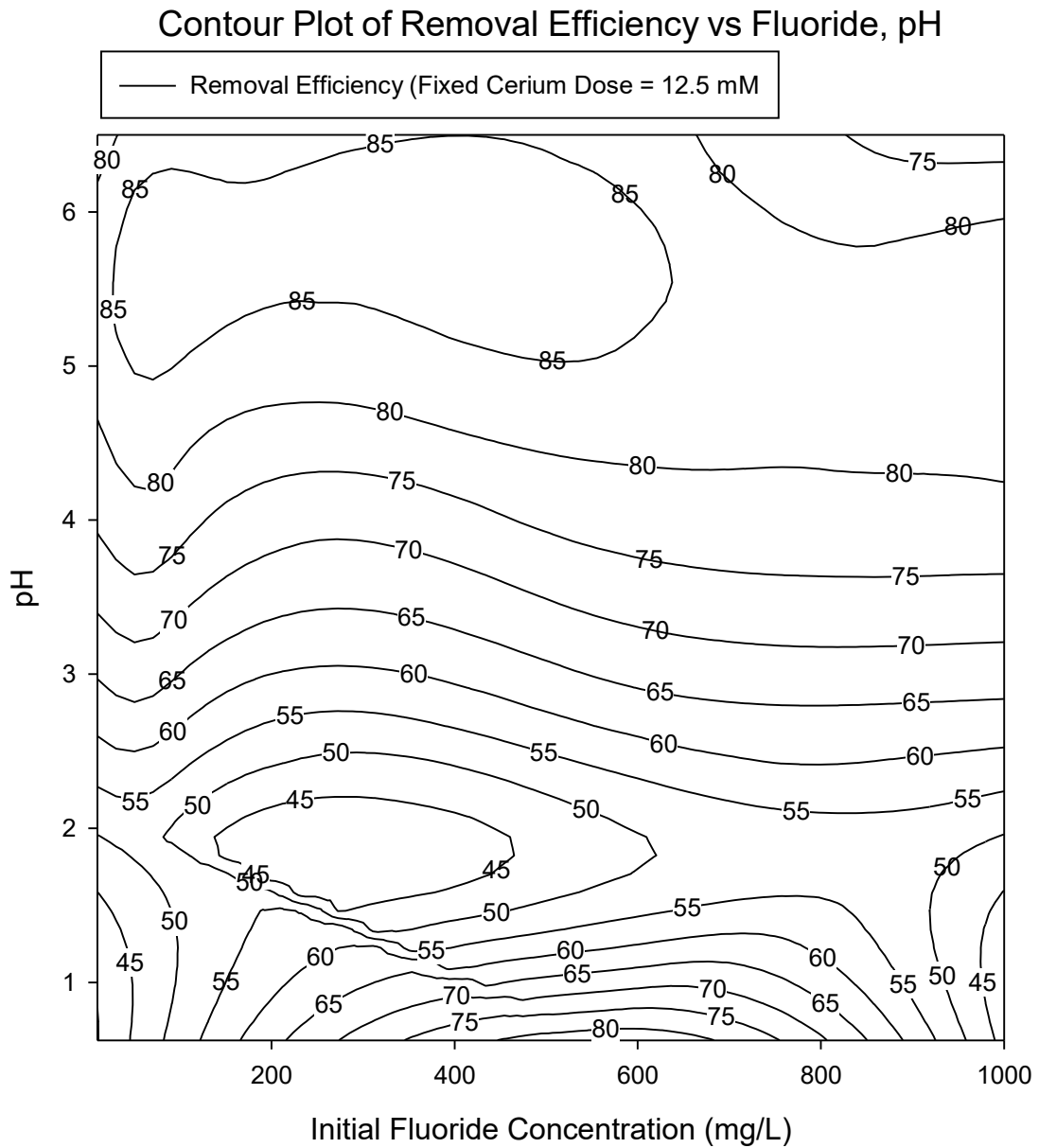


Figure8: Contour plot of predicted fluoride removal efficiency as a function of initial fluoride concentration at cerium dose of 12.50 mM and 1% salinity.

Contour Plot of Removal Efficiency vs Fluoride, pH

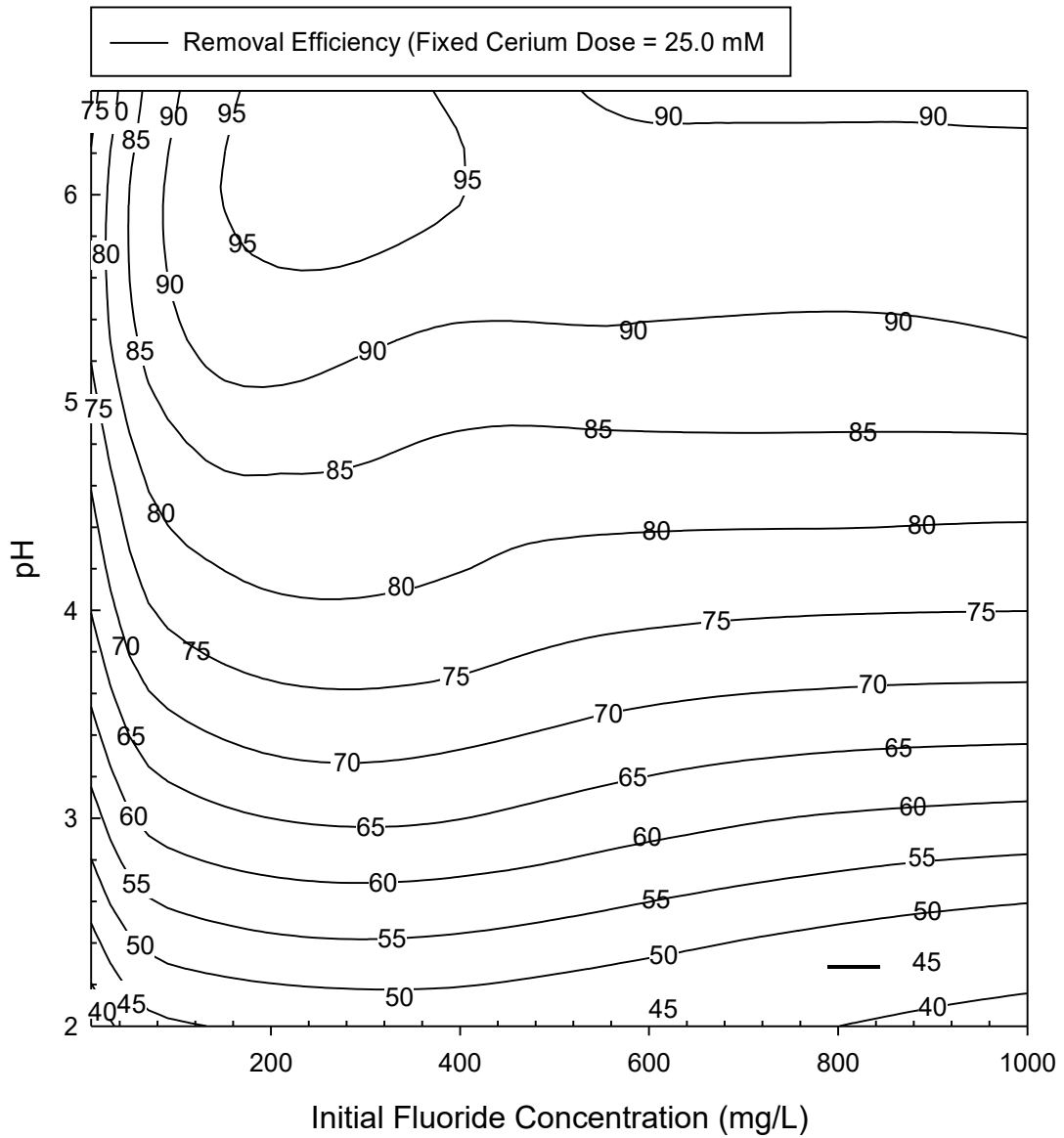


Figure 9: Contour plot of predicted fluoride removal efficiency as a function of initial fluoride concentration at cerium dose of 25.0 mM and 1% salinity.

Contour Plot of Removal Efficiency vs Cerium Dose, Fluoride

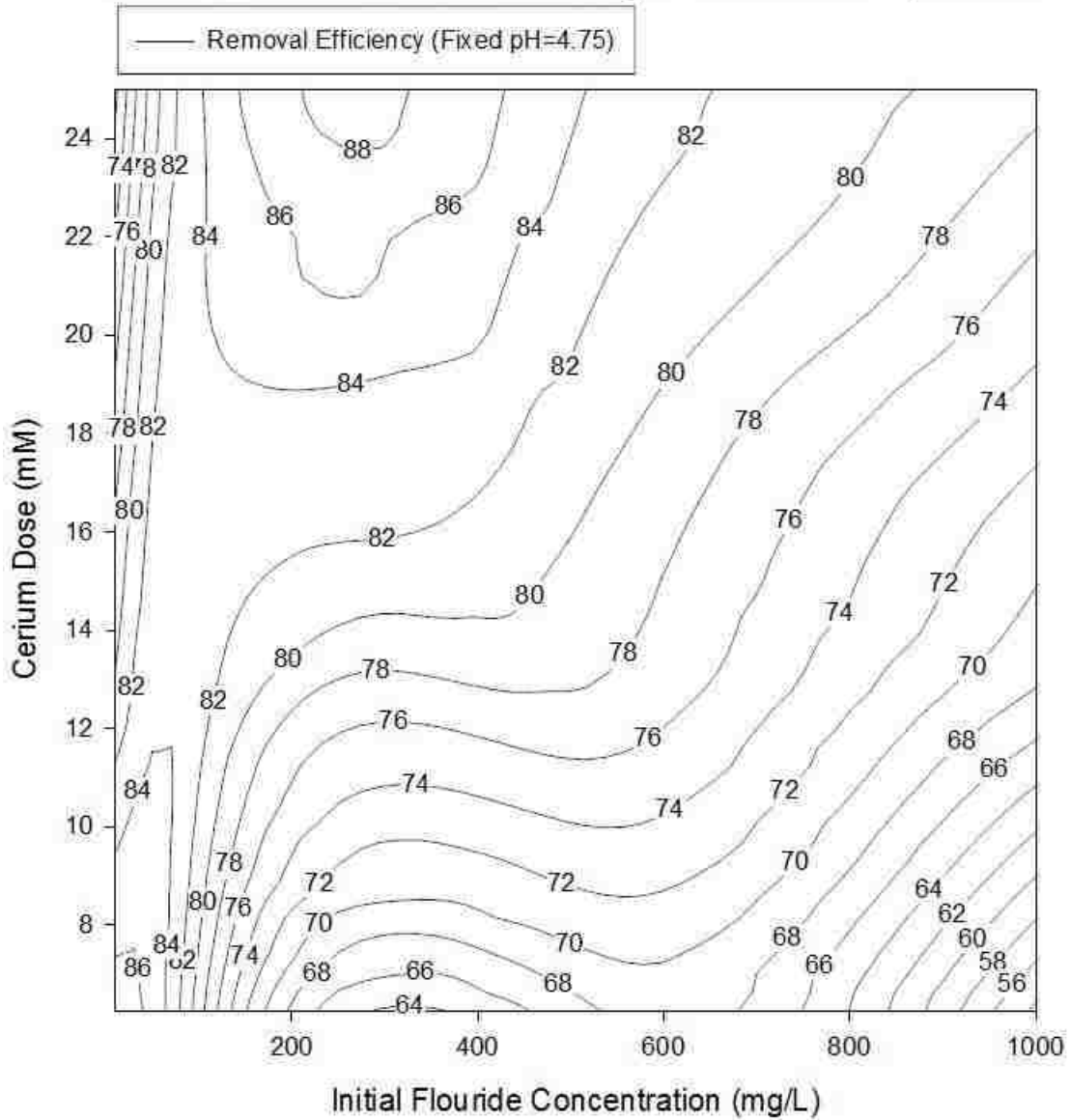


Figure 10: Contour plot of predicted fluoride removal efficiency as a function of initial fluoride concentration at pH level of 4.75 and 1% salinity.

4.2. Effect of pH and Cerium Dose on Fluoride Removal

The optimal operating pH plays a significant role in fluoride removal by precipitation as previously determined by other studies (Tomar & Kumar, 2013; Raichur & Basu, 2001). The CCD results helped identify which variables impact fluoride removal. Fluoride removal was evaluated with changing pH, while adding different doses of cerium. Fluoride removal efficiency, as a function of pH and increasing cerium dose is depicted in Figure 11.

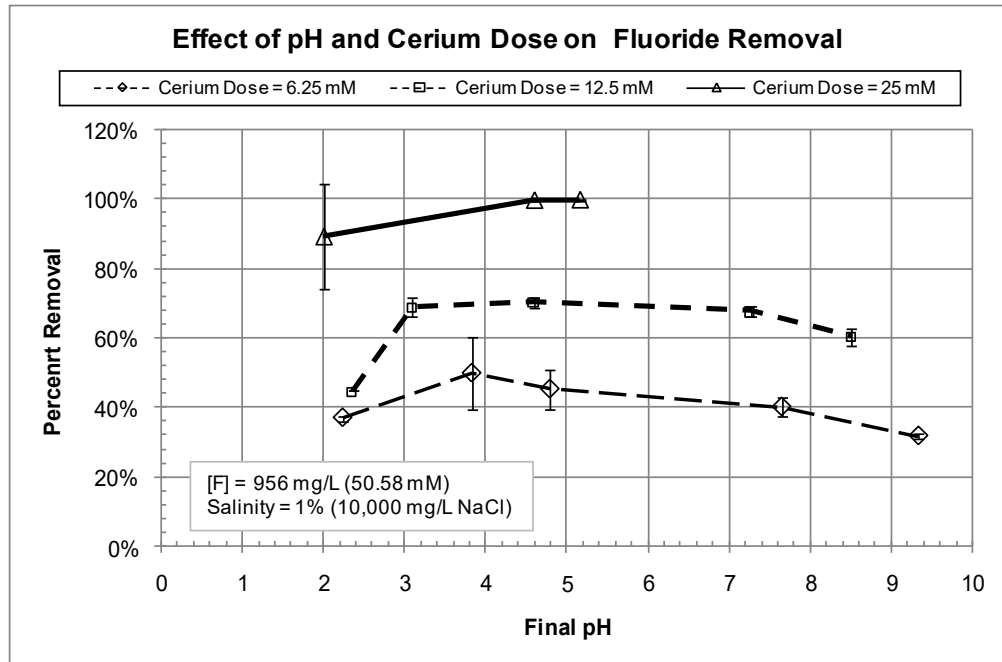


Figure 11: Fluoride removal efficiency as a function of pH and differential cerium dose (6.25, 12.5, and 25 mM), and with 1% salinity.

Three different doses were evaluated for fluoride removal while increasing the pH from 2 to 9.50, at a constant fluoride concentration of 1,000 mg/L (956 mg/L). Independent of the dosage of cerium applied, the highest removal of fluoride was

achieved at low pH values (between 3 and 5). At higher pH values, fluoride removal decreased. For the same pH value, a higher cerium dose resulted in higher fluoride removal. By increasing the pH from 4 to 9.25, fluoride removal was reduced to 30%. At a cerium dose of 12.50 mM (Ce/F=0.25), 70% removal was achieved at a pH of 3.0. No additional removal was achieved by increasing the pH to 7. However, the graph showed a dropping fluoride removal to 60% at pH 8.5.

Based on the experimental results from the CCD model, the highest removal was achieved at a pH of 4.78, at 105 mg-F/L (5.53 mM), and a cerium dose of 25.0 mM (Ce/F=4.52). Batch test results, run for these conditions, support the CCD model. A 98% removal of fluoride was, indeed, achieved at higher dose (25.0 mM; Ce/F=0.50), validating the model. The fluoride removal efficiency at 6.25 mM (Ce/F=0.12), 12.50 mM (Ce/F=0.25), and 25.0 mM (Ce/F=0.50) at pH <3, were 36%, 42%, and 80%, respectively. Based on the predicted responses (Table 14), the range of removal that can be achieved at that particular pH is from 35% to 50%. Therefore, both sets of experiments showed coherence with predicted fluoride removal.

4.3. Effect of Dose and Fluoride Concentration on Fluoride Removal

In this study, it was determined that the amount of cerium added and the final pH has an impact on fluoride removal; however, the impact of initial fluoride concentration and cerium dose needed further investigation. Therefore, additional batch experiments were performed. Fluoride removal efficiency based on the molar ratio (i.e. cerium dose) and initial fluoride concentration are plotted in Figure 12.

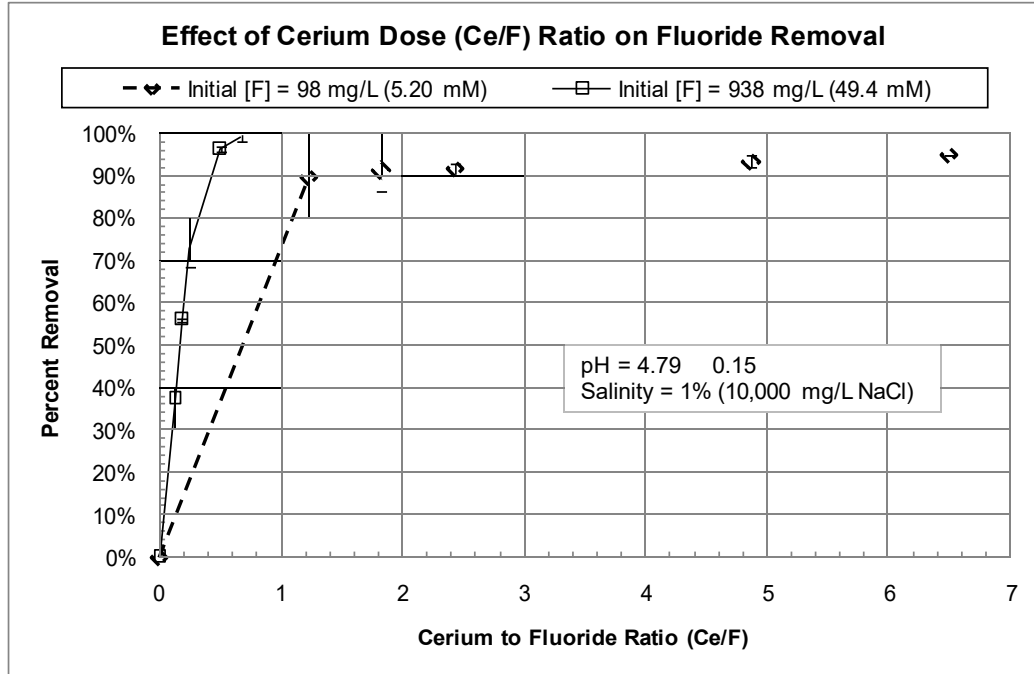


Figure 12: Fluoride removal efficiency as a function of Ce/F molar ratio and differential initial fluoride concentrations with 1% salinity, sulfate concentration of 20 mg/L, and final pH of 4.79 ± 0.24 .

At initial fluoride concentration of 98 mg/L, fluoride removal reached 90% at a molar ratio of 1.20 and by increasing the dose, no significant improvement was observed. At high fluoride concentrations, which are commonly found in industrial wastewater, a 96% removal was achieved at molar ratio of 0.60. In addition, a 98% removal was achieved at a molar ratio of 0.80 (cerium dose of 33.33 mM). Stoichiometrically, it only requires 1 mole of cerium for 3 moles of fluoride. Therefore, the data shows, particularly at $>1,000$ mg/L, more than $Ce/F = 0.33$ is required to achieve higher fluoride removal. On the other hand, at concentrations <100 mg/L, it is not advantageous to increase the molar ratio passed a Ce/F of 2.0. No additional removal was demonstrated (Figure 12) with molar ratio >2.0 .

Considering the prediction equation, at pH of 4.75, 1,000 mg-F/L, and cerium dose of 25 mM (Ce/F=0.50), 75%-80% can only be achieved. This predicted removal was less than that achieved experimentally. As previously mentioned, the CCD model cannot predict complex lanthanide formation or adsorption to hydroxides (Wood, 1990).

4.4. Impact of Competing Ions

Sulfate, bicarbonate, nitrate, and phosphate have been found to be the ions that typically affect fluoride removal by precipitation with coagulants other than cerium chloride (Drouiche et al., 2008; Drouiche et al., 2012; Hu et al., 2005).

Figure 13 shows the effect of sulfate on fluoride removal for a pH of 4.75, a salinity of 1% (10,000 mg/L as NaCl), a fixed fluoride concentration, and a Ce/F ratio of 0.33. These values represent the typical composition of industrial wastewaters contaminated with fluoride.

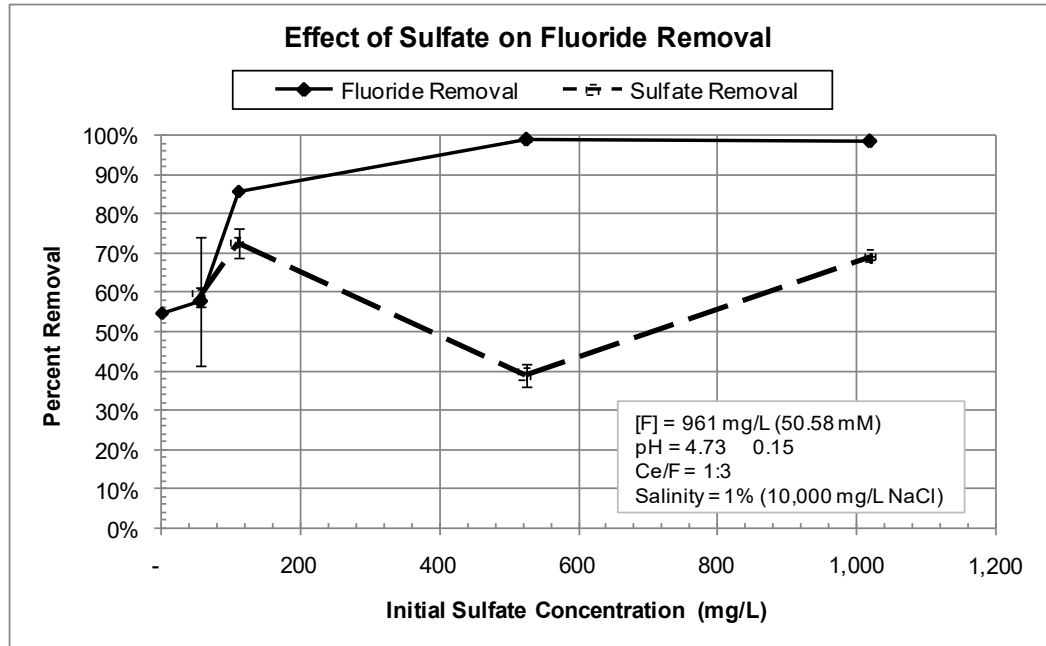
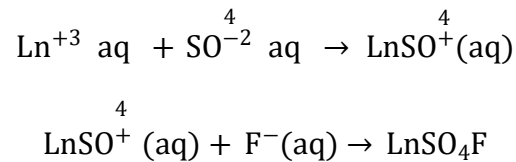


Figure 13: Fluoride and sulfate removal as a function of increasing initial sulfate concentration at initial fluoride concentration of 961 mg/L, molar ratio Ce/F of 0.33, 1% salinity and final pH of 4.73 ± 0.15.

The results show increasing fluoride removal with increasing sulfate concentration. The highest fluoride (>90%) removal was achieved for sulfate concentrations > 500 mg/L. By increasing the sulfate concentrations from 500 mg/L to 1000 mg/L, no additional fluoride removal was observed. Remaining sulfate concentrations show that sulfate was also removed and corresponded with increased fluoride removal. The highest sulfate (80%) removal was observed for the initial sulfate concentration of 100 mg/L. The initial hypothesis, in this thesis, was that sulfate would suppress fluoride removal because of reported negative impacts of sulfate on fluoride removal by adsorption. However, the data show the opposite. Increasing sulfate concentrations, up to 500 mg/L promoted increased fluoride removal from 55% (i.e. with no sulfate present) to over 90% at sulfate concentrations >50 mg/L. One of the

characteristics of cerium is that it forms many complexes (Wood, 1990). In the presence of sulfate ions, the formation of cerium complex, $CeSO_4^+$, may be observed.

Furthermore, Wood (1990), in a review of complex formation with REEs, concluded that various lanthanide elements (i.e. generally referred as to Ln to signify the lanthanide element) form complexes with sulfate; the most common complexes are $Ln(SO_4)_2^-$ and $LnSO_4^+$ in groundwater. The literature reveals that in the absence of other ions and with predominantly sulfate ions in water, $LnSO_4^+$ would be the dominant species. The Ln-sulfate complex, $LnSO_4^+$, occurs at sulfate concentrations of 10^{-4} M (9.6 mg/L) to 10^{-2} M (960 mg/L). At sulfate concentrations greater than 10^{-2} M, $Ln(SO_4)_2^-$ is the dominant species (Wedepohl, 1978; Wood, 1990). Wood (1990) cites work by Bilal and Koss (1982) and, Sinha and Moller (1983) that proposes the formation of mixed complexes, including carbonate ($Ln(CO_3)_nF$) and hydroxide of cerium. Although there is no confirmation of their existence in the literature, the possible formation of such complexes of fluoride could be expressed as:



Equation 18: Complex formation of lanthanides (expressed as Ln) with sulfate and then with a fluoride ion (Haas et al., 1995).

Similar to what is observed with the addition of coagulants such as alum and ferric chloride, when cerium chloride is added to water, it forms cerium hydroxide. Therefore, fluoride removal can be explained by two mechanisms, direct precipitation by the formation of cerium fluoride (CeF_3) and adsorption onto the surface of cerium

hydroxide. Tokunaga et al. (2007) has proposed potential mechanisms for fluoride removal through ion-exchange and adsorption means onto lanthanum oxide. Other researchers have also investigated adsorption mechanisms using REE oxides (Na & Park, 2010; Raichur & Basu, 2001). Although there is much literature that demonstrates REE complex formation (Wood, 1990; Wedepohl, 1978), such as the complexes of cerium with sulfate, there is not much information that supports the increased removal of fluoride in the presence of high sulfate concentrations. However, a relatively recent study by Kovacs et al. (2009) shed some light into the reactions between cerium fluoride and sulfate. They found that sulfate decreases the surface charge of the cerium fluoride particles enhancing the possibility of coagulation (Kovacs et al., 2009). In this study, the results show greater fluoride removal in the presence of sulfate. Independent of the exact mechanisms that promoted such outcome; these findings are significant to water treatment. For industrial wastewaters with high fluoride, addition of sulfate can promote better fluoride removal, using stoichiometric ratio of Ce/F.

Although many waters contaminated with high fluoride concentration do not contain significant amounts of phosphate, the fact that cerium forms strong complexes with phosphate supports the investigation of whether phosphate can promote higher fluoride removal. Cerium chloride has been shown to remove phosphate extremely well from wastewaters containing high and low concentrations of phosphate (Strileski, 2013). Figure 14 shows the effect of phosphate on fluoride removal for a pH of 4.75, 1% (10,000 mg/L) salinity, a fluoride concentration of 1,000 mg/L, and a Ce/F of 0.33.

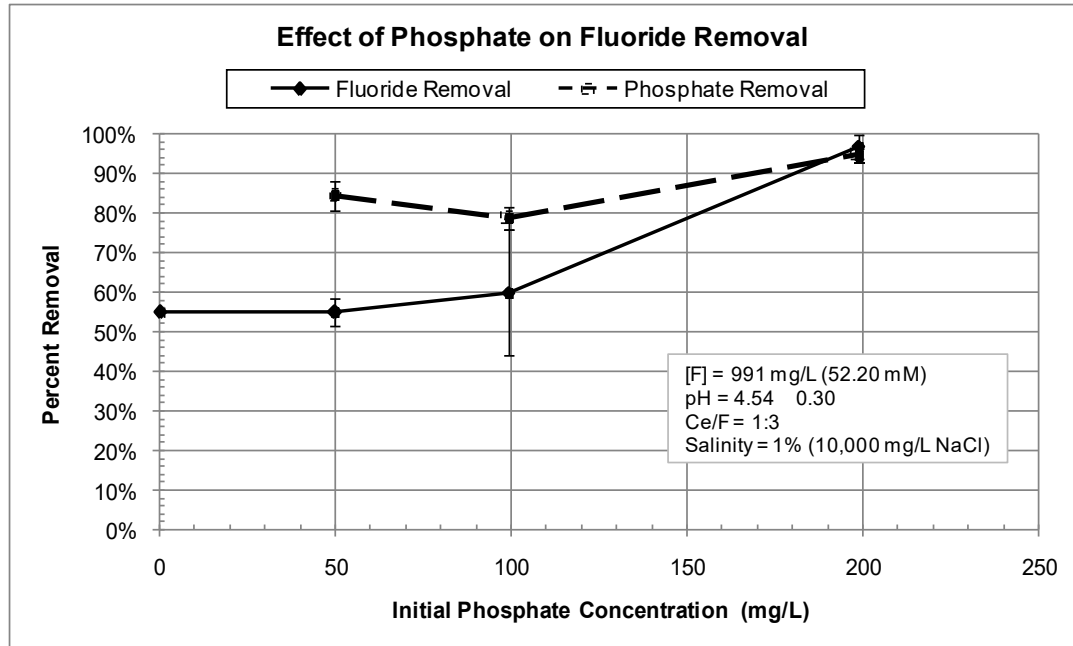
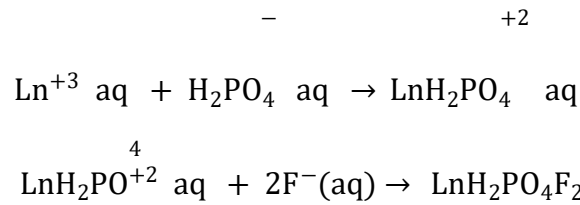


Figure 14: Fluoride and phosphate removal as a function of increasing initial phosphate concentration at initial fluoride concentration of 991 mg/L, molar ratio Ce/F of 0.33, 1% salinity and final pH of 4.54 ± 0.3.

The removal efficiency of fluoride increased following the increased phosphate concentration in water (Figure 14). The highest fluoride (98%) removal efficiency was achieved for initial phosphate concentration of 200 mg/L. Highest phosphate (98%) removal was achieved for initial phosphate of 200 mg/L.

One of the most important characteristic of lanthanides is their ability to react with phosphate to form mixed complexes (Wood, 1990). In most acidic waters, lanthanide reacts with phosphate to form the complex ion, $\text{LaH}_2\text{PO}_4^{2+}$ (Wood, 1990). Mayer and Schwartz (1950) identified the formation of CePO_4 in natural waters; however, this finding was not validated and was deemed to be incorrect (Mayer & Schwartz, 1950; Wood, 1990). Although there no literature identifying mixed complex formations of phosphate and fluoride, one can express the potential formation of such complexes as:



Equation 19: Equation for lanthanide complexes with phosphate and with fluoride in natural waters (Haas et al., 1995).

Previous studies by Yang et al. (2001) and Islam and Patel (2007) determined that presence of phosphates in water inhibits fluoride removal when calcium chloride and quick lime (Yang et al., 2001; Islam & Patel, 2007) are used. They identified that for the removal of fluoride with quick lime the presence of anions reduced fluoride removal in the order of, phosphate > sulfate > nitrate (Islam & Patel, 2007).

This is the opposite of that observed for cerium chloride. While coagulants like lime are negatively impacted by the presence of phosphate and sulfate, at lower pH values and using cerium chloride, higher removals of fluoride are observed in the presence of sulfate (Figure 13) and of phosphate (Figure 14).

Evaluation of phosphate removal shows its decrease in solution corresponding with increased fluoride removal. The concomitant removal of phosphate and fluoride removal can be explained by two mechanisms, co-precipitation by both simultaneous formation of cerium fluoride (CeF_3) and cerium phosphate (CePO_4) and adsorption onto the surface of cerium hydroxide, as previously identified for sulfate. In addition to the aforementioned mechanisms, the formation of phosphate complexes provides the opportunity for the formation of additional complexes with fluoride and/or adsorption to these complexes (Wood, 1990). However, there is very limited literature identifying such

mixed complex formations for REEs, phosphate and fluoride (Wood, 1990; Wedepohl, 1978).

Even though literature suggests REE form complexes, there are no available studies identifying the effect of increasing phosphate concentrations in aiding fluoride removal. In this research, higher fluoride removal was achieved at higher phosphate concentrations. Regardless of the removal mechanism using cerium chloride, in wastewaters containing high fluoride, addition of phosphate and sulfate could aid better removal as seen in this study. These findings can result in a treatment technology enhancement for industrial wastewaters containing high fluoride concentrations. Tables 20 and 21 show molar concentrations in all batch experiments.

Table 20: Distribution of sulfate, fluoride and cerium for batch tests examining the impact of sulfate on fluoride removal by cerium chloride precipitation

#	Ce ³⁺ (mM)	Fluoride			Sulfate		
		Initial (mM)	Final (mM)	Removal (%)	Initial (mM)	Final (mM)	Removal (%)
1	18	53.2	23.92	55.0	-	-	-
2	18	53.9	22.21	57.8	0.60	0.23	60.7
3	18	52.1	20.55	85.9	1.10	0.26	77.3
4	18	45.8	0.60	98.8	5.70	3.33	41.8
5	18	47.9	0.88	98.4	10.6	3.31	68.9

Table 21: Distribution of phosphate, fluoride and cerium for batch tests examining the impact of phosphate on fluoride removal

#	Ce^{3+} (mM)	Fluoride			Phosphate		
		Initial (mM)	Final (mM)	Removal (%)	Initial (mM)	Final (mM)	Removal (%)
1	18	53.2	23.92	55.0	-	-	-
2	18	52.6	22.21	57.8	0.90	0.04	60.7
3	18	50.0	20.55	58.9	1.77	0.41	77.3
4	18	50.3	0.60	98.8	8.77	1.11	41.8
5	18	55.3	0.88	98.4	16.5	0.50	68.9

Assuming that REE mixed complexes are formed, either with phosphate or sulfate, the data show that both sulfate and phosphate are limiting reactants. Evaluating molar concentrations of sulfate (Table 20) and phosphate (Table 21), fluoride removal was only achieved if either sulfate or phosphate is greater than 1 mM. As previously mentioned, there is no literature suggesting formation of higher form of mixed complexes with phosphates and sulfates. Evaluating the final sulfate (Table 20) molar concentrations, approximately 3 mM was remained non-reacted for samples 4 and 5. The tables do suggest two possible fluoride removal mechanisms: co-precipitation with sulfate or phosphate at molar concentrations <1 mM and adsorption onto cerium hydroxides, and complexes at molar concentrations >1mM.

The presence of nitrate in high concentrations in wastewaters containing fluoride is not well documented. However, waters from the metal and oil processing industries, which may contain fluoride, contain high concentrations of ammonium that can be converted to nitrate, depending on the treatment used (Wang et al., 2008). To evaluate the impact of nitrate on fluoride removal, nitrate solutions were used. Figure 15 shows the

fluoride removal efficiency as the nitrate concentration was increased with following water characteristics: initial fluoride concentration of 1,000 mg/L, 1% salinity, pH of 4.75, and a Ce/F ratio of 0.33.

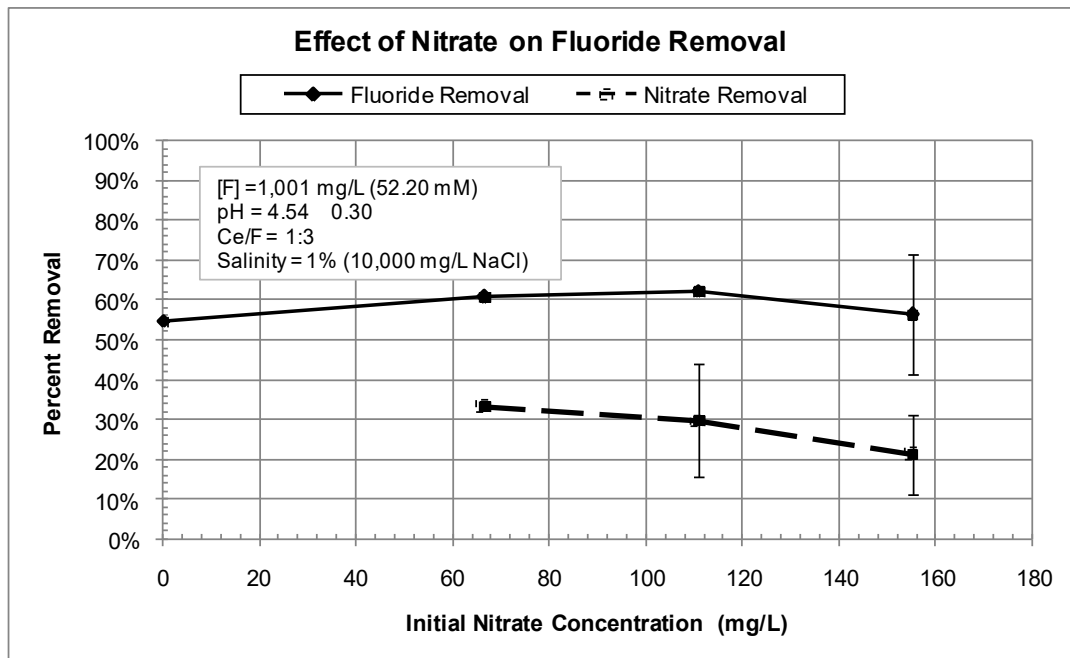


Figure 15: Fluoride removal as a function of increasing nitrogen concentration at an initial fluoride concentration of 1,001 mg/L, molar ratio Ce/F of 0.33, 1 % salinity, and final pH of 4.54 ± 0.24..

Based on the results, nitrate has no or little effect on fluoride removal. Fluoride removals ranged from 57% to 60%. With the addition of cerium chloride, very little nitrate removal was achieved. The literature indicated that nitrate only forms weak complexes with cerium (Wood, 1990). The most acceptable complex for lanthanides and nitrate is LnNO_3^{+2} . Due to relatively low stability constants, formation of LnNO_3^{+2} and other complexes of nitrates are negligible in most waters (Wood, 1990).

The literature also indicates REE forms very weak complexes with chloride. The acceptable lanthanides and chloride complex is LnCl_2^+ (Wood, 1990). Lanthanide and chloride complexes are not very stable in natural waters. However, these complexes appear in brine solutions with salinities greater than seawater ($> 30,000 \text{ mg/L}$)(Wood, 1990). In this study, the salinity was fixed at 1% (10,000 mg/L as NaCl); therefore, in such cases, chloride complexes with lanthanides can be neglected.

The impacts of carbonate alkalinity on fluoride removal were also evaluated because it is known that cerium (III) can form precipitates and complexes (e.g. $\text{Ce}_2(\text{CO}_3)_3$ (s), CeCO_3^+ , and $\text{Ce}(\text{CO}_3)_2^-$) with carbonate (Ferri et al., 1983). Researchers have suggested complex formation of LnCO_3^+ and LnHCO_3^{+2} in natural waters (Wedepohl, 1978; Wood, 1990; Haas et al., 1995; Cetiner & Xiong, 2008). Cetiner and Xiong (2008) identified the complex species, LnCO_3^+ and $\text{Ln}(\text{CO}_3)^{-1}$, which can be formed above neutral pH (Cetiner & Xiong, 2008).

Figures 16 and 17 show the impact of bicarbonate on the removal of fluoride for a fixed Ce/F ratio and 1% salinity. As the bicarbonate concentration increased, the final pH increased from 5.94 for 100 mg/L HCO_3^{-1} to 8.12 for 10,000 mg/L HCO_3^{-1} . Therefore, the removals shown in Figures 16 and 17 are for different pH values. The fluoride removal was decreasing likely because the cerium was being used to form cerium bicarbonate, cerium carbonate and related complexes.

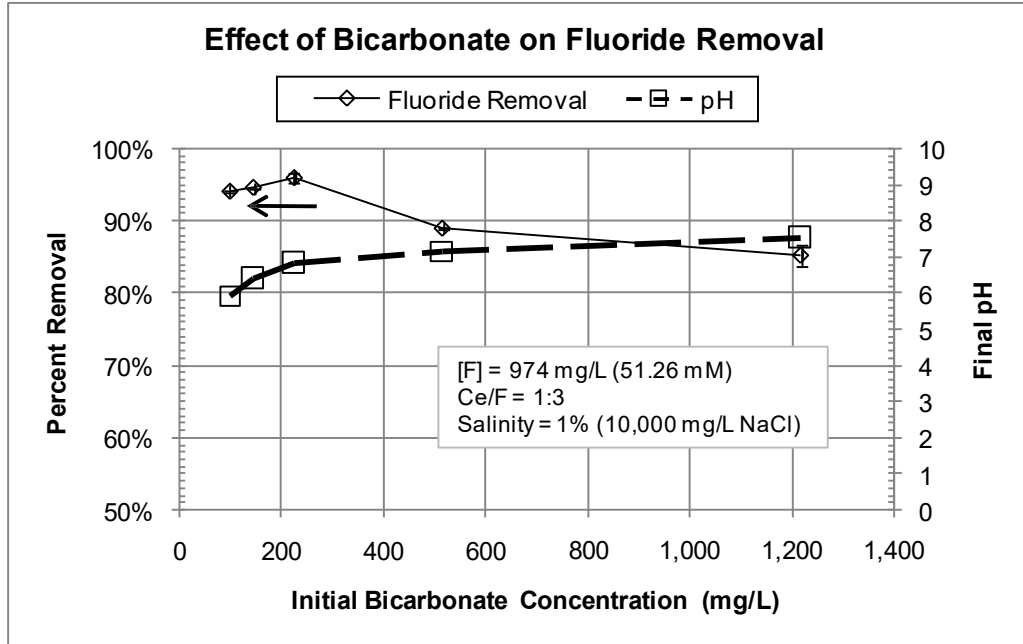


Figure 16: Effect of bicarbonate on fluoride removal with an initial fluoride concentration of 974 mg/L and Ce/F ratio of 0.33 and with initial bicarbonate concentrations from 50 to 1250 mg/L as HCO_3^{-1}

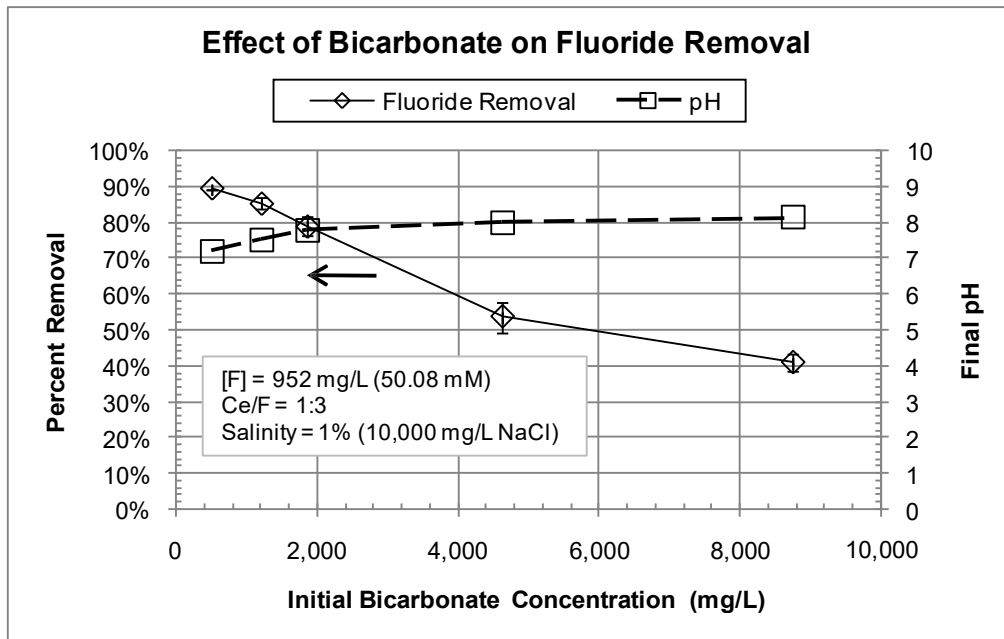


Figure 17: Effect of bicarbonate on fluoride removal with an initial fluoride concentration of 952 mg/L and Ce/F ratio of 0.33 and with initial bicarbonate concentrations from 500 to 8,900 mg/L as HCO_3^{-1}

The results show that the presence of bicarbonate alkalinity has a negative impact on fluoride removal with cerium chloride. With alkalinity less than 200 mg/L, the fluoride removal efficiency was effective. However, increasing the alkalinity from 500 mg/L to 9,000 mg/L, decreased the overall fluoride removal efficiency from 90% to 40%, respectively.

The impact of alkalinity on fluoride removal was also evaluated using varying Ce/F ratios. Fluoride removal efficiencies as a function of molar ratio and initial alkalinity are depicted on Figure 18.

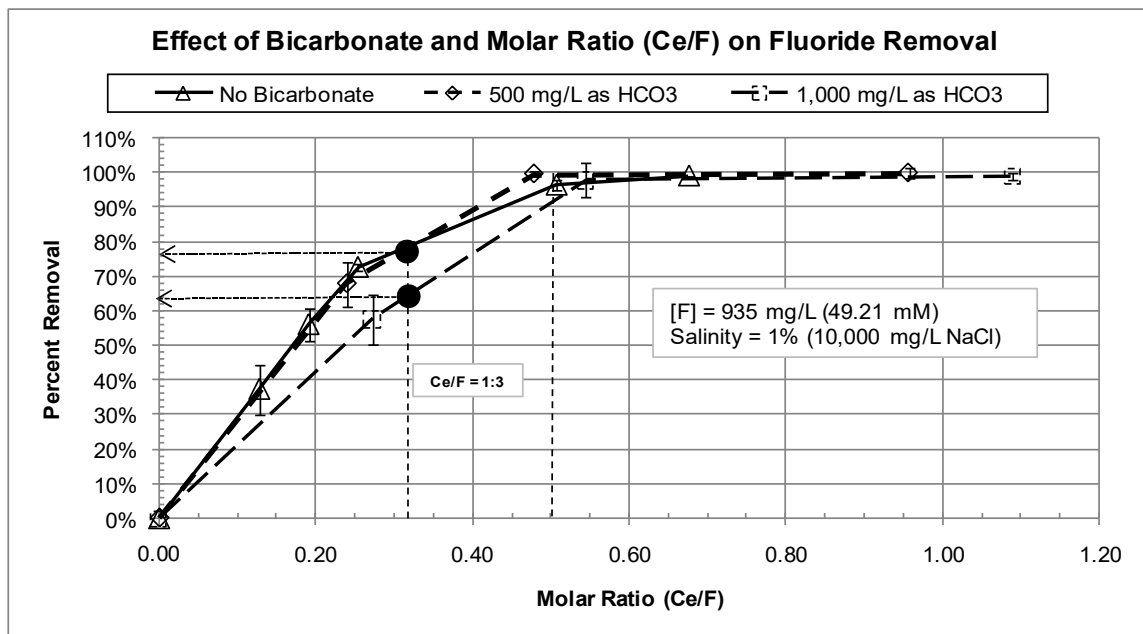


Figure 18: Fluoride removal as a function of Ce/F molar ratio and varying initial alkalinities, with constant initial fluoride concentration, and 1% salinity.

With no alkalinity present and for a fixed pH of 4.75, fluoride removal increased with increasing ratio up to a Ce/F ratio of 0.5. For higher ratios, no improvement on

removal was observed. The results show that the presence of alkalinity has a slight negative impact on fluoride removal for on stoichiometric Ce/F ratio of 0.33. Increasing the cerium dose (i.e. Ce/F molar ratio) above stoichiometric ratio, the overall fluoride did increase from 78% to 98% at a molar Ce/F ratio of 0.50. The controlled solution (without bicarbonate) showed similar results as the samples with 500 mg/L bicarbonate. A 78% removal was achieved for both samples. The fluoride removal in the presence of 500 mg/L bicarbonate was higher than that for 1,000 mg/L bicarbonate (70% removal). The reason for the lower removal of fluoride in the presence of higher alkalinity is a higher pH value as shown in Figure 19.

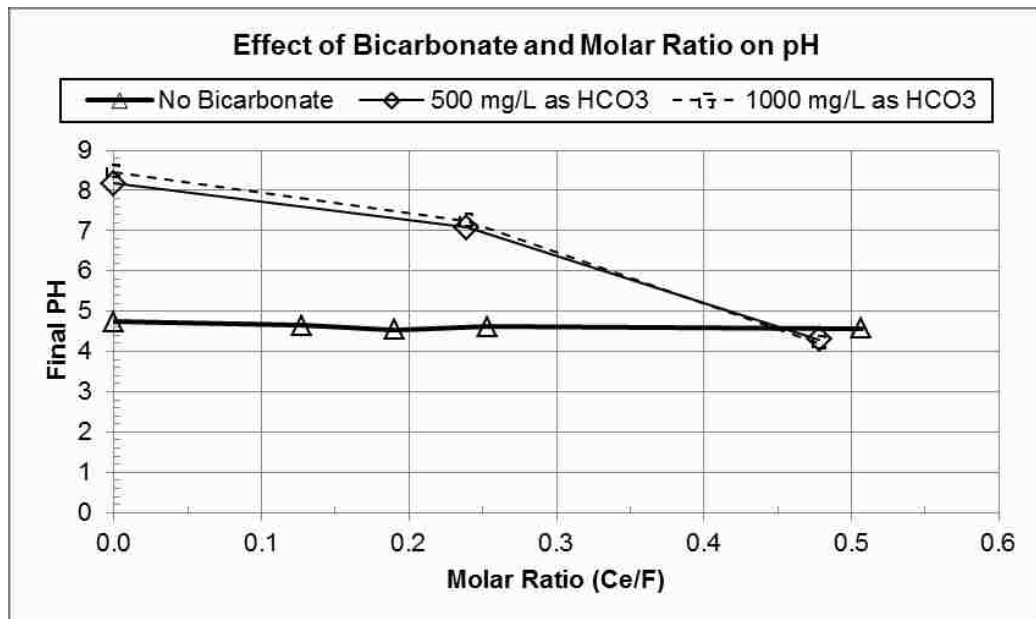


Figure 19: Final pH solution as a function of Ce/F molar ratio and varying initial alkalinities, with constant initial fluoride concentration, and 1% salinity.

Figure 19 shows that by increasing the molar Ce/F ratio, the pH of the solution decreased significantly. Based on these results, cerium chloride consumes a significant

amount of alkalinity that resulted in pH depression. The highest achievable fluoride (94%-98%) removal for all samples was determined at a molar ratio of 0.50, at which the final pH of the solution was reduced to 4.20. This suggests that pH adjustment is necessary for wastewaters with high alkalinity. In this study, it was determined that the optimal working pH for cerium chloride, to be effective, was 4.75.

4.5. Testing the Impact of Alkalinity on Fluoride Removal Using an Actual Fluoridated-Industrial Wastewater

To determine the effectiveness of cerium chloride in removing fluoride from industrial wastewater, an actual wastewater from the oil reprocessing industry was experimented with for fluoride removal in the presence of high alkalinity. The wastewater sample had initial fluoride concentration of 41 mg/L, extremely high alkalinity (100,000 mg/L as CaCO₃), and a pH of 13. Water quality characteristics for this wastewater sample are shown in Table 13 (Chapter 3-Materials and Methods).

A very striking result is obtained when cerium chloride is added to the wastewater. A very high amount of sludge is formed as a result of precipitation of supposedly cerium hydroxide and cerium carbonate (Figure 20).



Figure 20: Sludge production with increasing cerium dose on SCS solution, with initial fluoride concentration 41 mg/L.

The amount of sludge generated increases almost proportionally to the cerium chloride added (Figure 21). Figure 22 shows the removal of fluoride with increasing cerium chloride. As noted, no fluoride was removed. The reason is the extremely high concentration of alkalinity that is using up the cerium to form sludge.

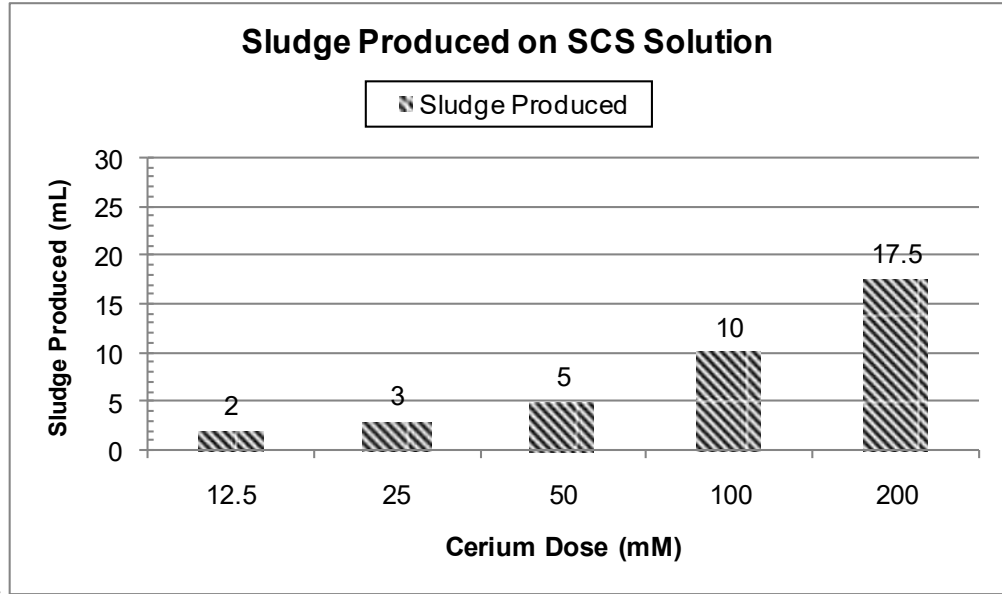


Figure 21: Sludge production and distribution, as a function of cerium dose (12.5, 12, 50, 100, and 200 mM).

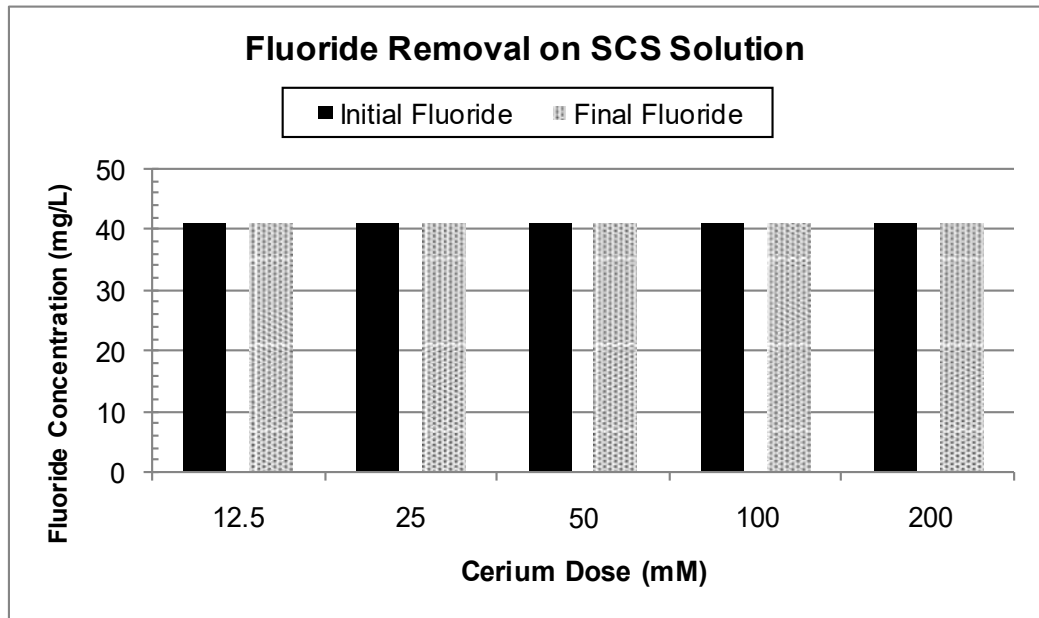


Figure 22: Fluoride removal efficiency as a function of cerium dose, with an initial fluoride concentration of 41 mg/L.

Even with an increasing dose of cerium chloride (i.e. as Ce (III)), the results showed no fluoride removal for this particular wastewater. It has been determined experimentally, that the optimal pH for fluoride removal was 4.75. For cerium chloride to be effective, pH adjustment is necessary for high alkalinity solutions by using strong acids (e.g. sulfuric acid or hydrochloric acid). Alkalinity must first be consumed to bring down the pH (<6.50) within the working condition. Hence, alkalinity has a direct effect on fluoride removal when cerium chloride is used.

CHAPTER 5: REMOVAL OF PHOSPHATE USING CERIUM CHLORIDE IMPREGNATED MEDIA

RESULTS AND DISCUSSION

Previous studies performed by UNLV using lanthanum chloride (Strileski, 2013) and others (Na & Park, 2010; Raichur & Basu, 2001; Zhang et al., 2012) have demonstrated that REEs remove phosphate very well from water. Preliminary testing performed for this research revealed, as expected, that cerium chloride (i.e. Sorbx-100), which is chemically very similar to lanthanum chloride, is also an excellent coagulant for phosphate removal. Although cerium chloride, in aqueous form, can be directly added to waters for this purpose, its impregnation to a solid media would increase its usefulness because such media could be used in granular filtration.

Following are results of column adsorption experiments performed using various media (i.e. GAC, zeolite, and anthracite) impregnated with Sorbx-100 for phosphate removal. One-hundred milliliters of GAC, anthracite, and natural zeolite were rinsed multiple times with distilled water. Once all the media were left to dry for 24 hours, 15 mL of Sorbx-100 was added to each 100 mL media. Depending on the preparation (Table 22), 15 mL of potassium hydroxide (KOH) was added and followed by air or oven dehydration. Some samples were then placed in a furnace and heated for a specific amount of time. The summarized preparations for the column testing are as follows:

Table 22: Media Preparation for Column Testing Using Activated Carbon and Anthracite, and Natural Zeolite

Parameter	Preparation				
	#1	#2	#3	#4	#5
Media Content			Sorbx-100	Sorbx-100	Sorbx-100
Preparation	None	Sorbx-100	0.10 N KOH	0.10 N KOH	0.10 N KOH
0.10 N KOH					
Volume (mL)	None	None	15	15	15
Sorbx-100					
Volume (mL)	None	15	15	15	-
Sorbx-100					
Concentration (M)	None	2.09	2.09	2.09	0.40
Media	GAC Anthracite	GAC Anthracite	GAC Anthracite	GAC Anthracite	GAC Zeolite
Drying Method	None	Air-dried (24-hr)	Air-dried (24-hr)	Air-dried (24-hr)	Oven-dried (24-hr)
Furnace-Drying Temperature (°C)	None	None	None	400°C (30 min)	600°C (30 min)
HRT (min)	0.60- 1.00	0.60- 1.00	0.60- 1.00	0.60- 1.00	1.20 2.20

All columns were run with an average contact time of 0.6 to 1.0 minute, except for the media of preparation 5, which ran with a hydraulic retention time of 1.50 and 2.20 minutes for zeolite and 1.20 to 1.30 minutes for GAC. Since literature suggested HRT affects adsorption, HRT was increased from 1.20 to 2.20 min. However, it was not evaluated further. Columns were run with 10 g of prepared media using 1-inch diameter plastic column fed with a peristaltic pump.

5.1. Adsorption of Impregnated Anthracite

Figure 23 shows effluent/influent phosphate concentration ratios (C/C_0) relative to the bed volumes of phosphate solution passed through the treated anthracite media.

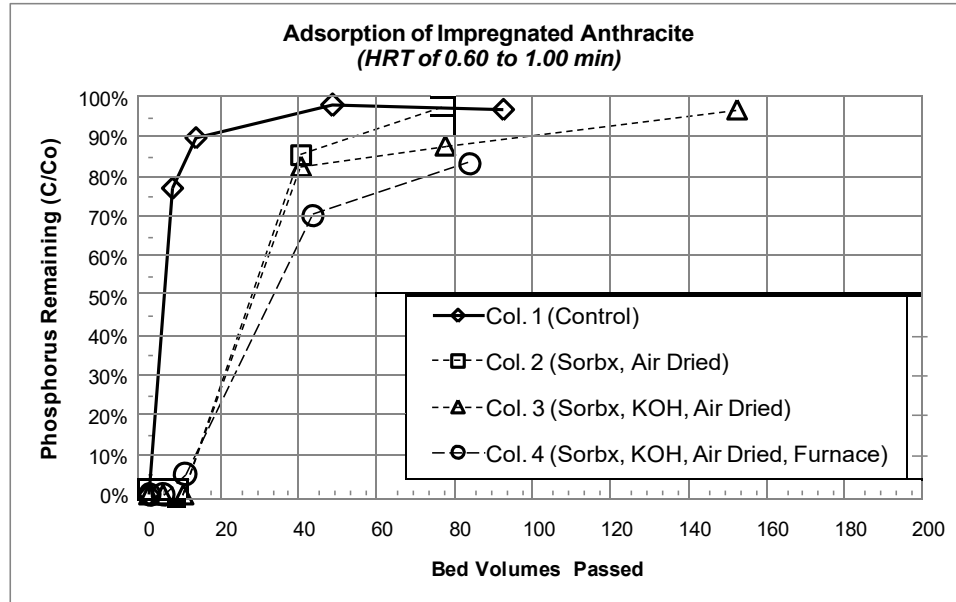


Figure 23: Relationship between C/C_0 and bed volumes passed (anthracite) with feed concentration (C_0) of 3 ppm PO_4^{3-} -P (C =effluent concentration, C_0 =influent/feed concentration). The column was then run with an average hydraulic retention time of 0.60 to 1.00 minute.

The data show that less than 20 bed volumes could be processed before breakthrough of phosphate in the effluent. All four treatments types were proven to be insufficient to promote significant phosphate removal. Neither the impregnation of anthracite with Sorbx-100 and potassium hydroxide, nor the furnace-dried impregnated anthracite at 400°C improves the removal of phosphate. The column reached breakthrough after approximately 15 bed volumes. It was observed during anthracite media preparation that significant aggregation of the material occurred. It was also observed that a large amount of cerium chloride solution that was used for impregnation

did not attach well to the media – a large amount of it was retained on the beaker, where the media and solution were mixed. Therefore, anthracite impregnation with cerium chloride is not a feasible process. As previously mentioned, cerium chloride is very acidic with a typical pH around 3.2 to 3.50. One of the weaknesses of anthracite media is its susceptibility to acid. In filtration systems, the potential for loss of anthracite material is determined by using an acid solubility method (Beverly, 2011). Anthracite is easily degraded when in contact with acidic or oxidizing solutions (Beverly, 2011), which explains its poor cerium chloride adsorption capacity.

5.2. Adsorption of Impregnated Natural Zeolite

Figure 24 shows that zeolite impregnated with Sorbx-100 did not remove phosphate well and breakthrough was reached after about 5 bed volumes.

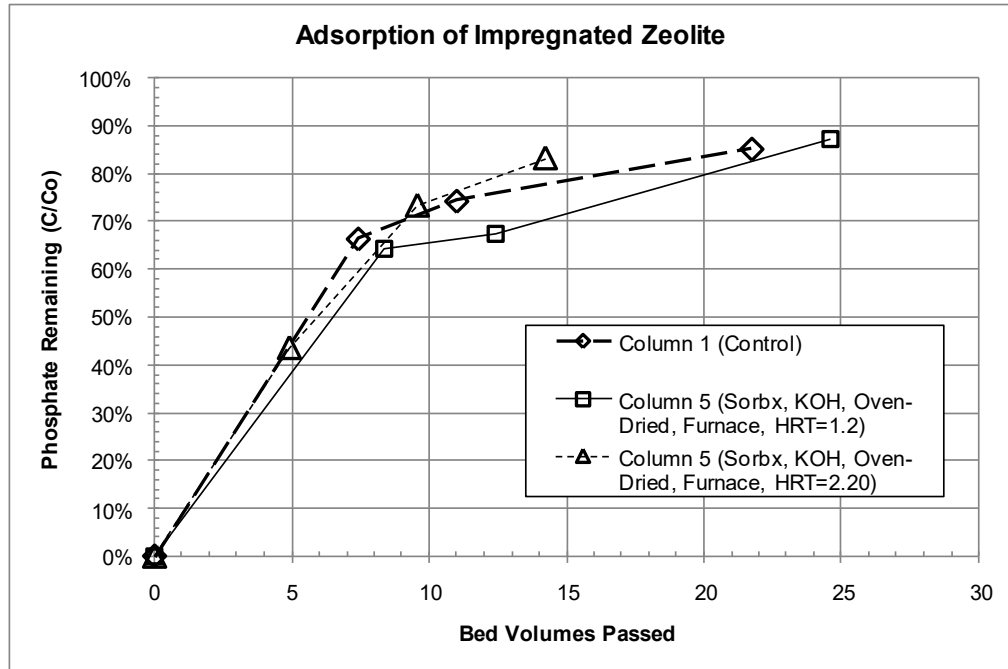


Figure 24: Relationship between C_3/Co and bed volumes passed (modified zeolite preparation) with feed concentration (Co) of 3 ppm $PO_4^{3-}P$ (C =effluent concentration, Co =influent/feed concentration).

The same procedures were followed for the column 5 (preparation #5). Two separate runs were performed with HRT of 1.2 min and of 2.0 min. However, even with a slower HRT (1.2 min), the column broke through after 5 bed volumes. Therefore, Sorbx-100 impregnation of zeolite did not result in media that can be used for phosphate removal.

5.3. Adsorption of Impregnated GAC

Fresh or Sorbx-impregnated granular activated carbon (GAC) were used for the column tests. Figure 25 shows no significant increase in bed volumes processed through the column for phosphate removal, when using GAC impregnated with Sorbx-100 alone under various conditions. However, the results show significant improvement in

phosphate removal when the GAC was heated at higher temperatures that allow for the formation of cerium oxide. About 120 bed volumes could be processed before breakthrough, demonstrating that impregnation of GAC followed by furnace-dehydration at 600°C is a feasible way to impregnate GAC to be used in filters to remove phosphate.

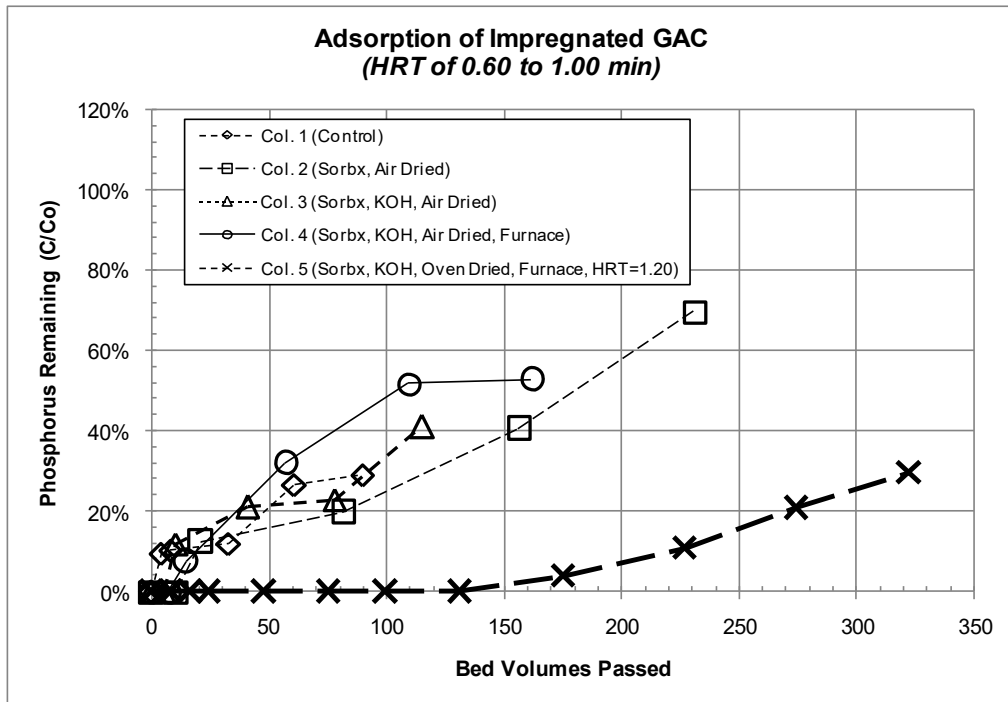


Figure 25; Relationship between C/Co and bed volumes passed (GAC) with feed concentration (Co) of 3 ppm PO₄³⁻-P (C=effluent concentration, Co=influent/feed concentration).The column was then run with an average hydraulic retention time of 0.60 to 1.2 (#5) minutes.

The results show significant improvement in phosphate removal when the GAC is heated at higher temperatures – column #4 at 400°C and column #5 at 600°C - that allowed for the formation of cerium oxide. The formation of cerium oxide under these conditions was confirmed by X-ray diffraction (Figure 26). For column #5, with an HRT of 1.20 minutes and furnace-dehydration at 600°C, approximately 120 bed volumes could be processed before breakthrough demonstrating that impregnation of GAC followed by

furnace-dehydration at 600°C may be a feasible way to adsorb cerium to the media and use it for the removal of phosphate. Therefore, with modified activated carbon furnace-heated at 600°C, at an HRT of 1.20 min, impregnation of GAC with cerium chloride seems to be a more feasible approach than for the other media tested. It is important to note that larger bed volumes of phosphate solution were processed with the impregnated media with somewhat longer HRT values. The impact of retention time on the impregnated media deserves further consideration, and it was not evaluated in this research.

For column #5 with an HRT of 1.20 minutes and furnace-dried at 600°C, the effluent samples were analyzed for cerium to determine any leakage. The cerium concentration in the effluent was measured using ICP at the Molycorp facility at Mountain Pass. Figure 26 shows the tracer cerium analysis for modified GAC preparation.

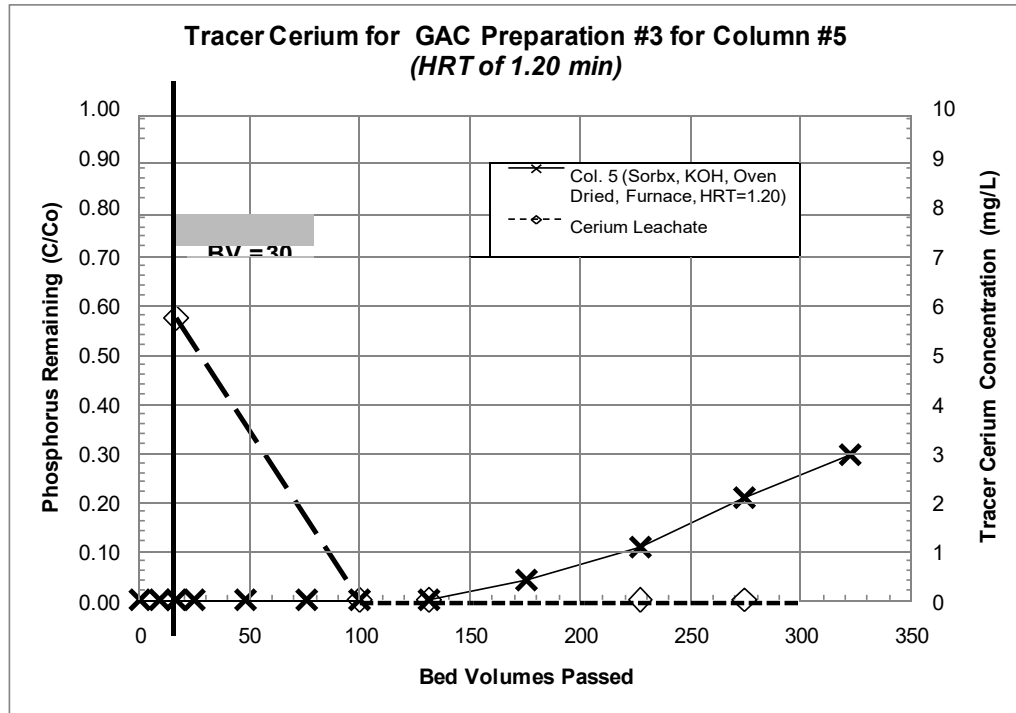


Figure 26: Tracer cerium analysis for modified GAC preparation (#5) as a function of phosphate ($\text{PO}_4^{3-}\text{-P}$) remaining.

After approximately 30 bed volumes, significant amount of cerium washed out of the media into the water phase. A significant loss of cerium solution was already observed during the preparation of all media. Figure 26 shows that cerium is leaking out of the GAC and promoting low phosphate removal. Although GAC impregnation worked better than for the other media, the process attempted does not work well. Typical activated carbon has thousands of square feet of internal surface area per gram of carbon. This is significantly larger than those of anthracite and zeolite. Even though this suggests feasibility for impregnation of GAC with cerium chloride, a significant amount of cerium was observed being washed out of the column hindering the process. Therefore, the results of this study show that cerium chloride impregnation to typical

filter media is not feasible. Adding liquid cerium chloride to the water and then using sedimentation or filtration to separate the sludge formed should then be the choice.

It is disappointing that cerium chloride cannot be impregnated to typical filter media because of its potential use in water treatment. As it was demonstrated in Chapter 4, cerium chloride is a good coagulant for fluoride removal. Fluoride is present in many rural and economically depressed regions of Africa and India. If one could impregnate media with cerium chloride, then point of use technologies could be developed for use in such regions.

5.4. Results of XRF Analysis and Oxide Distribution

XRF analysis results of GAC impregnated with cerium chloride using various preparations are shown in Figure 27. The analyses identified cerium oxide, lanthanum oxide, and other oxides presented in the prepared media. Other researchers have identified rare-earth elements to form rare-earth oxides at temperature from 550°C to 635°C (Lee & Rees, 1987; Hashimoto et al., 1997; Zhang et al., 2012).

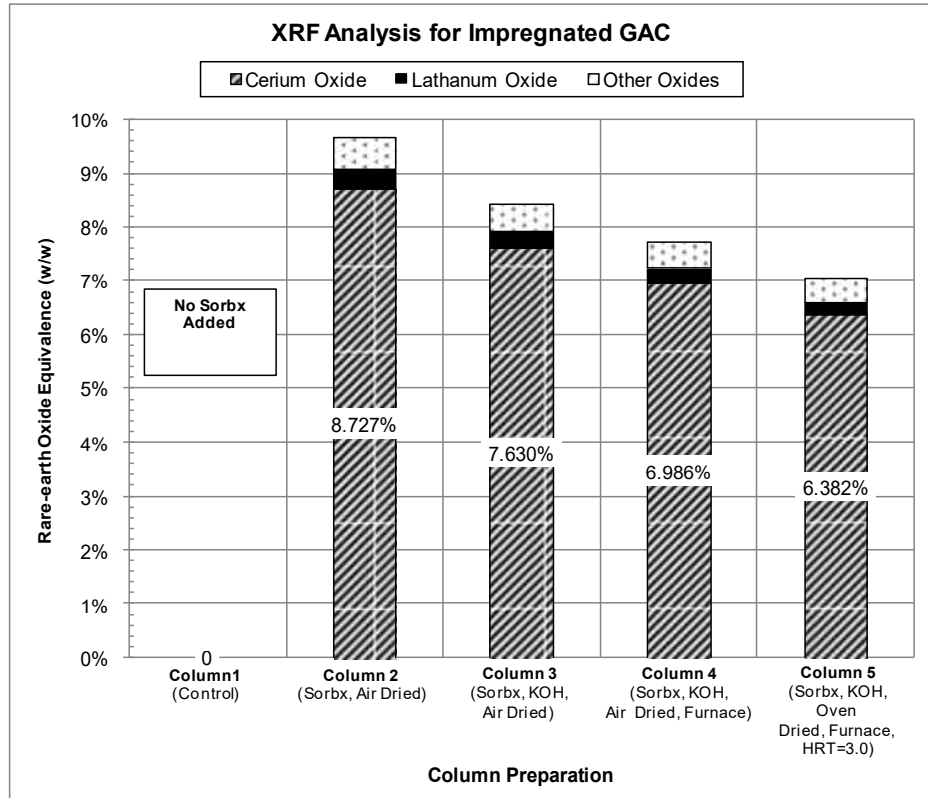


Figure 27: XRF analyses for all GAC preparation and identification of metal oxides on impregnated GAC

The analyses show that all media preparations resulted in the formation of some metal oxides. However, in this study, only limited formation of cerium oxides, lanthanum oxides, and various other Ln-oxides, were found in GAC. One possible explanation is the uneven distribution of cerium oxides on the media. The significant flaw in the estimation of removal is the assumption of even distribution of cerium chloride in the cavities of media (e.g. GAC). Therefore, in all cases, the preparations did not work effectively for cerium chloride impregnation.

CHAPTER 6: CONCLUSIONS, IMPLICATIONS AND FUTURE WORK

6.1. Conclusion

The objectives of this research were to evaluate the effectiveness of cerium chloride on the removal of both fluoride and phosphate from wastewaters. Batch experiments were performed to investigate fluoride removal. While the research on fluoride focus on using coagulation/precipitation, the research on phosphate removal focus on impregnating media with cerium chloride for use in wastewater filters.

The following conclusions can be draw from the results of this research:

1. The CCD model achieved an R-Squared = 0.8615 and adjusted R-Squared = 0.7368. The revised CCD model, where the non-significant coefficients were removed, estimated an R-Squared = 0.7884 and adjusted R-Squared = 0.7128. Based on the calculated responses of the CCD models, F-value are significantly greater than the F-critical. Furthermore, all P-values are less than P-critical ($P < 0.05$); therefore, the model is statistically significant. The CCD models forecast fluoride removals that are lower than those obtained experimentally. One limitation of the CCD model is that the cerium chloride dosage used assumes the formation of cerium fluoride (CeF_3) precipitate. It does not account for the formation of cerium hydroxide and cerium carbonate and the formation of cerium complexes that can promote fluoride removal by adsorption, rather than by precipitation. The optimal fluoride removal, based on the developed CCD model, was achieved at cerium doses of 12.50 mM and 25.0 mM and a pH of 4.75 to

5.00, regardless of the initial fluoride concentration. At lower pH (<2.00), the highest achievable fluoride removal is between 40% and 50%.

2. The effect of pH and cerium dose on fluoride removal was evaluated. Highest fluoride removal was achieved at a pH of 4.75 and 6.50. Below the pH of 4.75, less than 80% removal was achieved. Furthermore, at a pH greater than 7, fluoride removal deteriorated significantly and was less than 60%. Higher fluoride removal was observed with a higher cerium dose (25.0 mM), and lower removals were found for at a cerium dose of 6.25 mM.
3. For high fluoride concentrations (938 mg/L), 90% fluoride removal was achieved at a Ce/F molar ratio of 0.50. A 98% removal was achieved with molar ratio of 0.80. For 98 mg/L fluoride concentration, 90% removal was achieved with a Ce/F molar ratio of 1.2; no additional removal was achieved with molar Ce/F ratio >1.2. Therefore, high concentrations of fluoride required less dosages of cerium chloride.
4. Higher fluoride removals were achieved with the addition of sulfate and phosphate. The presence of nitrate showed no impact on fluoride removal. The positive impact of sulfate and phosphate and lack of impact of nitrate on fluoride removal can likely be attributed to the formation of complexes of these ions with cerium. The formation of strong complexes of cerium (III) and sulfate and phosphate. However, cerium (III) forms weak complexes with nitrate have been documented. In addition, it has been documented that fluoride can adsorb to the surface of oxides and hydroxides, including those formed by the addition of REEs, such as cerium chloride.

5. Fluoride removal, as investigated in this study can be attributed to two mechanisms: direct precipitation by the formation of cerium fluoride, and adsorption of fluoride ions onto the surfaces of cerium hydroxides or the formation of complexes with other ions.. The formation of various REE complexes have been investigated and reported in the literature including those of phosphate (e.g. $\text{LaH}_2\text{PO}_4^{2+}$, CePO_4) and sulfate (e.g. LnSO_4^+).
6. The presence of carbonate alkalinities $>1,000$ mg/L negatively impacted fluoride removal. At higher alkalinities ($>1,000$ mg/L), a lower fluoride removal was observed. Cerium (III) can form precipitates and complexes (e.g. $\text{Ce}_2(\text{CO}_3)_3(\text{s})$, CeCO_3^+ , and $\text{Ce}(\text{CO}_3)_2^-$) with bicarbonates and carbonates. The results show that fluoride removal is inversely proportional to the amount of alkalinity present. Therefore, fluoride removal is lower at high alkalinity, because cerium (III) is consumed to form cerium carbonates and its complexes. Therefore, water with high carbonate and hydroxide alkalinities are poor candidates for fluoride removal with cerium chloride, unless the pH of the water is lowered using strong acids. For an actual wastewater containing fluoride and high alkalinity, (100,000 as CaCO_3), a significant amount of sludge is observed when cerium chloride is added. The sludge is the result of the precipitation of cerium hydroxide – $\text{Ce}(\text{OH})_3$ and cerium carbonate ($\text{Ce}_2(\text{CO}_3)_3$). No fluoride removal was observed for this water because cerium chloride addition resulted in the formation of precipitates, other than those of fluoride.
7. The impregnation of various media types with cerium chloride was proven unsuccessful. Only a small number of bed volumes of contaminated water were

processed through beds of the media, before breakthrough occurred. The most reliable impregnation methods consisted of calcinations of GAC at 600°C. Treated GAC was able to sustain the processing of more bed volumes of contaminated water than the other media. X-ray diffraction of the treated media revealed that cerium oxide was formed by the treatment technique used. In addition, measurement of cerium in the effluents of the columns showed that cerium was being washed out from the media. Therefore, all preparation techniques used were ineffective in keeping cerium attached to the media.

6.2. Implications of the Research Results to the Treatment of Industrial Waters Contaminated with Fluoride

When using cerium chloride (i.e. Sorbx-100) for fluoride removal, the addition of sulfate and phosphate may be practiced to improve fluoride removal. This study suggested the formation of REE complexes that can aid fluoride removal. Researchers (Wedepohl, 1978; Wood, 1990; Haas et al., 1995; Cetiner & Xiong, 2008) have identified the formation of these complexes. With sulfate and phosphate, smaller amounts of cerium chloride can be added to achieve high removals of fluoride. Waters contaminated with fluoride and that have high alkalinity are challenging to treat by cerium chloride addition. Fluoride removal is inversely proportional to the amount of alkalinity present in water; cerium will react with alkalinity to form sludge before it will react with fluoride. Treatment of these waters would require a significant amount of acid to lower the pH to dischargeable levels.

6.3. Future Work

Cerium is a very new coagulant that has only recently become available. The use of cerium as a water/wastewater coagulant is still in its infancy. Therefore, many interesting applications of cerium chloride are still to be discovered. There is much potential in REE-based coagulants, but additional research must be conducted including:

1. Evaluate the mechanisms involved in fluoride removal in the presence of sulfate, phosphate, and carbonate by examining the sludge formed by X-ray diffraction.
2. Investigate further the role of sulfate and phosphate on fluoride removal at different pH values.
3. Evaluate the role of sulfate and phosphate in the enhancement of fluoride removal.
4. Evaluate the impact of organics on coagulation process using cerium chloride
5. In the investigations involving the role of sulfate, phosphate, and carbonate, identifies the amount of cerium used in the processes.
6. Evaluate the appropriate cerium dose and molar ratio for the removal of high fluoride levels from water under extremely high alkalinity conditions.

REFERENCES

- American Cancer Association, 2013. *American Cancer Association*. [Online] Available at: www.cancer.org/cancer/cancercauses/othercarcinogens/athome/water-fluoridation-and-cancer-risk [Accessed 29 September 2014].
- Asghar, A., Abdul-Raman, A.A. & Wan-Daud, W.M.A., 2014. A Comparison of Central Composite Design and Taguchi Method for Optimizing Fenton Process. *The Scientific World Journal*, 2014, pp.1-14.
- Ayoob, S. & Gupta, K., 2006. Fluoride in drinking water: A review on the status and stress effects. *Environmental Science and Technology*, pp.433-87.
- Bahena, J.L.R., Cabrera, A.R., Valdivieso, A.L. & Urbina, R.H., 2002. Fluoride Adsorption Onto alpha-Al₂O₃ and its Effect on the Zeta Potential at the Alumina - Aqueous Electrolyte Interface. *Separation Science and Technology*, 1973-1987, p.37.
- Bas, D. & Boyaci, I.H., 2007. Modeling and Optimization I: Usability of Response Surface Methodology. *Journal of Food Engineering*, 78, pp.836-45.
- Batsala, M. et al., 2012. Inductively Coupled Plasma Mass Spectrometry (ICP-MS). *International Journal of Research in Pharmaceutical Sciences*, 2(3), pp.671-80. Available at: <http://www.ijrpc.com/files/14-2111.pdf>.
- Beverly, R.P., 2011. Filter Media. In *Filter Troubleshooting and Design Handbook*. American Water Works Association. pp.76-116.
- Bezerra, M.A. et al., 2008. Response Surface Methodology (RSM) as a Tool for Optimization in Analytical Chemistry. *Talanta*, 76(5), pp.965-77.
- Bezerra, M.A. et al., 2008. Response Surface Methodology (RSM) as a Tool for Optimization in Analytical Chemistry. *Talanta*, 76, pp.965-77.
- Bhatnagar, A., Kumar, E. & Sillanpaa, M., 2011. Fluoride Removal from water by Adsorption - A Review. *Journal of Chemical Engineering*, 171, pp.811-40.
- Bleiwas, D.I. & Gambogi, J., 2013. *Preliminary Estimates of the Quantities of Rare-Earth Elements Contained in Selected Products in Imports of Semimanufactured Products to the United States*. U.S. Geological Survey.
- Burkes, S. & McCleskey, C.S., 1947. The bacteriostatic activity of cerium, lanthanum, and thallium. *Journal of Bacteriology*, 54, pp.417-24.
- Castor, S.B. & Hedrick, J.B., n.d. Rare-Earth Elements. pp.769-92.

- Cetiner, Z.S. & Xiong, Y., 2008. Chemical Controls on the Solubility, Speciation and Mobility of Lanthanum at near Surface Conditions: A Geochemical Modeling Study. *Applied Geochemistry*, 23, pp.2301-15.
- Chang, M.F. & Liu, J.C., 2007. Precipitation Removal of Fluoride from Semiconductor Wastewater. *Journal of Environmental Engineering*, 133, pp.419-25.
- Christoe, J.R., 1976. Removal of Sulfate from Industrial Wastewaters. *Water Pollution Control Federation*, 48(12), pp.2804-08.
- Cottrell, T.L., 1958. *The Strengths of Chemical Bonds*. 2nd ed. Butterworth, London.
- CSU Dominguez Hills, n.d. *Selected Solubility Products and Formation Constants at 25C*. [Online] Available at: <http://www.csudh.edu/oliver/chemdata/data-ksp.htm> [Accessed 22 July 2015].
- Darwent, D.d., 1970. *Bond Dissociation Energies in Simple Molecules*. 31st ed. Washington: National Bureau of Standards.
- De Gregorio, C., Caravelli, A.H. & Zaritzky, N.E., 2011. Application of a Combined Biological and Chemical System for the Treatment of Phosphorus-containing Wastewater from the Food Industry. *Procedia Food Science*, 1, pp.1841-47.
- Drouiche, N. et al., 2012. Fluoride Removal from pretreated Photovoltaic Wastewater by Electrocoagulation: An Investigation of The Effect of Operational Parameters. *Procedia Engineering*, 33, pp.385-91.
- Drouiche, N. et al., 2008. Electrochemical treatment of chemical mechanical polishing wastewater: removal of fluoride — sludge characteristics - operating cost. *Desalination*, 223, pp.134-42.
- Ebeling, J.M., Sibrell, P.L., Ogden, S.R. & Summerfelt, S.T., 2003. Evaluation of Chemical Coagulation - Flocculation Aids for the Removal of Suspended Solids and Phosphorus from Intensive Recirculating Aquaculture Effluent Discharge. *Aquacultural Engineering*, 29(1-2), pp.23-42.
- Edmunds, W.M. & Smedley, P.L., 2013. Fluoride in Natural Waters. In O. Selinus, ed. *Essentials of Medical Geology: Revised Edition*. Springer Science & Business Media. pp.311-36.
- Fan, X., Parker, D.J. & Smith, M.D., 2003. Adsorption Kinetics of Fluoride on Low Cost Materials. *Water Research*, 37(20), pp.4929-37.

- Feenstra, L., Vasak, L. & Griffioen, J., 2007. *Fluoride in Groundwater: Overview and Evaluation of Removal Methods*. Review. International Groundwater Resources Assessment Centre.
- Ferri, D., Grenthe, I., Hietanen, S. & Salvatore, F., 1983. Studies on Metal Carbonate Equilibria. 5. The Cerium (III) Carbonate Complexes in Aqueous Perchlorate Media. *Acta Chemica Scandinavica A*, 37, pp.359-65.
- Firsching, F.H. & Brune, S.N., 1991. Solubility Products of the Trivalent Rare-Earth Phosphates. *Journal of Chemical and Engineering Data*, 36(1), pp.93-95.
- Ghorai, S. & Pant, K.K., 2004. Investigations on the Column Performance of Fluoride Adsorption by Activated Alumina in a Fixed-Bed. *Journal of Chemical Engineering*, 165-173, p.98.
- Goswami, A. & Purkait, M.K., 2012. The Defluoridation of Water by Acidic Alumina. *Chemical Engineering Research and Design*, 90, pp.2316-24.
- Greaves, H., Hobbs, P., Chadwick, D. & Haygarth, P., 1999. Prospects for the Recovery of Phosphorus from Animal Manures: A Review. *Environmental Technology*, 20(7), pp.697-708.
- Grzmil, B. & Wronkowski, J., 2006. Removal of Phosphates and Fluorides from Industrial Wastewater. *Desalination*, 189, pp.261-68.
- Gupta, V.K., Ali, I. & Saini, V.K., 2007. Defluoridation of Wastwaters using Waste Carbon Slurry. *Water Research*, 41, pp.3307-16.
- Gurtubay, L. et al., 2010. Viability Study on Two Treatments for an Industrial Effluent Containing Sulphide and Fluoride. *Chemical Engineering Journal*, 162(1), pp.91-96.
- Haas, J.R., Shock, E.L. & Sassani, D.C., 1995. Rare-Earth Elements in Hydrothermal Systems: Estimates of Standard Partial Molal Thermodynamic Properties of Aqueous Complexes of the Rare-Earth Elements at High Pressures and Temperatures. *Geochemica et Cosmochimica Acta*, 59(21), pp.4329-50.
- Habuda-Stanic, M., Ravancic, M.E. & Flanagan, A., 2014. A Review on Adsorption of Fluoride from Aqueous Solution. *Materials*, 7, pp.6317-65.
- Hamdi, N. & Srasra, E., 2007. Removal of Fluoride from Acidic Wastewater by Clay Mineral: Effect of Solid-Liquid Ratios. *Desalination*, 206, pp.238-44.
- Haron, M.J. et al., 2008. Sorption Removal of Arsenic by Cerium-Exchanged Zeolite-P. *Materials Science and Engineering*, 146(2), pp.204-08.

- Hashimoto, K., Matzuo, K., Kominami, H. & Kera, Y., 1997. Cerium Oxides Incorporated into Zeolite Cavities and Their Reactivity. *Journal of The Chemical Society*, 93(20), pp.3729-32.
- Haynes, W.M., ed., 2015. *CRC Handbook of Chemistry and Physics*. 96th ed. Boca Raton: CRC Press.
- Huang, C.J. & Liu, J.C., 1999. Precipitate Flotation of Fluoride-Containing Wastewater from a Semiconductor Manufacturer. *Water Research*, 33(16), pp.3403-12.
- Hu, C.Y., Lo, S.L., Kuan, W.H. & Lee, Y.D., 2005. Removal of Fluoride from Semiconductor Wastewater by Electrocoagulation-Flotation. *Water Research*, 39, pp.895-901.
- Islam, M. & Patel, R.K., 2007. Evaluation of Removal Efficiency of Fluoride from Aqueous Solution using Quick Lime. *Journal of Hazardous Materials*, 143, pp.303-10.
- Jafari, A. et al., 2014. Process Optimization for Fluoride Removal from Water by Moringa oleifera Seed Extract. *Flouride*, 47(2), pp.152-60.
- Jagtap, S., Yenkie, M.K., Labhsetwar, N. & Rayalu, S., 2012. Fluoride in drinking water and defluoridation of water. *American Chemical Society*, pp.2454-66.
- Jenkins, D., Ferguson, J.F. & Menar, A.B., 1971. Chemical Processes for Phosphate Removal. *Water Research*, 5(7), pp.369-89.
- Johnson, P.N. & Amirtharajah, A., 1983. Ferric Chloride and Alum as Single and Dual Coagulants. *American Water Works Association*, 75(5), pp.232-39.
- Khatibikamal, V., Torabian, A., Janpoor, F. & Hoshyaripour, G., 2010. Fluoride Removal from Industrial Wastewater using Electrocoagulation and its Adsorption Kinetics. *Journal of Hazardous Materials*, 179, pp.276-80.
- Khuri, A.I. & Mukhopadyay, S., 2010. Response Surface Methodology. *WIREs Computational Statistics*, 2, pp.128-49.
- Kirschner, M., 2005. Hydrofluoric Acid. *Chemical Market Reporter*, 268(16), p.38.
- Kovacs, M. et al., 2009. Multi-Analytical Approach of the Influence of Sulphate Ion on the Formation of Cerium (III) Fluoride Nanoparticles in Precipitation Reaction. *Colloids and Surfaces A: Physicochemical and Engineering Aspects*, 352, pp.56-62.

- Kumar, S. & Jain, S., 2013. History, Introduction, and Kinetics of Ion Exchange Materials. *Journal of Chemistry*, 2013, pp.1-13.
- Lee, E.F.T. & Rees, L.V.C., 1987. Calcination of Cerium (III) Exchanged Y-Zeolite. *Zeolites*, 7(5), pp.446-50.
- Li, B., Ning, P., Deng, C.L. & Zhe, Z., 2005. Nitrogen and Phosphate Removal by Activated Zeolite with Lanthana. *Journal of Wuhan University Technology*, 27(9), pp.56-9.
- Li, H. et al., 2009. Removal of Phosphate from Polluted Water by Lanthanum Doped Vesuvianite. *Journal of Hazardous Materials*, 168(1), pp.326-30.
- Litke, D.W., 1999. *Review of Phosphorus Control Measures in the United States and Their Effects on Water Quality*. Investigations Report. Denver: U.S. GEOLOGICAL SURVEY U.S. GEOLOGICAL SURVEY.
- Loganathan, P., Vigheswaran, S., Kandasamy, J. & Naidu, R., 2013. Defluoridation of drinking water using adsorption processes. *Journal of Hazardous Materials*, pp.1-19.
- Lundstedt, T. et al., 1998. Experimental Design and Optimization. *Chemometrics and Intelligent Laboratory Systems*, 42, pp.3-40.
- Mandinic, Z. et al., 2010. Fluoride in drinking water and dental fluorosis. *Science of Total Environment*, pp.3507-12.
- Mayer, S.W. & Schwartz, S.D., 1950. The Association of Cerous Ion with Sulfite, Phosphate and Pyrophosphate Ions. *Journal of the American Chemical Society*, 72(11), pp.5106-10.
- McGill, P., 1995. Endemic Fluorosis. *Baillière's Clinical Rheumatology*, pp.75-81.
- Meas, Y., Ramirez, J.A., Villalon, M.A. & Chapman, T.W., 2010. Industrial Wastewaters Treated by Electrocoagulation. *Electrochimica Acta*, 55, pp.8165-71.
- Meas, Y., Ramirez, J.A., Villalon, M.A. & Chapman, T.W., 2010. Industrial Wastewaters Treated by Electrocoagulation. *Electrochimica Acta*, 55, pp.8165-71.
- Metcalf & Eddy, 2014. *Wastewater Engineering: Treatment and Resource Recovery*. 5th ed. New York: McGraw Hill.
- Minton, G.R. & Carlson, D.A., 1972. Combined Biological-Chemical Phosphorus Removal. *Water Pollution Control Federation*, 44(9), pp.1736-55.

- Mohammed, S.A. & Shanshool, H.A., 2009. Phosphorus Removal from Water and Waste Water by Chemical Precipitation Using Alum and Calcium Chloride. *Iraqi Journal of Chemical and Petroleum Engineering*, 10(2), pp.35-42.
- Mohapatra, M. et al., 2009. Review of fluoride removal from drinking water. *Journal of Environmental Management*, pp.67-77.
- Molycorp Minerals Incorporated, n.d. *SorbX-100*. [Online] Available at: www.molycorp.com [Accessed 30 September 2014].
- Morse, G.K., Brett, S.W., Guy, J.A. & Lester, J.N., 1998. Review: Phosphorus Removal and Recovery Technologies. *The Science of the Total Environment*, 212, pp.69-81.
- MWH Global, 2012. *MWH's Water Treatment: Principles and Design*. 3rd ed. Hoboken: John Wiley & Sons, Inc.
- Na, C.-K. & Park, H.-J., 2010. Defluoridation from aqueous solution by lanthanum hydroxide. *Journal of Hazardous Materials*, pp.512-20.
- National Institute of Standards and Technology, 2003. *Central Composite Design (CCD)*. [Online] Available at: www.itl.nist.gov/div898/handbook/pri/section3/pri3361.html [Accessed 8 August 2015].
- National Research Council, 2006. *Fluoride in Drinking Water: A Scientific Review of EPA's Standards*. Washington, DC: National Academy of Sciences.
- Ndiaye, P.I. et al., 2005. Removal of Fluoride from Electronic Industrial Effluent by RO Membrane Separation. *Desalination*, 173, pp.25-32.
- Ning, P. et al., 2008. Phosphate Removal from Wastewater by Model-La(III) Zeolite Adsorbents. *Journal of Environmental Sciences*, 20(6), pp.670-74.
- Ochoa-Herrera, V. et al., 2009. Toxicity of Fluoride to Micro-organisms in Biological Wastewater Treatment Systems. *Water Research*, 43, pp.3177-86.
- Olmez, T., 2009. The Optimization of Cr(VI) reduction and removal by Electrocoagulation using Response Surface Methodology. *Journal of Hazardous Material*, 162(2-3), pp.1371-78.
- Pakzadeh, B. & Batista, J.R., 2011. Chromium Removal from Ion-Exchange Waste Brines with Calcium Polysulfide. *Water Research*, 45, pp.3055-64.

- Parsons, S.A. & Smith, J.A., 2008. Phosphorus Removal and Recovery from Municipal Wastewaters. *Elements*, 4, pp.109-12.
- Patil, S.S. & Ingole, N., 2012. Studies on Defluoridation - A Critical Review. *Journal of Engineering Research and Studies*, 3(1), pp.111-19.
- Patil, S., Ingole, N.W., Bhakumi, T.S. & Sharma, N.N., 1970. Studies on Defluoridation- A Critical Review. *Studies on defluoridation Bulletin*, 7, pp.77-80.
- Pelletier, D. et al., 2010. Effects of engineered cerium oxide nanoparticles on bacterial growth and viability. *Applied and Environmental Microbiology*, 76(24), pp.7981-89.
- Qu, E. et al., 2007. Highly-efficient Phosphate Removal by Lanthanum-doped Mesoporous, SiO₂. *Colloids and Surfaces A: Physicochemical and Engineering Aspects*, 308(1-3), pp.47-53.
- Raichur, A.M. & Basu, M.J., 2001. Adsorption of fluoride onto mixed rare earth oxides. *Separation and Purification Technology*, pp.121-27.
- Rao, M. & Bhaskaran, C.S., 1998. Studies on Defluoridation of Water. *Journal of Fluoride Chemistry*, 41, pp.17-24.
- Rao, C.R.N. & Karthikeyan, J., 2011. Removal of fluoride from water by adsorption onto lanthanum oxide. *Water Air and Soil Pollution*, pp.1101-14.
- Recht, H.L., Ghassemi, M. & Kleber, E.V., 1970. Precipitation of Phosphates from Water and Wastewater using Lanthanum Salts. In *Proceedings of the 5th International Water Pollution Research.*, 1970. Pergamon.
- Renuka, P. & Pushpanjali, K., 2013. Review on Defluoridation Techniques of Water. *The International Journal Of Engineering And Science*, 2(3), pp.86-94.
- Salman, M.S., 2009. Removal of Sulfate from Wastewater by Activated Carbon. *Al-Khwarizmi Engineering Journal*, 5(3), pp.72-76.
- Schneiter, R.W. & Middlebrooks, E.J., 1983. Arsenic and Fluoride Removal from Groundwater by Reverse Osmosis. *Environment International*, 9, pp.289-91.
- Shen, F., Chen, X., Gao, P. & Chen, G., 2003. Electrochemical removal of fluoride ions from industrial wastewater. *Chemical Engineering Science*, pp.987-93.
- Sillanpaa, M. & Matilaninen, A., 2014. NOM Removal by Coagulation. In Sillanpaa, M. & Voigt, M. *Natural Organic Matter in Water: Characterization and Treatment Methods*. Waltham: Elsevier Science & Technology Books. pp.55-80.

- Stratflul, I., Scrimshaw, M.D. & Lester, J.N., 1999. Biological Phosphorus Removal, its Role in Phosphorus Recycling. *Environmental Technology*, 20, pp.681-95.
- Strileski, M., 2013. *Phosphorus Removal from EBPR Sludge Dewatering Liquors Using Lanthanum Chloride, Aluminum Sulfate, and Ferric Chloride*. MS Thesis. Las Vegas: University of Nevada, Las Vegas University of Nevada, Las Vegas.
- Szabo, A. et al., 2008. Significant of Design and Operational Variables in Chemical Phosphorus Removal. *Water Environment Research*, 80(5), pp.407-16.
- The Pennsylvania State University, 2015. *Lesson 11: Response Surface Methods and Designs*. [Online] Available at: <https://onlinecourses.science.psu.edu/stat503/node/57> [Accessed 21 July 2015].
- Thistleton, J., Clark, T.A., Pearce, P. & Parsons, S.A., 2002. Mechanisms of Chemical Phosphorus Removal II: Iron (III) Salts. *Transactions of the Institution of Chemical Engineers*, 80, pp.265-69.
- Tokunaga, S., Hakuta, T. & Wasay, S., 1999. Treatment of waters containing hazardous anions. *Journal of the National Institute of Materials and Chemical Research*, pp.291-334.
- Tokunaga, S., Hakuta, T. & Wasay, S.A., 1999. Treatment of waters containing hazardous anions. *Journal of the National Institute of Materials and Chemical Research*, pp.291-334.
- Tomar, V. & Kumar, D., 2013. A Critical Study on Efficiency of Different Materials for Fluoride Removal from Aqueous Media. *Chemistry Central Journal*, 7(51), pp.1-15.
- Tripathy, S.S., Bersillon, J.-L. & Gopal, K., 2006. Removal of Fluoride from Drinking Water by Adsorption onto Alum-Impregnated Activated Alumina. *Separation and Purification Technology*, 50, pp.310-17.
- U.S. Environmental Protection Agency, 2000. *Wastewater Technology Fact Sheet: Chemical Precipitation*. Fact Sheet. U.S. Environmental Protection Agency.
- United Steelworkers, 2013. *A Risk Too Great: Hydrofluoric Acid in U.S. Refineries*. [Online] United Steelworkers Available at: <http://assets.usw.org/resources/hse/pdf/A-Risk-Too-Great.pdf> [Accessed 28 July 2015].
- Vithanage, M. & Bhattacharya, P., 2015. Fluoride in the Environment: Sources, Distribution and Defluoridation. *Environmental Chemistry Letters*, 13, pp.131-47.

- Wang, Y. & Reardon, E.J., 2001. Activation and Regeneration of a Soil Sorbent for Defluoridation of Drinking Water. *Applied Geochemistry*, 16, pp.531-39.
- Wang, L.K., Shammam, N.K. & Hung, Y.-T., 2008. Waste Treatment in the Iron and Steel Manufacturing Industry. In L.K. Wang, N.K. Shammam & Y.-T. Hung, eds. *Waste Treatment in the Metal Manufacturing, Forming, Coating, and Finishing Industries*. CRC Press. pp.38-70.
- Wasay, S.A., Haron, M.J. & Tokunaga, S., 1996. Adsorption of Fluoride, Phosphate, Arsenate Ions, on Lanthanum-Impregnated Silica Gel. *Water Environment Research*, 68(3), pp.295-300.
- Wedepohl, K.H., 1978. *Handbook of Geochemistry*. New York: Springer.
- Wood, S.A., 1990. The Aqueous Geochemistry of the Rare-Earth Elements and Yttrium. *Chemical Geology*, 82, pp.159-86.
- Wu, R.S., Lam, K.H., Lee, J.M. & Lau, T.C., 2007. Phosphate Removal from Water by a Highly-Selective La(III)-chelex Resin. *Chemosphere*, 69(2), pp.289-94.
- Yang, Y., 2008. *Multiple Criteria Third-Order Response Surface Design and Comparison*. Thesis. Tallahassee: Florida State University Florida State University.
- Yang, M. et al., 2001. Precipitative Removal of Fluoride from Electronics Wastewater. *Journal of Environmental Engineering*, 127, pp.902-07.
- Zaroual, Z. et al., 2009. Optimizing the Removal of Trivalent Chromium by Electrocoagulation using Experimental Design. *Chemical Engineering Journal*, 148(2-3), pp.488-95.
- Zhang, L. et al., 2012. Batch and Fixed-Bed Column Performance of Phosphate Adsorption by Lanthanum-Doped Activated Carbon Fiber. *Water, Air, & Soil Pollution*, 223(9), pp.5893-902.
- Zhang, J. et al., 2010. Adsorption Behavior of Phosphate on Lanthanum (III)-doped Mesoporous Silicates Material. *Journal of Environmental Science (China)*, 22(4), pp.507-11.

CURRICULUM VITAE

Graduate College
University of Nevada, Las Vegas

John Michael O. Gonzales

Degrees

Bachelor of Science in Civil Engineering, 2013

University of Nevada, Las Vegas

Master of Science in Engineering, 2015

University of Nevada, Las Vegas

Thesis Title: Fluoride and Phosphate Removal from Industrial Domestic Wastewater
Using Cerium Chloride

Thesis Examination Committee:

Chairperson, Jacimaria Batista, Ph.D.

Committee Member, Daniel Gerrity, Ph.D.

Committee Member, David James, Ph. D.

Graduate College Representative, Spencer Steinberg, Ph.D.